MMNSA

Mathematical Modelling and Numerical Simulation with Applications

ISSN Online : 2791-8564

Year : 2022

Volume : 2

Issue : 2

www.mmnsa.org

VOLUME: 2 ISSUE: 2
ISSN ONLINE: 2791-8564

June 2022
https://www.mmnsa.org

MATHEMATICAL MODELLING AND NUMERICAL SIMULATION WITH APPLICATIONS

Editor-in-Chief and Publisher

Mehmet Yavuz
Department of Mathematics and Computer Sciences,
Faculty of Science, Necmettin Erbakan University,
Meram Yeniyol, 42090 Meram, Konya / TÜRKİYE
mehmetyavuz@erbakan.edu.tr

Editorial Board

Technical Editor

Halil İbrahim Özer
Department of Computer and Instructional Technologies
Education, Ahmet Keleşoğlu Faculty of Education,
Necmettin Erbakan University, Meram Yeniyol, 42090
Meram, Konya / TÜRKİYE
hiozer@gmail.com

English Editor

Abdulkadir Ünal
School of Foreign Languages, Foreign Languages, Alanya
Alaaddin Keykubat University, Antalya / TÜRKİYE
abdulkadir.unal@alanya.edu.tr

Editorial Secretariat

Fatma Özlem Coşar
Department of Mathematics and Computer Sciences,
Faculty of Science, Necmettin Erbakan University,
Meram Yeniyol, 42090 Meram, Konya / TÜRKİYE

Müzeyyen Akman
Department of Mathematics and Computer Sciences,
Faculty of Science, Necmettin Erbakan University,
Meram Yeniyol, 42090 Meram, Konya / TÜRKİYE

Contents

Research Articles

Mathematical Modelling and Numerical Simulation with Applications, 2022, 2(2), 59–72

https://www.mmnsa.org
ISSN Online: 2791-8564 / Open Access
https://doi.org/10.53391/mmnsa.2022.006

RESEARCH PAPER

Analysis of fractional-order vaccinated Hepatitis-B epidemic model with Mittag-Leffler kernels

Anwarud Din[1,‡,*] and Muhammad Zainul Abidin[2,‡]

[1]Department of Mathematics, Sun Yat-Sen University, Guangzhou 510275, China, [2]College of Mathematics and Computer Science, Zhejiang Normal University, Jinhua 321004, China

*Corresponding Author

‡anwarud@mail.sysu.edu.cn (Anwarud Din); mzainulabidin@zjnu.edu.cn (Muhammad Zainul Abidin)

Abstract

The current paper investigates a newly developed model for Hepatitis-B infection in sense of the Atangana-Baleanu Caputo (ABC) fractional-order derivative. The proposed technique classifies the population into five distinct categories, such as susceptible, acute infections, chronic infections, vaccinated, and immunized. We obtain the Ulam-Hyers type stability and a qualitative study of the corresponding solution by applying a well-known principle of fixed point theory. Furthermore, we establish the deterministic stability of the proposed model. For the approximation of the ABC fractional derivative, we use a newly proposed numerical method. The obtained results are numerically verified by MATLAB 2020a.

Key words: Fractional calculus; fractional-order model; hepatitis-B disease; ABC derivative; fixed-point theorem; numerical simulation

AMS 2020 Classification: 34A08; 34D20; 34K60; 92C50; 92D30

1 Introduction

Many pandemics and endemics around the world are first explored using a mathematical model based on data from various hospitals. These models explain the human disease origin, current development, and forecast. Mathematical formulations can then be used by researchers and scholars to discover the treatment or cure. The treatment may come in the form of precaution or vaccination for affected individuals of a certain population. Thus, vaccinations against several diseases such as pertussis, measles, polio, Hepatitis-B and influenza have been given and have led to healthy recovery, as mentioned in [1, 2, 3, 4, 5, 6]. Numerous mathematical models for various diseases have been developed recently, including stochastic, deterministic, and difference equation systems with several vaccination parameters for diagnosed infections, as seen in [5]. Among the most serious diseases is Hepatitis-B, which is transmitted by infected individuals. More than one million people have died worldwide due to this outbreak. [7, 8] shows that around 200 million individuals were infected by the pandemic and that three and a half billion people were in a chronic condition. A combination of long-term planning and frequent vaccinations can reduce the spread of the disease in the population in the case of a major epidemic [8]. Strong immunization and dose for the infected persons will rapidly decrease the cases of HBV. To investigate the qualitative analysis Hepatitis-B disease, we consider [9] model as below:

➤ **Received:** 22.03.2022 ➤ **Revised:** 11.05.2022 ➤ **Accepted:** 24.05.2022 ➤ **Published:** 29.05.2022

$$\begin{aligned}
\acute{\Omega}(\sigma) &= \Pi\Lambda - \frac{\gamma\Omega(\sigma)\mathcal{J}^a(\sigma)}{N} + \lambda\mathcal{H}(\sigma) - (\delta+\mu)\Omega(\sigma),\\
\acute{\mathcal{J}}^a(\sigma) &= \frac{\gamma\Omega(\sigma)\mathcal{J}^a(\sigma)}{N} - (\mu+\alpha+\kappa)\mathcal{J}^a(\sigma),\\
\acute{\mathcal{J}}^c(\sigma) &= \kappa\mathcal{J}^a(\sigma) - (\mu+\rho+\eta)\mathcal{J}^c(\sigma),\\
\acute{\mathfrak{R}}(\sigma) &= \alpha\mathcal{J}^a(\sigma) + \eta\mathcal{J}^c(\sigma) - \mu\mathfrak{R}(\sigma),\\
\acute{\mathcal{H}}(\sigma) &= \Lambda(1-\Pi) + \delta\Omega(\sigma) - (\lambda+\mu)\mathcal{H}(\sigma),
\end{aligned} \tag{1}$$

where the parameters and variables in the above equation are listed below:

- vaccinated cases, susceptible population, acute infection cases, chronic carriers cases and immunized cases have been represented by $\mathcal{H}(\sigma)$, $\Omega(\sigma)$, $\mathcal{J}^a(\sigma)$, $\mathcal{J}^c(\sigma)$ and $\mathfrak{R}(\sigma)$ respectively.
- Λ: Recruitment/Birth rate.
- λ: Waning vaccine-induced immunity.
- μ: Natural death rate.
- ρ: The HBV death rate.
- γ: Contact rate among infected and non-infected individuals.
- α: The rate of recovery for infected individuals.
- η: The rate of recovery of individuals infected chronically.
- κ: The rate at which acute cases are transformed into chronic cases.
- Π: Ratio of new-borns who have not received proper immunization.
- δ: Hepatitis immunization rate.

Riemann-Liouville, Euler, and Fourier made significant contributions to the development of ordinary calculus in the 18th century. At the time, many authors made significant contributions to the field of fractional calculus (FC), see [10, 11, 12]. This is due to the fact that ordinary calculus lacks the applications of modern calculus in many mathematical modeling domains, such as the process of memory and hereditary data. FC, as a general form of integer order calculus, has significantly larger freedom in their derivative than is found in integer-order derivative due to its local behavior. Several applications of FC are discussed in [13, 14, 15, 16, 17, 18, 19, 20, 21]. Researchers and scientists have become more interested in analyzing non-integer order (FO) of differential and integral calculus because of its applications. Non-local and non-singular concepts were introduced in FC articles, replacing singular and local kernels with these new concepts. The most useful feature of this newly developed kernel is its memory property combined with the system's hereditary. Atangana, Baleanu, and Caputo (ABC) [13] proposed a novel FO operator, in 2016, depending on the general non-local and non-singular kernel of Mittag-Leffler (ML) mapping. As seen in [22, 23, 24, 25, 26], the ABC order fractional order operator has been used in many mathematical schemes describing different physical problems. More specifically, this generalized ML function is a precise tool to deal with real word problems.
Scientists and researchers across a wide range of fields are working to stop or slow down the spread of these diseases, as evidenced by these references [27, 28, 29, 30, 31, 32, 33, 34, 35, 36, 37, 38, 39, 40, 41, 42, 43, 44]. Many authors have investigated various models for a number of diseases; for a detailed study see [45, 46, 47, 48, 49, 50]. Epidemic models by the researcher are widely used nowadays to investigate the dynamic spreading of disease and to follow the efficient method for its controlling. Ordinary differential equation with integer-order derivative could be generalized to the fractional-order larger degree freedom derivative of fractional order. Also FO differential equations with $0 < \wp \leq 1$ have been studied in [26]. Generally, biological models and FDEs are theoretically related to memory-based systems [23, 25, 50]. Furthermore, the history factor is a major source of disease transmission. In the coming days, the development of totality and historical effects on existing levels will be a source of transmission. Heterogeneity and historical effect show the spread of the previous infections. Thus, the mentioned properties can be examined via fractional derivatives, as well as their effect on disease transmission [39, 50].
The purpose of this work is to investigate the dynamic behavior of the fractional HBV epidemic model's solutions (2). We established the stability and equilibria analysis for the given system based on the diseases free equilibrium point. We additionally addressed some basic principles and gave theoretical solutions. Furthermore, we simulate the unknown quantities to verify and explain the fractional order mathematical model. We note from the existing research that limited study has been done on non-integer order epidemic models using ABC derivatives. There has not been enough research done on the ML kernel-based arbitrary order HBV vaccinated model. Thus, the primary motivation for this study is to develop a HBV FO-vaccinated system. Under the ABC derivative with $\wp \in (0,1]$ we reexamine the HBV model (1) in the following fractional form

$$\begin{cases}
{}^{ABC}D^{\wp}\Omega(\sigma) = \Pi\Lambda - \dfrac{\wp\Omega(\sigma)\mathcal{J}^a(\sigma)}{N} + \lambda\mathcal{H}(\sigma) - (\delta+\mu)\,\Omega(\sigma),\\
{}^{ABC}D^{\wp}\mathcal{J}^a(\sigma) = \dfrac{\wp\Omega(\sigma)\mathcal{J}^a(\sigma)}{N} - (\mu+\alpha+\kappa)\,\mathcal{J}^a(\sigma),\\
{}^{ABC}D^{\wp}\mathcal{J}^c(\sigma) = \kappa\mathcal{J}^a(\sigma) - (\mu+\rho+\eta)\,\mathcal{J}^c(\sigma),\\
{}^{ABC}D^{\wp}\mathfrak{R}(\sigma) = \alpha\mathcal{J}^a(\sigma) + \eta\mathcal{J}^c(\sigma) - \mu\mathfrak{R}(\sigma),\\
{}^{ABC}D^{\wp}\mathcal{H}(\sigma) = \Lambda\,(1-\Pi) + \delta\,\Omega(\sigma) - (\lambda+\mu)\,\mathcal{H}(\sigma).
\end{cases} \tag{2}$$

with the initial conditions

$$S(0) \geq 0,\ \ \mathcal{J}^a(0) \geq 0,\ \ \mathcal{J}^c(0) \geq 0,\ \ \mathfrak{R}(0) \geq 0,\ \ \mathcal{H}(0) \geq 0. \tag{3}$$

Our remaining paper has the following arrangement as follows. In Section Fundamental we recall some basic results of fractional calculus.

In this way, we manage the remainder of the contents of the current examination as follows. During Section 2, essential definitions are provided. The existence theory of model and stability is given in Section 3. Also, numerical methods to solve the considered problems are given in Section 4. Indeed, numerical results of the proposed models under practising different values of fractional orders are supplied in section Section 5. Finally, the conclusion of the current investigation can be observed in Section 6.

2 Preliminaries

In this section, we give some important definitions which we will use in the rest of the paper [23, 25, 26, 50].

Definition 1 *Let $\xi(\sigma)$ be a function satisfying $\xi(\sigma) \in \mathbb{H}^1[0,T]$ the $\mathbb{ABC}$ fractional derivative of order $0 \leq \ell \leq 1$ and is defined by*

$$^{ABC}D_t^{\wp}(\xi(\sigma)) = \frac{\mathbb{M}(\wp)}{1-\wp}\int_0^t \mathbf{E}_{\wp}\left[\frac{-\wp}{1-\wp}\left(t-z\right)^{\wp}\right]\frac{d}{dz}\xi(z)dz, \tag{4}$$

where $\mathbb{M}(\wp) = \frac{\wp}{2-\wp}$ is the normalization constant, $\mathbb{M}(0) = \mathbb{M}(1) = 1$ and $\mathbf{E}_{\wp}$ is the Mittag-Leffler operator given by

$$\mathbf{E}_{\wp}(y) = \sum_{k=0}^{\infty}\frac{y^k}{\Gamma(\wp k+1)}.$$

Theorem 1 *[51] The Atangana-Baleanu fractional differential equation*

$$^{ABC}D_t^{\wp}\xi(\sigma) = f(\sigma)$$

has a unique solution in the form

$$\xi(\sigma) = \frac{1-\wp}{\mathbb{M}(\wp)}f(\sigma) + \frac{\wp}{\mathbb{M}(\wp)\Gamma(\wp)}\int_0^{\sigma} f(\vartheta)(\sigma-s)^{\wp-1}d\vartheta. \tag{5}$$

Definition 2 *[52] Let*

$$\begin{cases} ^{ABC}D_0^{\wp}\xi(\sigma) = f(t,\xi(\sigma)), \\ \xi(0) = \xi_0 \end{cases}$$

is a non-linear fractional ordinary differential equation. The new formula for the numerical scheme of the ABC fractional derivative can be written as

$$\begin{aligned} \xi_{m+1} = \xi_0 + \frac{1-\wp}{\mathbb{M}(\wp)}f(\xi(t_m),t_m) + \frac{\wp}{\mathbb{M}(\wp)}\sum_{n=0}^{m}\Bigg\{\frac{h^{\wp}f(\xi_n,t_n)}{\Gamma(\wp+2)}[(m+1-n)^{\wp}(m-n+2+\wp) \\ -(m-n)^{\wp}(m-n+2+2\wp)] - \frac{h^{\wp}f(\xi_s,t_s)}{\Gamma(\wp+2)}[(m+1-n)^{\wp+1}-(m-n)^{\wp}(m-n+1+\wp)] + E_m^{\wp}\Bigg\}, \end{aligned} \tag{6}$$

where $E_m^{\wp}$ is given by

$$E_m^{\wp} = \frac{\wp}{\mathbb{M}(\wp)\Gamma(\wp)}\sum_{k=0}^{m}\int_{t_n}^{t_{n-1}}\frac{(y-t_n)(y-\sigma_{n-1})}{2}\frac{\partial^2}{\partial y^2}[f(\xi(y),y)]_{y=\lambda_y}(\sigma_{m+1}-y)^{\wp-1}dy. \tag{7}$$

Theorem 2 *Let B be a convex subset of Z and suppose that the two operators Υ_1, Υ_2 with*
(1). $\Upsilon_1 u + \Upsilon_2 u \in \mathbb{B}$ for each $u \in B$.
(2). Υ_1 is "contraction".
(3). A continuous and compact set is Υ_2.
satisfying the operator equation $\Upsilon_1 u + \Upsilon_2 u = u$, has one or more solution(s).

3 Existence theory of model (2)

In this part, we established the existence and uniqueness of the solution for the proposed system (2). We find the solution and stability of the proposed model under ABC derivative with FO using Banach fixed point principles. We rearrange the proposed model in the following way

$$\begin{cases} \aleph_1(\sigma,\Omega,\mathcal{J}^a,\mathcal{J}^c,\mathcal{H},\Re) = \Pi\Lambda - \frac{\wp\Omega(\sigma)\mathcal{J}^a(\sigma)}{N} + \lambda\mathcal{H}(\sigma) - (\delta+\mu)\,\Omega(\sigma), \\ \aleph_2(\sigma,\Omega,\mathcal{J}^a,\mathcal{J}^c,\mathcal{H},\Re) = \frac{\wp\Omega(\sigma)\mathcal{J}^a(\sigma)}{N} - (\mu+\alpha+\kappa)\,\mathcal{J}^a(\sigma), \\ \aleph_3(\sigma,\Omega,\mathcal{J}^a,\mathcal{J}^c,\mathcal{H},\Re) = \kappa\mathcal{J}^a(\sigma) - (\mu+\rho+\eta)\,\mathcal{J}^c(\sigma), \\ \aleph_4(\sigma,\Omega,\mathcal{J}^a,\mathcal{J}^c,\mathcal{H},\Re) = \alpha\mathcal{J}^a(\sigma) + \eta\mathcal{J}^c(\sigma) - \mu\Re(\sigma), \\ \aleph_5(\sigma,\Omega,\mathcal{J}^a,\mathcal{J}^c,\mathcal{H},\Re) = \Lambda(1-\Pi) + \delta\Omega(\sigma) - (\lambda+\mu)\,\mathcal{H}(\sigma). \end{cases} \tag{8}$$

For $0 < \wp \leq 1$, using (8) we write the proposed model in the following form

$$\begin{aligned} {}^{ABC}D^{\wp}_{+0}\mathcal{H}(\sigma) &= \aleph(\sigma, \nu(\sigma)), \\ \nu(0) &= \nu_0. \end{aligned} \tag{9}$$

By Theorem 1, the system (9) becomes

$$\nu(\sigma) = \nu_0(\sigma) + \left[\aleph((\sigma, \nu(\sigma)) - \aleph_0(\sigma)\right]\frac{1-\wp}{M(\wp)} + \frac{\wp}{M(\wp)\Gamma(\wp)}\int_0^{\sigma}(\sigma - s)^{\wp-1}\aleph(\vartheta, \nu(\vartheta))d\vartheta, \tag{10}$$

where

$$\nu(\sigma) = \begin{cases} \Omega(\sigma) \\ \mathcal{J}^a(\sigma) \\ \mathcal{J}^c(\sigma) \\ \Re(\sigma) \\ \mathcal{H}(\sigma) \end{cases}, \nu_0(\sigma) = \begin{cases} \Omega_0 \\ \mathcal{J}^a_0 \\ \mathcal{J}^c_0 \\ \Re_0 \\ \mathcal{H}_0 \end{cases}, \aleph(\sigma, \nu(\sigma)) = \begin{cases} \aleph_1(\sigma, \Omega, \mathcal{J}^a, \mathcal{J}^c, \mathcal{H}, \Re) \\ \aleph_2(\sigma, \Omega, \mathcal{J}^a, \mathcal{J}^c, \mathcal{H}, \Re) \\ \aleph_3(\sigma, \Omega, \mathcal{J}^a, \mathcal{J}^c, \mathcal{H}, \Re) \\ \aleph_4(\sigma, \Omega, \mathcal{J}^a, \mathcal{J}^c, \mathcal{H}, \Re) \\ \aleph_5(\sigma, \Omega, \mathcal{J}^a, \mathcal{J}^c, \mathcal{H}, \Re) \end{cases}, \aleph_0(\sigma) \begin{cases} \aleph_1(0, \Omega_0, \mathcal{J}^a_0, \mathcal{J}^c_0, \mathcal{H}_0, \Re_0) \\ \aleph_2(0, \Omega_0, \mathcal{J}^a_0, \mathcal{J}^c_0, \mathcal{H}_0, \Re_0) \\ \aleph_3(0, \Omega_0, \mathcal{J}^a_0, \mathcal{J}^c_0, \mathcal{H}_0, \Re_0) \\ \aleph_4(0, \Omega_0, \mathcal{J}^a_0, \mathcal{J}^c_0, \mathcal{H}_0, \Re_0) \\ \aleph_5(0, \Omega_0, \mathcal{J}^a_0, \mathcal{J}^c_0, \mathcal{H}_0, \Re_0) \end{cases}. \tag{11}$$

Using (10) and (11), define two operators Υ_1 and Υ_2, using (10)

$$\begin{aligned} \Upsilon_1 u &= \nu_0(\sigma) + \left[\aleph(\sigma, \nu(\sigma)) - \aleph_0(\sigma)\right]\frac{1-\wp}{M(\wp)}, \\ \Upsilon_2 u &= \frac{\wp}{M(\wp)\Gamma(\wp)}\int_0^{\sigma}(\sigma - s)^{\wp-1}\aleph(\vartheta, \nu(\vartheta))d\vartheta. \end{aligned} \tag{12}$$

Next, we have to determine the qualitative analysis for the proposed model by using fixed point principle.
(L_1) there exist some constants ϵ_1 and ϵ_2,

$$|\aleph(\sigma, \nu(\sigma))| \leq \epsilon_1|\nu(\sigma)| + \epsilon_2.$$

(L_2) there exists a positive constant K_p, for each $u, u_1 \in \mathbb{X}$,

$$|\aleph(\sigma, \nu(\sigma)) - \aleph(\sigma, \nu_1(\sigma))| \leq K_p\|u - u_1\|.$$

Theorem 3 *The system* (10) *has at least one solution, if* (L_1) *and* (L_2) *hold, then the proposed system* (2) *also has a unique solution if*

$$\frac{(1-\wp)K_p}{M(\wp)} < 1.$$

Proof First we have to show that Υ_1 is contraction by using Banach contraction principle. Let $u_1 \in \mathbf{B}$, : $\mathbf{B} = \{u \in \mathfrak{Z} : ||u|| \leq r, r > 0\}$ be a closed convex set. From the operator Υ_1 defined in (12), we have

$$\begin{aligned} \|\Upsilon_1 u - \Upsilon_1 u_1\| &= \frac{(1-\wp)}{M(\wp)}\max_{\sigma\in[0,T]}\left|\aleph(\sigma, \nu(\sigma)) - \aleph(\sigma, \nu_1(\sigma))\right|, \\ &\leq \frac{(1-\wp)_p}{M(\wp)}\|u - u_1\|. \end{aligned} \tag{13}$$

Hence, the operator Υ_1 is closed and therefore contraction.
Next, we have to show that the operator Υ_2 is compact, continuous and bounded. Also, obviously the operator Υ_2 is defined on all domains, so $\aleph$ is continuous. Let $u \in \mathbb{B}$, we have

$$\begin{aligned} |\Upsilon_2(u)| &= \max_{\sigma\in[0,T]}\frac{\wp}{M(\wp)\Gamma(\wp)}\left|\left|\int_0^{\sigma}(\sigma - s)^{\wp-1}\aleph(\vartheta, \nu(\vartheta))d\vartheta\right|\right|, \\ &\leq \frac{\wp}{M(\wp)\Gamma(\wp)}\int_0^{\sigma}(\sigma - s)^{\wp-1}|\aleph(\vartheta, \nu(\vartheta))|d\vartheta, \\ &\leq \frac{T^{\wp}}{M(\wp)\Gamma(\wp)}[\epsilon_1 r + \epsilon_2]. \end{aligned} \tag{14}$$

So by (14) the operator Υ_2 is bounded. For equi-continuous, $\sigma_1 > \sigma_2 \in [0, T]$, such that

$$\begin{aligned} |\Upsilon_2\nu(\sigma_1) - \Upsilon_2\nu(\sigma_2)| &= \frac{\wp}{M(\wp)\wp(\wp)}\left|\int_0^{\sigma_1}(\sigma_1 - s)^{\wp-1}\aleph(y), \nu(y)d\vartheta - \int_0^{\sigma_2}(\sigma_2 - s)^{\wp-1}\aleph(\vartheta, \nu(\vartheta))d\vartheta\right|, \\ &\leq \frac{[\epsilon_1 r + \epsilon_2]}{M(\wp)\Gamma(\wp)}[\sigma_1^{\wp} - \sigma_2^{\wp}]. \end{aligned} \tag{15}$$

As $\sigma_1 \to \sigma_2$, R.H.S of (15) tends to 0. Also, by continuous operator Υ_2 we have

$$|\Upsilon_2 v(\sigma_1) - \Upsilon_2 v(\sigma_2)| \to 0, \ as \ \ \sigma_1 \to \sigma_2.$$

Hence we proved that Υ_2 is continuous and bounded. So Υ_2 is also uniformly continuous. Using "Arzela$'$-Ascoli theorem", we have that Υ_2 is relatively compact and therefore completely continuous. By (3) and (10) it is easy to obtain that the system has at least one solution.

Uniqueness of the solution

Theorem 4 *Assume* (L_2) *and the integral form* (10) *has a unique solution. Then the system* (2) *has also a unique solution if*

$$\left[\frac{(1-\wp)K_p}{M(\wp)} + \frac{T^\wp K_p}{M(\wp)\Gamma(\wp)}\right] < 1.$$

Proof Let the operator $\mathcal{T} : \mathfrak{Z} \to \mathfrak{Z}$ be defined by

$$\mathcal{T}v(\sigma) = v_0(\sigma) + \left[\aleph(\sigma, v(\sigma)) - \aleph_0(\sigma)\right]\frac{1-\wp}{M(\wp)} + \frac{\wp}{M(\wp)\Gamma(\wp)}\int_0^\sigma (\sigma - s)^{\wp-1}\aleph(\vartheta, v(\vartheta))d\vartheta, \ \ \sigma \in [0, T]. \tag{16}$$

and $u, u_1 \in \mathfrak{Z}$, then

$$\begin{aligned} ||\mathcal{T}u - \mathcal{T}u_1|| &\leq \frac{(1-\wp)}{M(\wp)}\max_{\sigma\in[0,T]}\left|\aleph(\sigma, v(\sigma)) - \aleph(\sigma, v_1(\sigma))\right|, \\ &+ \frac{\wp}{M(\wp)\Gamma(\wp)}\max_{\sigma\in[0,T]}\left|\int_0^\sigma (\sigma - s)^{\wp-1}\aleph(\vartheta, v(\vartheta))d\vartheta - \int_0^\sigma (\sigma - s)^{\wp-1}\aleph(\vartheta, v_1(\vartheta))d\vartheta\right|, \\ &\leq \left[\frac{(1-\wp)K_p}{M(\wp)} + \frac{\wp T^\wp K_p}{M(\wp)\Gamma(\wp)}\right]||u - u_1||, \\ &\leq \Theta||u - u_1||, \end{aligned} \tag{17}$$

where

$$\Theta = \left[\frac{(1-\wp)K_p}{M(\wp)} + \frac{T^\wp K_p}{M(\wp)\Gamma(\wp)}\right]. \tag{18}$$

By (17), the operator $\mathcal{T}$ is contraction. Therefore, the equation (10) has a unique solution. Consequently, the proposed system (2) has also a unique solution.

Ulam-Hyers stability

Next, we obtain the stability of the proposed system, consider small change $\varphi \in C[0, T]$ satisfying $0 = \wp(0)$, we have
(1) $|\varphi(\sigma)| \leq \xi$, *for* $\xi > 0$
(2) ${}^{ABC}D^\wp_{+0}(v(\sigma)) = \aleph(\sigma, v(\sigma)) + \varphi(\sigma)$,for all $\sigma \in [0, T]$.

Lemma 1 *The solution to the changed problem can be expressed by*

$$\begin{cases} {}^{ABC}_{0}D^\wp_{+0}v(\sigma) = \aleph(\sigma, v(\sigma)) + \varphi(\sigma), \\ v(0) = v_0, \end{cases} \tag{19}$$

satisfying

$$\left|v(\sigma) - \left(v_0(\sigma) + \left[\aleph(\sigma, v(\sigma)) - \aleph_0(\sigma)\right]\frac{1-\wp}{M(\wp)} + \frac{\wp}{M(\wp)\Gamma(\wp)}\int_0^\sigma (\sigma - \vartheta)^{\wp-1}\aleph(\vartheta, v(\vartheta))d\vartheta\right)\right| \leq \wp_{T,\wp}\xi, \tag{20}$$

where

$$\wp_{T,\wp} = \frac{\Gamma(\wp)(1-\wp) + T^\wp}{M(\wp)\Gamma(\wp)}.$$

Proof The proof is obvious, therefore the details are omitted.

Theorem 5 *Consider* (L_2) *together with equation* (20)*, the solution of equation* (10) *is UH stable and hence, the analytical solution for the proposed system is UH stable for* $\Theta < 1$.

Proof Let $u_1 \in 3$ be a unique solution and u $\in$ 3 be any solution of equation (10), we have

$$\begin{aligned}
|\nu(\sigma)-\nu_1(\sigma)| &= \left|\nu(\sigma)-\left(\nu_0(\sigma)+\left[\aleph(\sigma,\nu_1(\sigma))-\aleph_0(\sigma)\right]\frac{1-\wp}{M(\wp)}+\frac{\wp}{M(\wp)\Gamma(\wp)}\int_0^\sigma(\sigma-\vartheta)^{\wp-1}\aleph(\vartheta,\nu_1(\vartheta))d\vartheta\right)\right|,\\
&\le \left|\nu(\sigma)-\left(\nu_0(\sigma)+\left[\aleph(\sigma,\nu(\sigma))-\aleph_0(\sigma)\right]\frac{1-\wp}{M(\wp)}+\frac{\wp}{M(\wp)\Gamma(\wp)}\int_0^\sigma(\sigma-\vartheta)^{\wp-1}\aleph(\vartheta,\nu(\vartheta))d\vartheta\right)\right|\\
&+\left|\left(\nu_0(\sigma)+\left[\aleph(\sigma,\nu(\sigma))-\aleph_0(\sigma)\right]\frac{1-\wp}{M(\wp)}+\frac{\wp}{M(\wp)\Gamma(\wp)}\int_0^\sigma(\sigma-\vartheta)^{\wp-1}\aleph(\vartheta,\nu(\vartheta))d\vartheta\right)\right.\\
&\left.-\left(\nu_0(\sigma)+\left[\aleph(\sigma,\nu_1(\sigma))-\aleph_0(\sigma)\right]\frac{1-\wp}{M(\wp)}+\frac{\wp}{M(\wp)\Gamma(\wp)}\int_0^\sigma(\sigma-\vartheta)^{\wp-1}\aleph(\vartheta,\nu_1(\vartheta))d\vartheta\right)\right|,\\
&\le \xi_{\wp_{T,\wp}}+\frac{(1-\wp)K_p}{M(\wp)}||u-u_1||+\frac{\wp T^\wp K_p}{M(\wp)\Gamma(\wp)}||u-u_1||\\
&\le \xi_{\wp_{T,\wp}}+\Theta||u-u_1||.
\end{aligned} \tag{21}$$

From (21), we can write

$$||\nu-\nu_1|| \le \frac{\xi_{\wp_{T,\wp}}}{1-\Theta}. \tag{22}$$

From (22), we obtained that the solution of (10) is Ulam-Hyers stable and hence by considering $\aleph_\nu(\xi) = \wp_{T,\wp}\xi$, $\aleph_\nu(0) = 0$ the solution is generalized Ulam-Hyers Stable. This proves that the solution of the considered model is Ulam-Hyers stable and also generalized Ulam-Hyers stable.

Now we postulate the assumptions given below
(1) $|\varphi(\sigma)| \le \nabla(\sigma)\xi$, *for* $\xi > 0$
(2) ${}^{ABC}D^{\wp}_{+0}(\nu(\sigma)) = \aleph(\sigma,\nu(\sigma)) + \varphi(\sigma)$, for all $\sigma \in [0,T]$.

Lemma 2 *The next equation will satisfy* (19)

$$\begin{aligned}
&\left|\nu(\sigma)-\left(\nu_0(\sigma)+\left[\aleph(\sigma,\nu(\sigma))-\aleph_0(\sigma)\right]\frac{1-\wp}{M(\wp)}+\frac{\wp}{M(\wp)\Gamma(\wp)}\int_0^\sigma(\sigma-\vartheta)^{\wp-1}\aleph(\vartheta,\nu(\vartheta))d\vartheta\right)\right|\\
&\le \nabla(\sigma)\xi_{\wp_{T,\wp}}.
\end{aligned} \tag{23}$$

Proof The proof is obvious, therefore the details are omitted.

Theorem 6 *By Lemma* (2)*, the solution to the considered system is Ulam-Hyers-Rassias (UHR) stable and hence, the generalized UHR stable.*

Proof Let $u_1 \in 3$ be a unique solution and $u \in 3$ be a solution of (10), we have

$$\begin{aligned}
|\nu(\sigma)-\nu_1(\sigma)| &= \left|\nu(\sigma)-\left(\nu_0(\sigma)+\left[\aleph(\sigma,\nu_1(\sigma))-\aleph_0(\sigma)\right]\frac{1-\wp}{M(\wp)}+\frac{\wp}{M(\wp)\Gamma(\wp)}\int_0^\sigma(\sigma-\vartheta)^{\wp-1}\aleph(\vartheta,\nu_1(\vartheta))d\vartheta\right)\right|,\\
&\le \left|\nu(\sigma)-\left(\nu_0(\sigma)+\left[\aleph(\sigma,\nu(\sigma))-\aleph_0(\sigma)\right]\frac{1-\wp}{M(\wp)}+\frac{\wp}{M(\wp)\Gamma(\wp)}\int_0^\sigma(\sigma-\vartheta)^{\wp-1}\aleph(\vartheta,\nu(\vartheta))d\vartheta\right)\right|\\
&+\left|\left(\nu_0(\sigma)+\left[\aleph(\sigma,\nu(\sigma))-\aleph_0(\sigma)\right]\frac{1-\wp}{M(\wp)}+\frac{\wp}{M(\wp)\Gamma(\wp)}\int_0^\sigma(\sigma-\vartheta)^{\wp-1}\aleph(\vartheta,\nu(\vartheta))d\vartheta\right)\right.\\
&\left.-\left(\nu_0(\sigma)+\left[\aleph(\sigma,\nu_1(\sigma))-\aleph_0(\sigma)\right]\frac{1-\wp}{M(\wp)}+\frac{\wp}{M(\wp)\Gamma(\wp)}\int_0^\sigma(\sigma-\vartheta)^{\wp-1}\aleph(\vartheta,\nu_1(\vartheta))d\vartheta\right)\right|,\\
&\le \nabla(\sigma)\xi_{\wp_{T,\wp}}+\frac{(1-\wp)K_p}{M(\wp)}||u-u_1||+\frac{\wp T^\wp K_p}{M(\wp)\Gamma(\wp)}||u-u_1||,\\
&\le \nabla(\sigma)\xi_{\wp_{T,\wp}}+\Theta\|u-u_1\|.
\end{aligned} \tag{24}$$

From (24), we get

$$\|\nu-\nu_1\| \le \frac{\nabla(\sigma)\xi_{\wp_{T,\wp}}}{1-\Theta}. \tag{25}$$

Therefore, the solution of (10) is stable.

4 Numerical solution of the proposed model

Numerous numerical techniques have been suggested for the approximation of the fractional derivative of Atangana-Baleanu in the sense of Caputo. In [53, 54] Atangana and Owolabi proposed a new form of the Adams-Bashforth approach based on the Mittag-Leffler kernel for the ABC fractional derivative approximation. The purpose of this section of the article is to demonstrate how to apply the numerical technique described in [52], which has recently been proven for accuracy and reliability [55, 56] to solve any fractional differential equation. The numerical technique for approximating ABC is defined in (2). To learn more about this numerical approach in detail, we suggest our readers to [52].
To determine the approximate solution to the given model, we use theorem (1) for each of $\Omega(\sigma)$, $\mathcal{J}^a(\sigma)$, $\mathcal{J}^c(\sigma)$, $R^v(\sigma)$, $V^v(\sigma)$ of the system (2) and obtain the following result:

$$
\begin{aligned}
\Omega(\sigma) &= S(0) + \frac{1-\wp}{\mathbb{M}(\wp)}\left[\Pi\Lambda - \frac{\gamma\Omega(\sigma)\mathcal{J}^a(\sigma)}{N} + \lambda V(\sigma) - (\delta+\mu)\,\Omega(\sigma)\right] \\
&\quad + \frac{\wp}{\mathbb{M}(\wp)\Gamma(\wp}\int_0^\sigma (\sigma-y)^{\wp-1}\left[\Pi\Lambda - \frac{\gamma\Omega(\sigma)\mathcal{J}^a(\sigma)}{N} + \lambda V(\sigma) - (\delta+\mu)\,\Omega(\sigma)\right]dy, \\
\mathcal{J}^a(\sigma) &= \mathcal{J}^a(0) + \frac{1-\wp}{\mathbb{M}(\wp)}\left[\frac{\gamma\Omega(\sigma)\mathcal{J}^a(\sigma)}{N} - (\mu+\alpha+\kappa)\,\mathcal{J}^a(\sigma)\right] + \frac{\wp}{\mathbb{M}(\wp)\Gamma(\wp}\int_0^\sigma (\sigma-y)^{\wp-1}\left[\frac{\wp\Omega(\sigma)\mathcal{J}^a(\sigma)}{N}\right. \\
&\quad \left. - (\mu+\alpha+\kappa)\,\mathcal{J}^a(\sigma)\right]dy, \\
\mathcal{J}^c(\sigma) &= \mathcal{J}^c(0) + \frac{1-\wp}{\mathbb{M}(\wp)}\left[\kappa\mathcal{J}^a(\sigma) - (\mu+\rho+\eta)\,\mathcal{J}^c(\sigma)\right] + \frac{\wp}{\mathbb{M}(\wp)\Gamma(\wp}\int_0^\sigma (\sigma-y)^{\wp-1}\left[\kappa\mathcal{J}^a(\sigma) - (\mu+\rho+\eta)\,\mathcal{J}^c(\sigma)\right]dy, \\
\mathfrak{R}(\sigma) &= \mathfrak{R}(0) + \frac{1-\wp}{\mathbb{M}(\wp)}\left[\alpha\mathcal{J}^a(\sigma) + \eta\mathcal{J}^c(\sigma) - \mu\mathfrak{R}(\sigma)\right] + \frac{\wp}{\mathbb{M}(\wp)\Gamma(\wp}\int_0^\sigma (\sigma-y)^{\wp-1}\left[\alpha\mathcal{J}^a(\sigma) + \eta\mathcal{J}^c(\sigma) - \mu\mathfrak{R}(\sigma)\right]dy, \\
\mathcal{H}(\sigma) &= \mathcal{H}(0) + \frac{1-\wp}{\mathbb{M}(\wp)}\left[\Lambda(1-\Pi) + \delta\Omega(\sigma) - (\lambda+\mu)\,\mathcal{H}(\sigma)\right] + \frac{\wp}{\mathbb{M}(\wp)\Gamma(\wp}\int_0^\sigma (\sigma-y)^{\wp-1}\left[\Lambda(1-\Pi)\right. \\
&\quad \left. + \delta\Omega(\sigma) - (\lambda+\mu)\,\mathcal{H}(\sigma)\right]dy.
\end{aligned}
\tag{26}
$$

At $\sigma = \sigma_{m+1}$ and by applying (6) on (26), we get the result as

$$
\begin{aligned}
\Omega_{m+1} &= \Omega_0 + \frac{1-\wp}{\mathbb{M}(\wp)}\nabla_1(S(\sigma_m),\sigma_m) + \frac{\wp}{\mathbb{M}(\wp)}\sum_{n=0}^{m}\left\{\frac{h^\wp\nabla_1(\Omega_n,\sigma_n)}{\Gamma(\wp+2)}\left[(m+1-n)^\wp(m-n+2+\wp)\right.\right. \\
&\quad \left.\left. - (m-n)^\wp(m-n+2+2\wp)\right] - \frac{h^\wp\nabla_1(\Omega_{n-1},\sigma_{n-1}}{\Gamma(\wp+2)}\left[(m+1-n)^{\wp+1} - (m-n)^\wp(m-n+1+\wp)\right]\right\} + E^\wp_{1,m}, \\
\mathcal{J}^a_{m+1} &= \mathcal{J}^a_0 + \frac{1-\wp}{\mathbb{M}(\wp)}\nabla_2(\mathcal{J}^a(\sigma_m),\sigma_m) + \frac{\wp}{\mathbb{M}(\wp)}\sum_{n=0}^{m}\left\{\frac{h^\wp\nabla_2(\mathcal{J}^a_n,\sigma_n)}{\Gamma(\wp+2)}\left[(m+1-n)^\wp(m-n+2+\wp)\right.\right. \\
&\quad \left.\left. - (m-n)^\wp(m-n+2+2\wp)\right] - \frac{h^\wp\nabla_2(\mathcal{J}^a_{n-1},\sigma_{n-1}}{\Gamma(\wp+2)}\left[(m+1-n)^{\wp+1} - (m-n)^\wp(m-n+1+\wp)\right]\right\} + E^\wp_{2,m}, \\
\mathcal{J}^c_{m+1} &= \mathcal{J}^c_0 + \frac{1-\wp}{\mathbb{M}(\wp)}\nabla_3(\mathcal{J}^c(\sigma_m),\sigma_m) + \frac{\wp}{\mathbb{M}(\wp)}\sum_{n=0}^{m}\left\{\frac{h^\wp\nabla_3(\mathcal{J}^c_n,\sigma_n)}{\Gamma(\wp+2)}\left[(m+1-n)^\wp(m-n+2+\wp)\right.\right. \\
&\quad \left.\left. - (m-n)^\wp(m-n+2+2\wp)\right] - \frac{h^\wp\nabla_3(\mathcal{J}^c_{n-1},\sigma_{n-1}}{\Gamma(\wp+2)}\left[(m+1-n)^{\wp+1} - (m-n)^\wp(m-n+1+\wp)\right]\right\} + E^\wp_{3,m}, \\
\mathfrak{R}_{m+1} &= \mathfrak{R}_0 + \frac{1-\wp}{\mathbb{M}(\wp)}\nabla_4(\mathfrak{R}(\sigma_m),\sigma_m) + \frac{\wp}{\mathbb{M}(\wp)}\sum_{n=0}^{m}\left\{\frac{h^\wp\nabla_4(\mathfrak{R}_n,\sigma_n)}{\Gamma(\wp+2)}\left[(m+1-n)^\wp(m-n+2+\wp)\right.\right. \\
&\quad \left.\left. - (m-n)^\wp(m-n+2+2\wp)\right] - \frac{h^\wp\nabla_4(\mathfrak{R}_{n-1},\sigma_{n-1}}{\Gamma(\wp+2)}\left[(m+1-n)^{\wp+1} - (m-n)^\wp(m-n+1+\wp)\right]\right\} + E^\wp_{4,m}, \\
\mathcal{H}_{m+1} &= \mathcal{H}_0 + \frac{1-\wp}{\mathbb{M}(\wp)}\nabla_5(\mathcal{H}(\sigma_m),\sigma_m) + \frac{\wp}{\mathbb{M}(\wp)}\sum_{n=0}^{m}\left\{\frac{h^\wp\nabla_5(\mathcal{H}_n,\sigma_n)}{\Gamma(\wp+2)}\left[(m+1-n)^\wp(m-n+2+\wp)\right.\right. \\
&\quad \left.\left. - (m-n)^\wp(m-n+2+2\wp)\right] - \frac{h^\wp\nabla_5(\mathcal{H}_{n-1},\sigma_{n-1}}{\Gamma(\wp+2)}\left[(m+1-n)^{\wp+1} - (m-n)^\wp(m-n+1+\wp)\right]\right\} + E^\wp_{5,m},
\end{aligned}
\tag{27}
$$

where

$$
\begin{aligned}
\nabla_1 &= \Pi\Lambda - \frac{\gamma\Omega(\sigma)\mathcal{J}^a(\sigma)}{N} + \lambda\mathcal{H}(\sigma) - (\delta+\mu)\,\Omega(\sigma), \\
\nabla_2 &= \frac{\gamma\Omega(\sigma)\mathcal{J}^a(\sigma)}{N} - (\mu+\alpha+\kappa)\,\mathcal{J}^a(\sigma), \\
\nabla_3 &= \kappa\mathcal{J}^a(\sigma) - (\mu+\rho+\eta)\,\mathcal{J}^c(\sigma), \\
\nabla_4 &= \alpha\mathcal{J}^a(\sigma) + \eta\mathcal{J}^c(\sigma) - \mu\mathfrak{R}(\sigma), \\
\nabla_5 &= \Lambda(1-\Pi) + \delta\Omega(\sigma) - (\lambda+\mu)\,\mathcal{H}(\sigma),
\end{aligned}
$$

and $E^\wp_{1,m}$, $E^\wp_{2,m}$, $E^\wp_{3,m}$, $E^\wp_{4,m}$, $E^\wp_{5,m}$ are of the form of $E^\wp_m$ given in (7).

5 Numerical simulations

In order to make our obtained results more understandable, we continue with some approximations, such as simulations of the system (2). By the values of all of the parameters in a biologically possible manner given in table 1 and to perform simulations to study the qualitative analysis of deterministic and fractional stability, it is necessary to assign values to all parameters of model (2).

Parameters	Value	Source
Λ	0.8	estimated
μ	0.03	estimated
ρ	0.005	estimated
γ	0.05	estimated
α	0.03	estimated
η	0.07	estimated
κ	0.009	estimated
λ	0.07	estimated
δ	0.07	estimated
Π	0.04	estimated
$S(0)$	100	estimated
$\mathcal{J}^a(0)$	10	estimated
$\mathcal{J}^c(0)$	70	estimated
$\mathfrak{R}(0)$	60	estimated
$\mathcal{H}(0)$	50	estimated

Table 1. Parameters values

Our simulation has been performed by applying a newly introduced numerical scheme for the approximation of ABC fractional derivative to model (1). Further, the parameters from Table 1 can be used. Time ranges from $[0 - 20]$ and the initial population for the compartment susceptible class $\Omega(\sigma)$, acutely infected class $\mathcal{J}^a(\sigma)$, chronically carrier class $\mathcal{J}^c(\sigma)$, recovery class $\mathfrak{R}(\sigma)$, and immunized class $\mathcal{H}(\sigma)$ have been chosen from Table 1 as well. Figures 1,2 and 3 illustrate the simulation of several compartments in the proposed model as a result of applying the previously given data. Figures 2(a)–2(e) represent the comparison of model (2) and (1), and Figures 1(a)–1(e) represent the comparison of the (2) and (1), when $\wp = 1.0$. Secondly, we apply iterative approaches developed from (27) to simulate the model (2) under the ABC non-integer order operator. All of the compartments ($\Omega(\sigma)$, $\mathcal{J}^a(\sigma)$, $\mathcal{J}^c(\sigma)$, $\mathfrak{R}(\sigma)$, $\mathcal{H}(\sigma)$) of the said fractional order system were plotted for the table 1 parameters for various arbitrary order values as $\wp = 1.0, 0.95, 0.90, 0.85$. Non-integer order operators of the ABC type have been used. According to these figures 2(a)–2(e), we can see the dynamic behavior of several compartments of the system (2). At first, the decay in the susceptible class is pretty rapid, but subsequently becomes stable with time. Similarly, infection cases decayed at various fractional orders of $\wp$. The recovery achieves their maximum at this point. The graphical findings show that the proposed model is dependent on the fractional order $\wp$ and provides more flexible data about the behavior of the model that cannot be achieved with the classic integer-order model.

(a) $\Omega-$Susceptible population

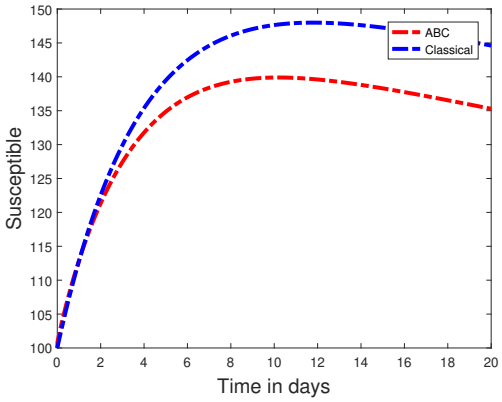

(b) $\mathcal{J}^a-$Acutely infected population

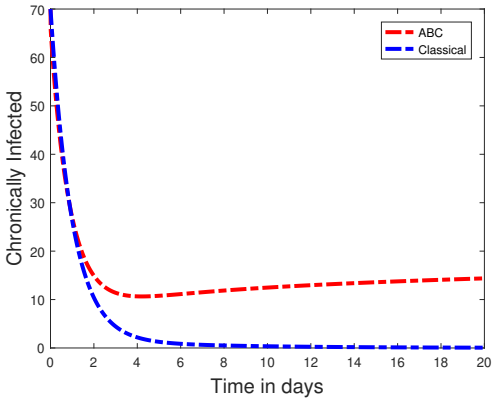

(c) $\mathcal{J}^c-$Chronically infected population

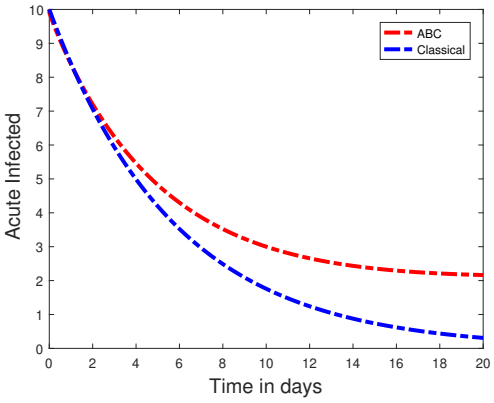

(d) $\mathfrak{R}-$Recovered population

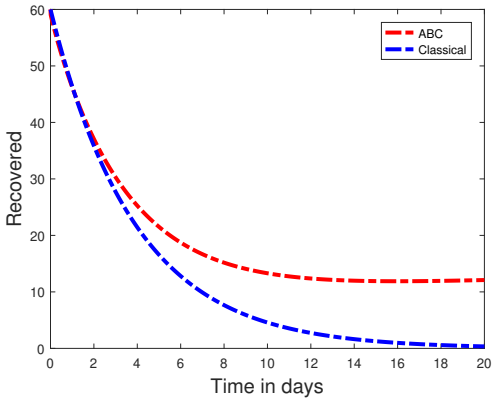

(e) $\mathcal{H}-$Vaccinated population

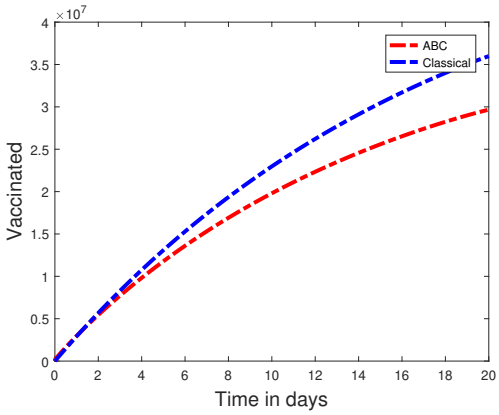

Figure 1. Simulations of susceptible, acute infections, chronic carriers, recovered and vaccinated individuals of model (1), when $\wp = 0.90$.

(a) Ω–Susceptible population

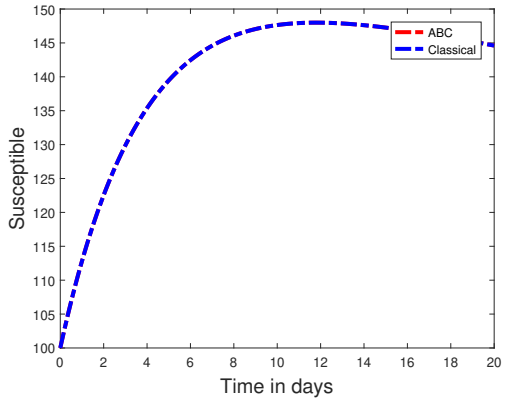

(b) $\mathcal{J}^a$–Acutely infected population

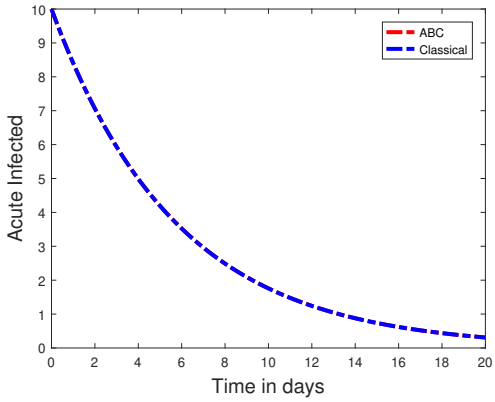

(c) $\mathcal{J}^c$–Chronically infected population

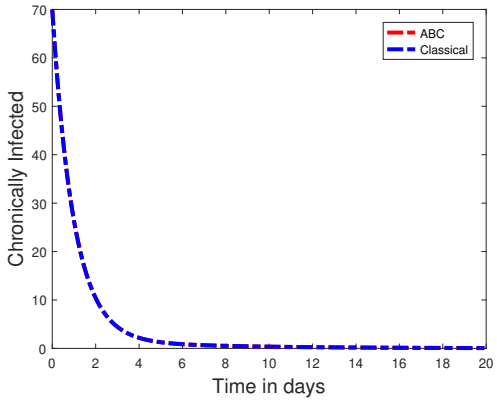

(d) $\mathfrak{R}$–Recovered population

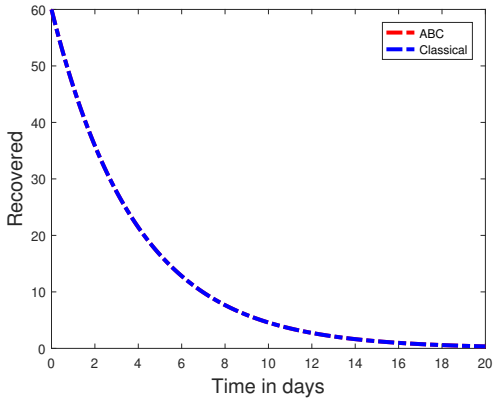

(e) $\mathcal{H}$–Vaccinated population

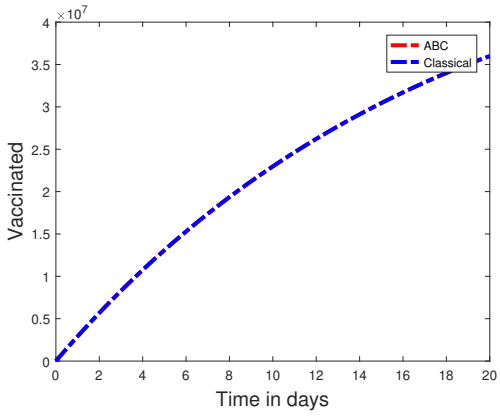

Figure 2. Simulations of susceptible, acute infections, chronic carriers, recovered and vaccinated individuals of model (2), when $\wp = 1$.

(a) $\Omega-$Susceptible population

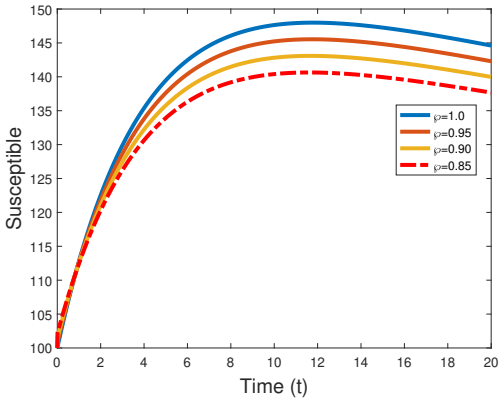

(b) [$\mathcal{J}^a-$Acutely infected population

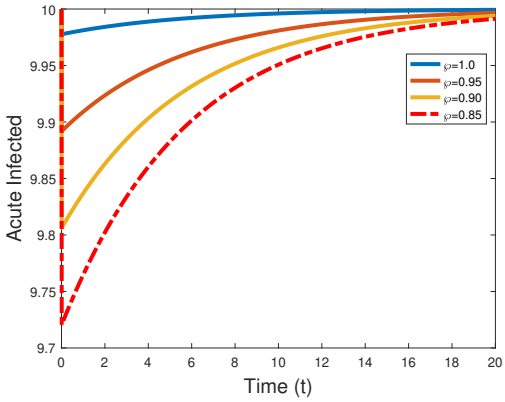

(c) $\mathcal{J}^c-$Chronically infected population

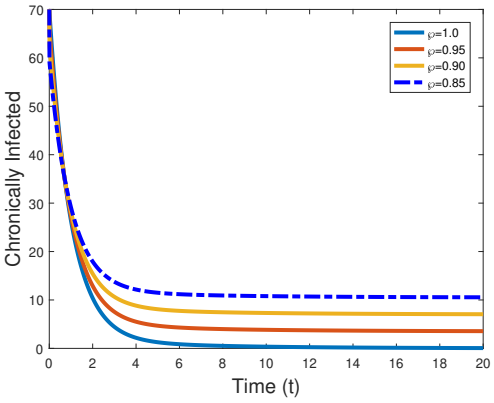

(d) $\mathfrak{R}-$Recovered population

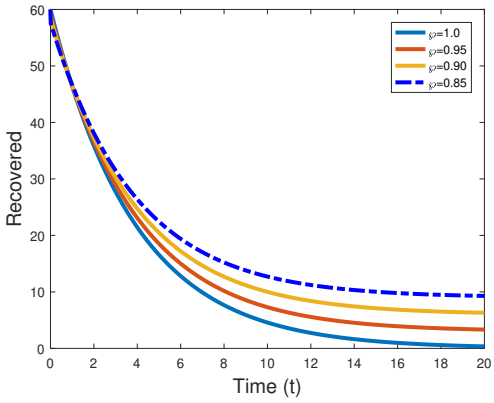

(e) $\mathcal{H}-$Vaccinated population

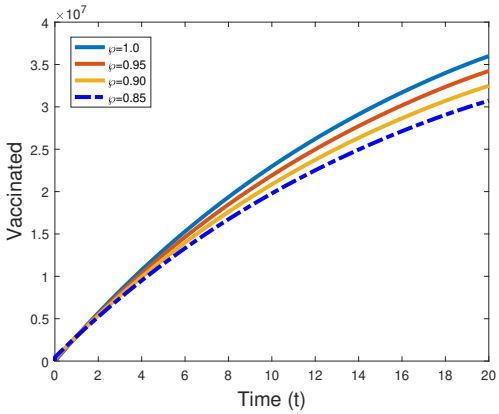

Figure 3. Simulations of susceptible, acute infections, chronic carriers, recovered and vaccinated individuals of model (2) when $\wp$ = (1.0, 0.95, 0.90, 0.85).

6 Conclusions

In the end we concluded that the proposed fractional system describing the vaccinated Hepatitis-B behaviors has been studied qualitatively using the contraction theorems of closed norm space. This investigation is taken under non-singular kernel related to the ABC fractional order derivative. By disease free equilibrium points, the proposed system also has been studied for existence, uniqueness, and stability. With the use of a newly defined numerical technique, a numerical simulation has been made for the approximation of ABC fractional derivative at different fractional orders. Such type of techniques can also can also be achieved by other different fractional operators like He's derivative. Taking the initial populations bigger than zero for $t > 0$ we have simulated the compartment of the proposed model. Moreover, we can declare that the result properly satisfying the initial data when the proposed system's right hand side approaches to zero under certain conditions. We can also control the epidemic by taking the optimal control strategy and with suitable variable or a parameter to minimised the infected class like unscreened blood, the reuse of dental and surgical instruments, etc. As seen in the graphs, the fractional derivative gives a more accurate and flexible data for investigating the complexity of the dynamics of the HBV model, see Figures 1–3.

Declarations

Consent for publication

Not applicable.

Conflicts of interest

The authors declare that they have no conflict of interests.

Funding

Not applicable.

Author's contributions

A.D.: Conceptualization, Methodology, Software, Data Curation, Investigation, Writing-Original draft. M.Z.A.: Conceptualization, Methodology, Supervision, Investigation. All authors discussed the results and contributed to the final manuscript.

Acknowledgements

Not applicable.

References

[1] Wang, L., Liu, Z., & Zhang, X. Global dynamics of an SVEIR epidemic model with distributed delay and nonlinear incidence. *Applied Mathematics and Computation*, 284, 47–65, (2016). [CrossRef]
[2] Din, A., & Li, Y. Mathematical analysis of a new nonlinear stochastic hepatitis B epidemic model with vaccination effect and a case study. *The European Physical Journal Plus*, 137(5), 1-24, (2022). [CrossRef]
[3] Veeresha, P. A numerical approach to the coupled atmospheric ocean model using a fractional operator. *Mathematical Modelling and Numerical Simulation with Applications*, 1(1), 1-10, (2021). [CrossRef]
[4] Din, A., & Li, Y. Lévy noise impact on a stochastic hepatitis B epidemic model under real statistical data and its fractal–fractional Atangana–Baleanu order model. *Physica Scripta*, 96(12), 124008, (2021). [CrossRef]
[5] Duan, X., Yuan, S., & Li, X. Global stability of an SVIR model with age of vaccination. *Applied Mathematics and Computation*, 226, 528–540, (2014). [CrossRef]
[6] Din, A., Li, Y., & Liu, Q. Viral dynamics and control of hepatitis B virus (HBV) using an epidemic model. *Alexandria Engineering Journal*, 59(2), 667-679, (2020). [CrossRef]
[7] Poland, G.A., & Jacobson, R.M. Prevention of hepatitis B with the hepatitis B vaccine. *New England Journal of Medicine*, 351(27), 2832-2838, (2004). [CrossRef]
[8] McAleer, W.J., Buynak, E.B., Maigetter, R.Z., Wampler, D.E., Miller, W.J., & Hilleman, M.R. Human hepatitis B vaccine from recombinant yeast. *Nature*, 307(5947), 178-180, (1984). [CrossRef]
[9] Din, A., & Li, Y. Stationary distribution extinction and optimal control for the stochastic hepatitis B epidemic model with partial immunity. *Physica Scripta*, 96(7), 074005, (2021). [CrossRef]
[10] Atangana, A. Non validity of index law in fractional calculus: A fractional differential operator with Markovian and non-Markovian properties. *Physica A: Statistical Mechanics and its Applications*, 505, 688-706, (2018). [CrossRef]
[11] Veeresha, P., Prakasha, D.G., & Baleanu, D. An efficient technique for fractional coupled system arisen in magnetothermoelasticity with rotation using Mittag–Leffler kernel. *Journal of Computational and Nonlinear Dynamics*, 16(1), (2021). [CrossRef]
[12] Hammouch, Z., Yavuz, M., & Özdemir, N. Numerical solutions and synchronization of a variable-order fractional chaotic system. *Mathematical Modelling and Numerical Simulation with Applications*, 1(1), 11-23, (2021). [CrossRef]
[13] Atangana, A., & Baleanu, D. New fractional derivatives with non-local and non-singular kernel: theory and application to heat transfer model. *Thermal Science*, 20(2), 763-769, (2016). [CrossRef]
[14] Jajarmi, A., & Baleanu, D. A new iterative method for the numerical solution of high-order non-linear fractional boundary value problems. *Frontiers in Physics*, 8, 220, (2020). [CrossRef]

[15] Shah, K., Khalil, H., & Khan, R.A. Investigation of positive solution to a coupled system of impulsive boundary value problems for nonlinear fractional order differential equations. *Chaos, Solitons and Fractals*, 77, 240-246, (2015). [CrossRef]
[16] Din, A., Liu, P., & Cui, T. Stochastic stability and optimal control analysis for a tobacco smoking model. *Applied and Computational Mathematics*, 10(6), 163-185, (2021). [CrossRef]
[17] Cui, T., Liu, P., & Din, A. Fractal–fractional and stochastic analysis of norovirus transmission epidemic model with vaccination effects. *Scientific Reports*, 11(1), 1-25, (2021). [CrossRef]
[18] Li, X.P., Din, A., Zeb, A., Kumar, S., & Saeed, T. The impact of Lévy noise on a stochastic and fractal-fractional Atangana–Baleanu order hepatitis B model under real statistical data. *Chaos, Solitons & Fractals*, 154, 111623, (2021). [CrossRef]
[19] Naik, P.A., Yavuz, M., Qureshi, S., Zu, J., & Townley, S. Modeling and analysis of COVID-19 epidemics with treatment in fractional derivatives using real data from Pakistan. *The European Physical Journal Plus*, 135(10), 1-42, (2020). [CrossRef]
[20] Chen, S.B., Soradi-Zeid, S., Jahanshahi, H., Alcaraz, R., Gómez-Aguilar, J.F., Bekiros, S., & Chu, Y.M. Optimal control of time-delay fractional equations via a joint application of radial basis functions and collocation method. *Entropy*, 22(11), 1213, (2020). [CrossRef]
[21] Ikram, R., Khan, A., Zahri, M., Saeed, A., Yavuz, M., & Kumam, P. Extinction and stationary distribution of a stochastic COVID-19 epidemic model with time-delay. *Computers in Biology and Medicine*, 141, 105115, (2022). [CrossRef]
[22] Joshi, H., & Jha, B.K. Chaos of calcium diffusion in Parkinson's infectious disease model and treatment mechanism via Hilfer fractional derivative. *Mathematical Modelling and Numerical Simulation with Applications*, 1(2), 84-94, (2021). [CrossRef]
[23] Din, A., Shah, K., Seadawy, A., Alrabaiah, H., & Baleanu, D. On a new conceptual mathematical model dealing the current novel coronavirus-19 infectious disease. *Results in Physics*, 19, 103510, (2020). [CrossRef]
[24] Gholami, M., Ghaziani, R.K., & Eskandari, Z. Three-dimensional fractional system with the stability condition and chaos control. *Mathematical Modelling and Numerical Simulation with Applications*, 2(1), 41-47, (2022). [CrossRef]
[25] Khan, A., Hussain, G., Inc, M., & Zaman, G. Existence, uniqueness, and stability of fractional hepatitis B epidemic model. *Chaos: An Interdisciplinary Journal of Nonlinear Science*, 30(10), 103104, (2020). [CrossRef]
[26] Atangana, A., Akgül, A., & Owolabi, K.M. Analysis of fractal fractional differential equations. *Alexandria Eng. J*, 59(3), 1117–1134, (2020). [CrossRef]
[27] Kumar, P., & Erturk, V.S. Dynamics of cholera disease by using two recent fractional numerical methods. *Mathematical Modelling and Numerical Simulation with Applications*, 1(2), 102-111, (2021). [CrossRef]
[28] Alzahrani, E.O., & Khan, M.A. Modeling the dynamics of Hepatitis E with optimal control. *Chaos, Solitons & Fractals*, 116, 287-301, (2018). [CrossRef]
[29] Din, A., & Li, Y. The extinction and persistence of a stochastic model of drinking alcohol. *Results in Physics*, 28, 104649, (2021). [CrossRef]
[30] Din, A., Li, Y., & Shah, M.A. The complex dynamics of hepatitis B infected individuals with optimal control. Journal of Systems Science and Complexity, 34(4), 1301-1323, (2021). [CrossRef]
[31] Daşbaşı, B. Stability analysis of an incommensurate fractional-order SIR model. *Mathematical Modelling and Numerical Simulation with Applications*, 1(1), 44-55, (2021). [CrossRef]
[32] Naik, P.A., Eskandari, Z., Yavuz, M., & Zu, J. Complex dynamics of a discrete-time Bazykin-Berezovskaya prey-predator model with a strong Allee effect. *Journal of Computational and Applied Mathematics*, 413, 114401, (2022). [CrossRef]
[33] Özköse, F., Yavuz, M., Şenel, M. T., & Habbireeh, R. Fractional order modelling of omicron SARS-CoV-2 variant containing heart attack effect using real data from the United Kingdom. *Chaos, Solitons & Fractals*, 157, 111954, (2022). [CrossRef]
[34] Rossikhin, Y.A., & Shitikova, M.V. Applications of fractional calculus to dynamic problems of linear and nonlinear hereditary mechanics of solids. *Applied Mechanics Reviews*, 50(1), 15-67, (1997). [CrossRef]
[35] Atangana, A., & Qureshi, S. Modeling attractors of chaotic dynamical systems with fractal–fractional operators. *Chaos, Solitons & Fractals*, 123, 320-337, (2019). [CrossRef]
[36] Özköse, F., & Yavuz, M. Investigation of interactions between COVID-19 and diabetes with hereditary traits using real data: A case study in Turkey. *Computers in Biology and Medicine,* 141, 105044, (2022). [CrossRef]
[37] Jena, R.M., Chakraverty, S., Yavuz, M., & Abdeljawad, T. A new modeling and existence–uniqueness analysis for Babesiosis disease of fractional order. *Modern Physics Letters B*, 35(30), 2150443, (2021). [CrossRef]
[38] Din, A., Khan, A., & Baleanu, D. (2020). Stationary distribution and extinction of stochastic coronavirus (COVID-19) epidemic model. *Chaos, Solitons & Fractals*, 139, 110036, (2020). [CrossRef]
[39] Din, A., Khan, T., Li, Y., Tahir, H., Khan, A., & Khan, W.A. Mathematical analysis of dengue stochastic epidemic model. *Results in Physics*, 20, 103719, (2021). [CrossRef]
[40] Yavuz, M., Coşar, F.Ö., Günay, F., & Özdemir, F.N. A new mathematical modeling of the COVID-19 pandemic including the vaccination campaign. *Open Journal of Modelling and Simulation*, 9(3), 299-321, (2021). [CrossRef]
[41] Allegretti, S., Bulai, I.M., Marino, R., Menandro, M.A., & Parisi, K. Vaccination effect conjoint to fraction of avoided contacts for a Sars-Cov-2 mathematical model. *Mathematical Modelling and Numerical Simulation with Applications*, 1(2), 56-66, (2021). [CrossRef]
[42] Li, X.P., Al Bayatti, H., Din, A., & Zeb, A. A vigorous study of fractional order COVID-19 model via ABC derivatives. *Results in Physics*, 29, 104737, (2021). [CrossRef]
[43] Sene, N. Second-grade fluid with Newtonian heating under Caputo fractional derivative: analytical investigations via Laplace transforms. *Mathematical Modelling and Numerical Simulation with Applications*, 2(1), 13-25, (2022). [CrossRef]
[44] Özköse, F., Şenel, M.T., & Habbireeh, R. Fractional-order mathematical modelling of cancer cells-cancer stem cells-immune system interaction with chemotherapy. *Mathematical Modelling and Numerical Simulation with Applications*, 1(2), 67-83, (2021). [CrossRef]
[45] Din, A., Li, Y., Khan, T., & Zaman, G. Mathematical analysis of spread and control of the novel corona virus (COVID-19) in China. *Chaos, Solitons & Fractals*, 141, 110286, (2020). [CrossRef]
[46] Atangana, A., & Koca, I. Chaos in a simple nonlinear system with Atangana–Baleanu derivatives with fractional order. *Chaos, Solitons & Fractals*, 89, 447-454, (2016). [CrossRef]
[47] Din, A., Li, Y., Khan, T., Anwar, K., & Zaman, G. Stochastic dynamics of hepatitis B epidemics. *Results in Physics*, 20, 103730, (2021). CrossRef]
[48] Atangana, E., & Atangana, A. Facemasks simple but powerful weapons to protect against COVID-19 spread: Can they have sides effects?. *Results in Physics*, 19, 103425, (2020). [CrossRef]

[49] Din, A., & Li, Y. Controlling heroin addiction via age-structured modeling. *Advances in Difference Equations*, 2020(1), 1-17, (2020). [CrossRef]
[50] Atangana, A. Modelling the spread of COVID-19 with new fractal-fractional operators: Can the lockdown save mankind before vaccination?. *Chaos, Solitons & Fractals*, 136, 109860, (2020). [CrossRef]
[51] Owolabi, K.M., Gómez-Aguilar, J.F., & Karaagac, B. Modelling, analysis and simulations of some chaotic systems using derivative with Mittag-Leffler kernel. *Chaos, Solitons & Fractals*, 125, 54-63, (2019). [CrossRef]
[52] Toufik, M., & Atangana, A. New numerical approximation of fractional derivative with non-local and non-singular kernel: application to chaotic models. *The European Physical Journal Plus*, 132(10), 1-16, (2017). [CrossRef]
[53] Owolabi, K.M., & Atangana, A. On the formulation of Adams–Bashforth scheme with Atangana–Baleanu–Caputo fractional derivative to model chaotic problems. *Chaos: An Interdisciplinary Journal of Nonlinear Science*, 29, 023111, (2019). [CrossRef]
[54] Atangana, A., & Owolabi, K.M. New numerical approach for fractional differential equations. *Mathematical Modelling of Natural Phenomena*, 13(1), 3, (2018). [CrossRef]
[55] Atangana, A., & Bonyah, E. Fractional stochastic modeling: new approach to cap ture more heterogeneity. *Chaos: An Interdisciplinary Journal of Nonlinear Science*, 29(1), 013118, (2019). [CrossRef]
[56] Koca, I. Modelling the spread of ebola virus with Atangana–Baleanu fractional operators. *The European Physical Journal Plus*, 133, 100, (2018). [CrossRef]

Mathematical Modelling and Numerical Simulation with Applications (MMNSA) (https://www.mmnsa.org)

Mathematical Modelling and Numerical Simulation with Applications, 2022, 2(2), 73–87

https://www.mmnsa.org
ISSN Online: 2791-8564 / Open Access
https://doi.org/10.53391/mmnsa.2022.007

RESEARCH PAPER

On a new approach to distributions with variable transmuting parameter: The concept and examples with emerging problems

Jordan Hristov[1,*,‡]

[1]Department of Chemical Engineering, University of Chemical Technology and Metallurgy, Sofia, Bulgaria

[*]Corresponding Author
[‡]jordan.hristov@mail.bg or jyh@uctm.edu (Jordan Hristov)

Abstract

A new concept in the transmutation of distribution applying variable transmuting function has been conceived. Test examples with power function by quadratic and cubic transmutations have been demonstrated by the applications of the error-function and standard logistic function variable transmuting functions. The efficiency and properties of the new approach by numerical examples addressing the rate constants of the transmuting functions and the shape parameter of the test power function have been demonstrated. An additional example with a quadratic transmutation of the exponential distribution through the error function as a variable transmuting parameter has been developed.

Key words: Transmutation; variable transmuting parameter; transmuted distributions; power function
AMS 2020 Classification: 62E17; 62P35; 62P99

1 Introduction

Distributions are widely implemented to fit experimental data dominantly in statistical applications. Applications of certain statistical tools are strongly dependent on the used probabilistic models of considered data. The increase in the variety of statistical data that should be fitted (modelled) revealed that many classical distributions are unsatisfactory in statistical data fitting. Hence, there are appeals to create more generalized distributions allowing modeling of more complicated phenomena more flexibly. Motivated by the need to add more parameters to distribution functions thus making them more flexible in data analyzes [1]. In this context, there are several attempts to consider compound distributions [2, 3, 4], exponentiated distributions [5], beta class of distributions [6, 7], generalized exponential distribution [8], weighted distributions [9]. The weighted distributions, for instance, take into consideration the verification method for adjustment probability distributions by introducing weights [10] which to some extent is close to the transmutation method considered in this work.

Here we address a class of weighted distributions developed by the so-called transmutation method [11] which results in a specific class of mixture distributions. In the approach conceived by Shaw and Buckley [11] the generalization of the distributions is achieved by the application of a transmutation map. Precisely, the transmutation map is a functional composition of the cumulative distribution function (cdf) of a certain distribution with the inverse cumulative distribution (quantile) function of another [1]. In statistical publications, there are numerous examples of transmutations of classical distributions such as Weibull distribution [12, 13, 14, 15, 16, 17], power distribution [18], minimax distribution [19], linear exponential distribution [20, 21, 22], Frechet distribution [23], Gumbel distribution [20, 23], Gamma distributions [20], etc.

This article introduces the idea to replace the transmutation parameter with a function (called here also activation function) dependent on the probability variable and varying only in range , as in the case when the transmutation parameter is a discrete value and resulting in a

➤ **Received:** 29.04.2022 ➤ **Revised:** 15.06.2022 ➤ **Accepted:** 17.06.2022 ➤ **Published:** 19.06.2022

specific class of mixture distributions. For a better understanding of the main idea of the transmutations, the technique is explained in the next section (Background) from a general point of view and with two simple examples further used in this work.

2 Background

The increasing number applications fitting real-world data, from life science, economics or advanced technologies, are raising problems for more flexibility which some of statistical distributions cannot provide adequate answers. Particularly, to capture the skewness and kurtosis (see the definitions in Appendix (Section 10) associate with such applications it was introduced a transmutation mapping [11]. This map is *a functional composition of a cumulative distribution function* (*cdf*) *of a particular distribution with the inverse cumulative distribution (quantile) of another distribution* [1]. This approach increases the distribution flexibility to fit experimental data. The common approach is to use *discrete values of the transmuting parameters* (commonly denoted by the symbol λ) [1, 11, 16, 21, 22, 24, 25, 26, 27, 28, 29]. This work addresses transmutations of statistical distributions by variable transmuting parameters, precisely, transmuting parameters dependent on random variables. For the sake of clarity, and creating the exposition gradually understandable, as well as to present the new approach we will start with some basic definitions explained next.

Theory of distribution transmutations

If there are absolutely *continuous cumulative distribution functions* (*cdf*s) $F_1(x)$ and $F_2(x)$ with the corresponding *pdf*s $f_1(x)$ and $f_2(x)$, on a common sample space, then the general rank of transmutation, following Shaw and Buckley [11], is formulated as

$$G_{R_{12}}(u) = F_2\left[F_1^{-1}(u)\right], \quad G_{R_{21}}(u) = F_1\left[F_2^{-1}(u)\right], \tag{1}$$

where both functions $G_{R_{12}}(u)$ and $G_{R_{21}}(u)$ map the compact $[0,1]$ into itself as well as they are mutually inverse with $G_{R_{ij}}(0) = 0$ and $G_{R_{ij}}(1) = 1$ when $i = 1, 2$.
In accordance with the definition of [11] a random variable x has a transmuted distribution of family of rank k if the cumulative distribution function (*cdf*) is defined in a general form as [11, 16, 24, 21]

$$F(x) = G(x) + [1 - G(x)] \sum_{i=1}^{k} \lambda_i [G(x)]^i, \tag{2}$$

with $\lambda_i \in [-1, 1]$ for $i = 1, 2, 3, \ldots, k$ and $-k \leq \sum_{i=1}^{k} \lambda_i < 1$.
The general transmuted family reduces to the base function (base cumulative distribution) (*cdf*) $G(x)$ for $\lambda_i = 0$. Two simple transmutations, undoubtedly explaining the idea of this mapping, and used in this work, are briefly presented next.

Transmutations of quadratic and cubic ranks: Examples

Before demonstrating simple examples we have to stress the attention on two important issues in applications of the transmutation approach, namely

- When the task is to demonstrate how the transmutation of certain rank transforms the base function (distribution) then the choice of the *transmuting parameter* λ (can be termed also as *activating parameter*) is to some extent arbitrary, with discrete values, from $\lambda \in [-1, 1]$, as it will be done in the following examples. This can be considered as a *forward problem*.That is, in the forward problem a given value of λ activates (results in) a particular shifted distribution.

- When a certain transmuted version of base function (distribution) has to be applied in fitting procedure to a given set of statistical data, then the determination of λ is a task related to an inverse problem. That is, in such a case the problem is to find particular value of λ so that the transmuted distribution to fit the statical data. This can be considered as a *backward problem*. This step is beyond the scope of this work, because the primary task addressed here is to demonstrate how the new approach in generation of transmuted distributions works.

It is worth noting that, in both cases, the tasks are performed with discrete values of the transmuting parameter λ as it follows from the basic formulation of Shaw and Buckley [11].
Here, for the seek of the clarity of the method applied and its development conceived in this work, we give demonstrative examples of the two most popular transmutations [11] with particular sets of values of λ chosen arbitrarily from the range $\lambda \in [-1, 1]$ as it has been done in all works cited above.

Quadratic transmutation

For $k = 1$, applying (2), we have a *cdf*

$$F_1(x) = (1 + \lambda) G(x) - \lambda G^2(x), \quad |\lambda| < 1, \tag{3}$$

and a corresponding *pdf* $f_1(x) = \frac{d}{dx} F_1(x)$

$$f_1(x) = (1 + \lambda) g(x) - 2\lambda g(x) G(x), \quad g(x) = \frac{dG(x)}{dx}. \tag{4}$$

It is obvious that for $\lambda = 0$ the transmuted function $F_1(x)$ reduces to $G(x)$. To illustrate this, we present examples of quadratic transmutations of the power function (distribution) (Eqs. (5) and (6)), with a shape parameter α and cumulative density function (*cdf*) [18]

$$G(x) = 1 - (1-x)^{\alpha}, \quad 0 < x < 1, \quad \alpha > 0, \tag{5}$$

and corresponding probability density function (*pdf*)

$$g(x) = \alpha(1-x)^{\alpha-1}, \quad 0 < x < 1, \quad \alpha > 0. \tag{6}$$

Applying (3) and (4) to (5), we get

$$F_1 = (1+\lambda)\left[1-(1-x)^{\alpha}\right] - \lambda\left[1-(1-x)^{\alpha}\right]^2, \tag{7}$$

$$f_1 = (1+\lambda)\left[\alpha(1-\alpha)^{\alpha-1}\right] - 2\alpha\left[1-(1-x)^{\alpha}\right]\left[\alpha(1-x)^{\alpha-1}\right]. \tag{8}$$

This function is a special case of beta distribution describing random data confined in the open interval $(0,1)$ [1, 18]. The numerical tests shown in figure 1 demonstrate the variations of the cumulative density function for various values of the transmuting parameter λ as well as the effect of the shape parameter for $\alpha < 1$ and $\alpha > 1$. The changes in both the skewness and kurtosis are obvious.

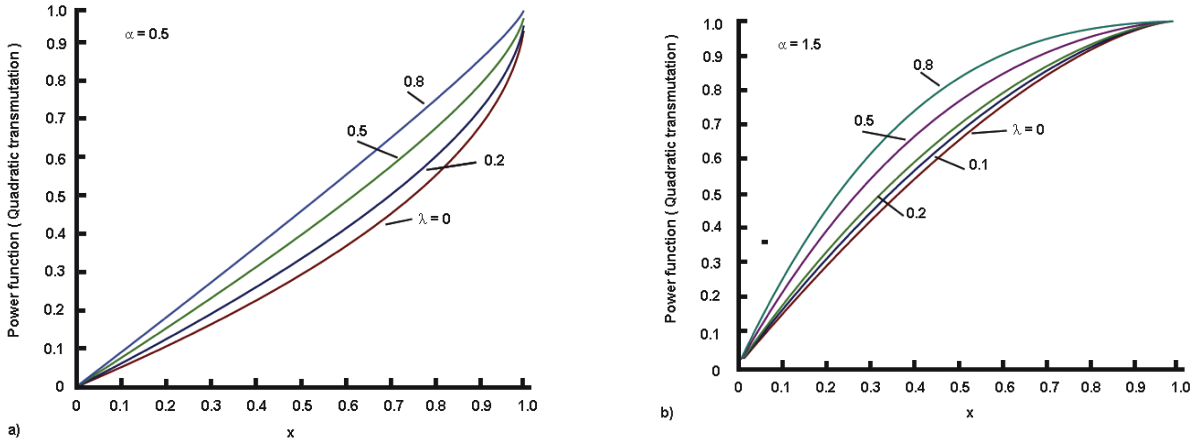

Figure 1. Two cases of quadratic transmuted power function (distribution): a) with $\alpha = 0.5$; b) with $\alpha = 1.5$

Cubic transmutation

For $k = 2$, applying (2), we have a *cdf*

$$F_2(x) = G(x) + \lambda_1 G(x)\left[1-G(x)\right] + \lambda_2 G^2(x)\left[1-G(x)\right]. \tag{9}$$

This can be presented also as

$$F_2(x) = (1+\lambda_1)G(x) + (\lambda_2-\lambda_1)G^2(x) - \lambda_2 G^3(x), \tag{10}$$

and a corresponding *pdf*

$$f_2(x) = (1+\lambda_1)g(x) + 2(\lambda_2-\lambda_1)g(x)G(x) - 3\lambda_2 g(x)G^2(x), \tag{11}$$

where $\lambda_1 \in [-1,1]$ and $\lambda_2 \in [-1,1]$, and $-2 < \lambda_1 + \lambda_2 < 1$. For this specific case, following Granzotto et al. [16], we have $\lambda_1 \in [0,1]$ and $\lambda_2 \in [-1,1]$.

If we try to minimize the number of transmuting parameters, it is possible to suggest that $\lambda_1 = \lambda$ and $\lambda_2 = -\lambda$ where $|\lambda| < 1$. Then, from (10) we get a simpler form of $F_2(x)$, namely

$$\tilde{F}_2(x) = (1+\lambda)G(x) - 2\lambda G^2(x) + \lambda G^3(x), \tag{12}$$

$$\tilde{f}_2(x) = (1+\lambda)g(x) - 4\lambda g(x)G(x) + 3\lambda g(x)G^2(x). \tag{13}$$

In the case with the power distribution (5), we have

$$\bar{F}_2 = (1+\lambda)\left[1-(1-x)^{\alpha}\right] - 2\lambda\left[1-(1-x)^{\alpha}\right]^2 + \lambda\left[1-(1-x)^{\alpha}\right]^3, \tag{14}$$

$$\bar{f}_2 = (1-\lambda)\left[\alpha(1-x)^{\alpha-1}\right] - 4\lambda\left[1-(1-x)^{\alpha}\right]\left[\alpha(1-x)^{\alpha-1}\right] + 3\lambda\left[1-(1-x)^{\alpha}\right]^2\left[\alpha(1-x)^{\alpha-1}\right]. \tag{15}$$

Examples of cubic transmutations of the power function (distribution), the same as used in the tests of the quadratic transmutation, are shown in Figure 2. The effect of the transmutation on the distributions is more obvious since there is a strong effect of the shape parameter α.

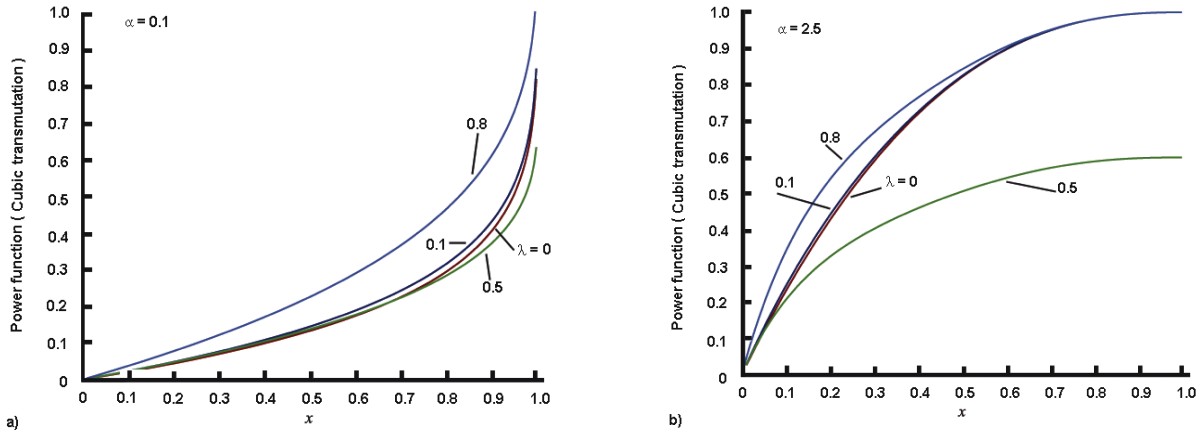

Figure 2. Two cases of cubic transmuted power function: Left- with $\alpha = 0.1$; Right- with $\alpha = 2.5$

There exist many examples of transmuted distributions [1] (see the detailed analysis in this article and references quoted therein) but here we address a different approach rather than selecting values of λ (the case with $k = 1$) or pairs (λ_1, λ_2) when $k = 2$, as it was done in most of the articles cited above. It is worth remarking that for the sake of clarity in the explanation of the idea developed in this article the numerical examples with power function are provided with $\alpha = 0.5$ and $\alpha = 1.5$, but there are no restrictions to demonstrate similar behaviours with different values of the shape parameter α; the effect of the shape parameter on the transmuted distribution in the light of the new concept is beyond the scope of this work.

3 Aim

This article conceives a new approach in transmutation of distributions by applying variable transmuting parameters (activation functions) instead of its particular (discrete) counterparts used in the original concept. To some extent, this leads to new distributions obeying all desired properties of transmuted basic functions. The power function is used as a test distribution with two transmuting (activating) functions: the Gaussian Error-function and the Standard Logistic Function. In fact, this is an experimental work, in sense of experimental mathematics, on the *forward transmuting problem*, when a new idea about transmutation of functions (distributions) is directly demonstrated.

4 Further paper organization

In the sequel the concept of a variable transmuting parameter (Section 5) with two functions as examples: Error Function $erf(x)$ (Section 5) and the Standard Logistic Function $LogF(x)$ (Section 5) is presented. Further, two examples with the application of these continuous transmuting functions (Section 6) to the power function distribution demonstrate all features and problems emerging in application of this new approach.

5 Variable transmuting parameter: The concept

Now, we have to stress the attention on the fact that *there is no rule for choice of the value of the transmuting parameter* λ, *when the forward problem is at issue*, despite the restriction $\lambda \in [-1, 1]$ as the references [11, 16, 21, 24] (and see the references therein) widely used to obtain new distributions in statistics. Only, by selections of pairs λ_1, λ_2 it is possible to get a variety of transmuted functions [1, 11, 16, 20, 21, 22, 24, 25, 26, 27, 28, 29]. One attempt to resolve the problem is the simplification of the cubic transmutation (12) avoiding the use of λ_1 and λ_2. In what follows we conceive the idea that λ can be dependent on the argument of the transmuted function, but at the same time to satisfy the condition $\lambda \in [-1, 1]$, that is

$$\lambda(x) = \Lambda(x), \quad \Lambda(x) \in [-1, 1], \quad x \in (-\infty, \infty). \tag{16}$$

In this context, both the quadratic (17) and cubic (18) transmuted profiles are

$$F_1^{\lambda}(x) = G(x) + \Lambda(x)\left[G(x) - G^2(x)\right], \tag{17}$$

$$F_2^{\lambda}(x) = G(x) + \Lambda(x)\left[G(x) - 2G^2(x) + G^3(x)\right]. \tag{18}$$

Therefore, we have a superposition of the basic function $G(x)$ and a term (functional relationship) deforming the entire transmuted profile (distribution). In such a case the *pdfs* of these transmuted *cdfs* are

$$f_1^{\lambda}(x) = f(x) + L(x)\left[G(x) - G^2(x)\right] + \Lambda(x)\, g(x)\left[1 - 2G(x)\right], \quad L(x) = \frac{d\Lambda(x)}{dx}, \tag{19}$$

$$f_2^{\lambda}(x) = g(x) + L(x)\left[G(x) - 2G^2(x) + G^3(x)\right] + \Lambda(x)\, g(x)\left[1 - 2G(x) + 3G^2(x)\right]. \tag{20}$$

It is important to stress the attention on the requirement coming from the new formulation the function $\Lambda(x)$ to be *smooth and differentiable with respect to x*.

The functional relationship of $\Lambda(x)$

We realize that there exists a variety of such functions defined by (16), but skipping a discussion on this problem which is beyond the scope of the present study, we suggest the following functional relationships:

Error function

In this case, we suggest

$$\Lambda(x) = erf[p \cdot x] = \frac{2}{\sqrt{\pi}}\int_0^x e^{-p^2 \cdot z^2} dz, \quad p > 0, \quad x(-\infty, \infty). \tag{21}$$

This is an *ad hoc* selection of $\Lambda(x)$ where the derivative with respect to x is

$$L(x) = \frac{d\Lambda(x)}{dx} = \frac{2p}{\sqrt{\pi}} e^{-p^2 x^2}. \tag{22}$$

In addition, the integral of $\Lambda(x)$ is

$$\int erf(px)dx = \frac{(px)\, erf(px)}{p} + \frac{1}{p}\frac{e^{-p^2x^2}}{\sqrt{\pi}} + C. \tag{23}$$

The parameter p controls the rate of growth of $\Lambda(x)$ as it is shown in Fig. 3 (left panel). It is obvious that for $p = 1$, we get the basic $erf(x)$, growing rapidly to 1.

Logistic function

Here we select only the standard logistic function along the axis $x \gg 0$, namely

$$V(x) = \frac{1}{1 + e^{-px}}, \quad x \gg 0, \quad p > 0, \quad 0.5 \le V(x) \le 1, \tag{24}$$

with the following basic properties

$$V(x) = \frac{1}{1 + e^{-px}} = \frac{e^{px}}{1 + e^{px}}, \quad \frac{dV(x)}{dx} = \frac{ke^{-px}}{(1 + e^{-px})^2}, \quad \int V(x)dx = \frac{1}{p}\ln\left(1 + e^{px}\right) + C. \tag{25}$$

As in the case of the error function (21) the parameter p controls the rate of growth (see figure 3 (right panel)) There are no restriction using other versions of the logistic function but here the standard version was chosen for its simplicity allowing to demonstrate the main idea of the variable transmuting parameter (function).

6 Distributions with variable transmuting parameter: Demonstrative examples

Example 1: Power distribution with Error-function as a variable activation function

Here, we consider again the power function (5), which allows comparing the new approach in the transmutation with the classical approach (with discrete λ) demonstrated in Section 2.

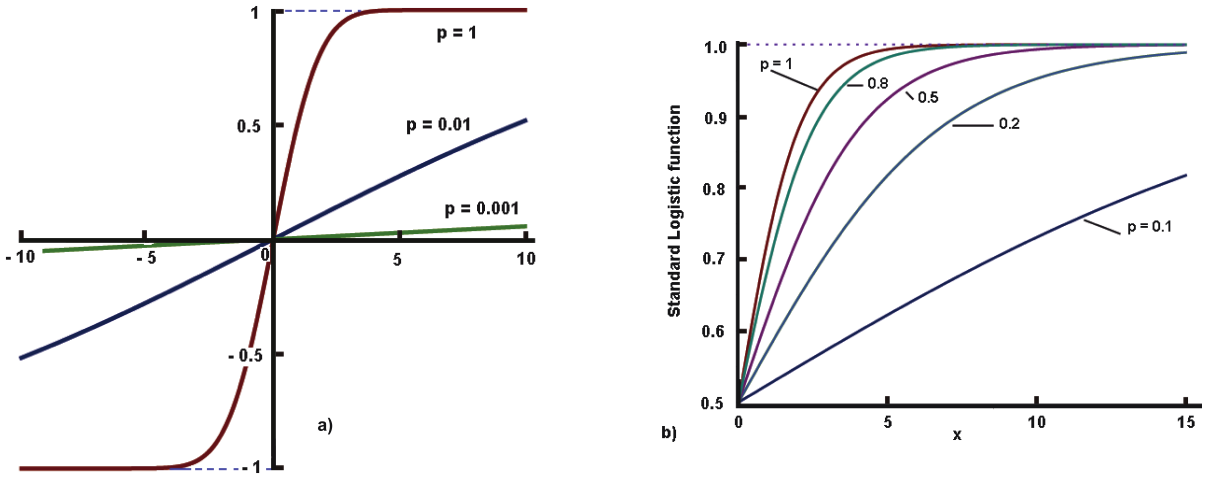

Figure 3. Two examples of variable functions $\Lambda(x)$. Left: Error function (ERF); Right: Standard Logistic function (SLF). The dotted lines show the lower (−1) and the upper (1) limits of variations of the functions (the same in all figures in the sequel).

Quadratic transmutation

Plots of the quadratic transmuted *cfd*s power function are shown in Figure 4. The behaviours of the transmuted functions reveal that in general the character of the effect of the transmuting parameter on the skewness and kurtosis resembles the effects of the discrete values of λ.

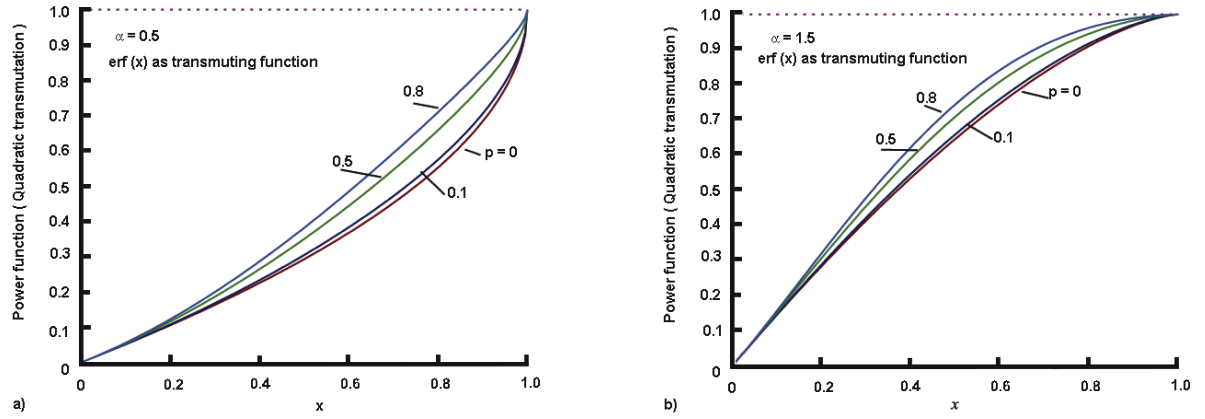

Figure 4. Two examples of variable functions $\Lambda(x)$ to the quadratic transmuted power function. Left: $\alpha = 0.5$; Right: $\alpha = 1.5$. See the plots in Fig. 1

The corresponding *pdf*s are shown in Figures 5a-5b.

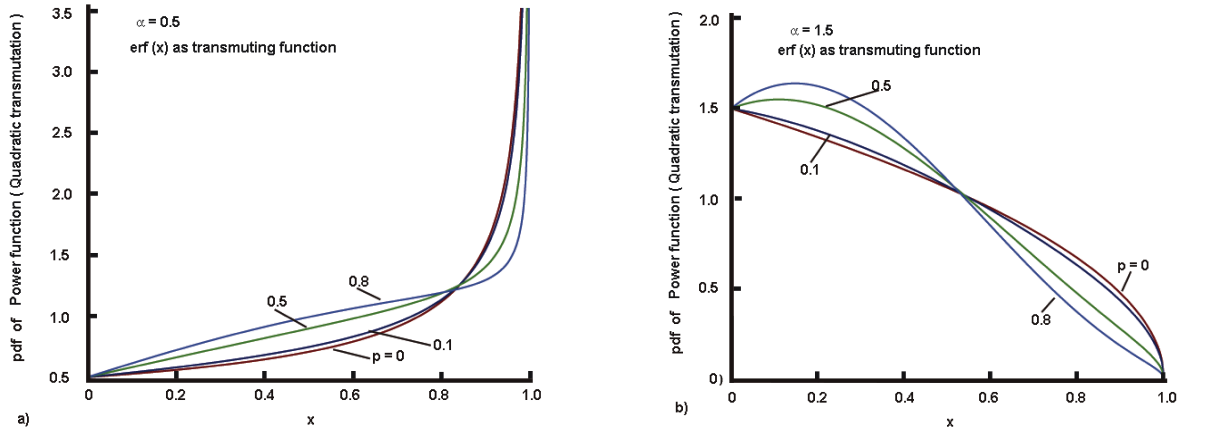

Figure 5. Two examples of *pdf*s with variable functions $\Lambda(x) = erf(x)$ to the quadratic transmuted power function. Left: $\alpha = 0.5$; Right: $\alpha = 1.5$.

Cubic transmutation

The cubic transmuted profiles ($k = 2$) in Figure 6 have almost the same behaviour as the quadratic counterparts ($k = 1$) but now they are located too close and the effect on the skewness and kurtosis is not so distinguished as in the case with $k = 1$. Only in the central zone, we can see some differences (see the inserts).

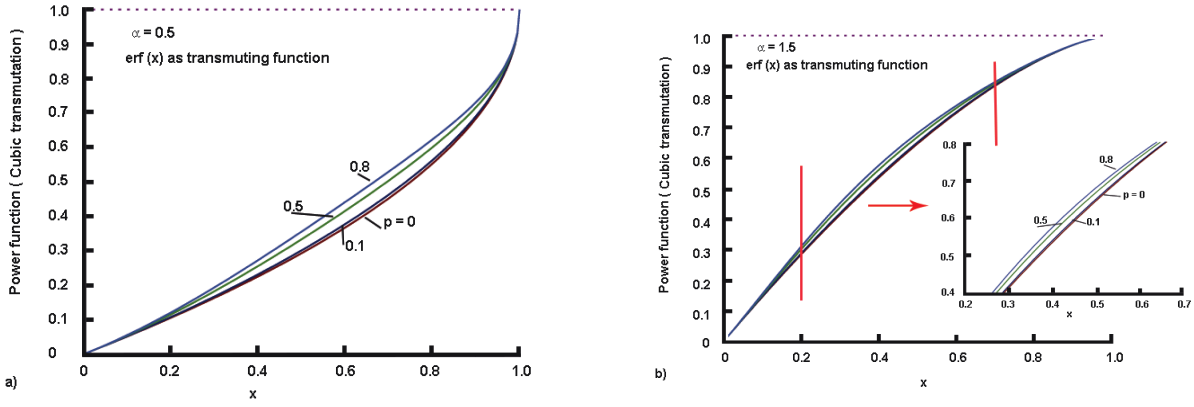

Figure 6. Two examples of variable functions $\Lambda(x)$ to the cubic transmuted power function. Left: $\alpha = 0.5$; Right: $\alpha = 1.5$

The corresponding *pdf*s are shown in Figures 7a-7b.

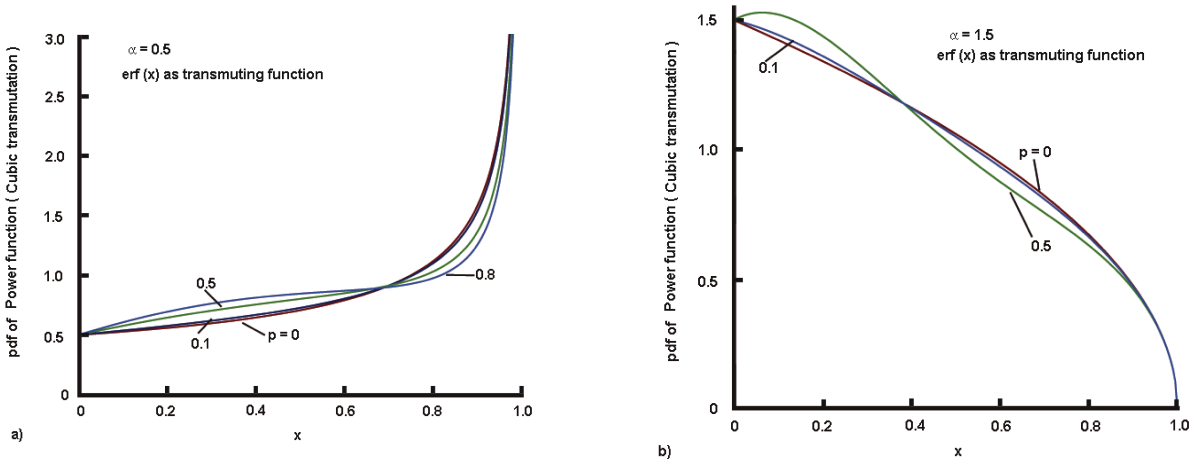

Figure 7. Two examples of *pdf*s with variable functions $\Lambda(x)$ to the cubic transmuted power function. Left: $\alpha = 0.5$; Right: $\alpha = 1.5$.

Reliability analysis: Survival and Hazard functions of transmuted distributions

The survival function $S_k(x)$ of $F_k(x)$ is the probability of an item not falling prior to a given x and is defined as

$$S_k(x) = 1 - F_k(x), \tag{26}$$

and the Hazard function $H_k(x)$ is given by

$$H(x) = \frac{f_k(x)}{S_k(x)}. \tag{27}$$

These functions, related to quadratic transmutation at issue, are shown in Fig. 8.

Example 2: Power function with standard logistic function as a variable transmuting parameter

Quadratic transmutation

The quadratic transmuted profiles of the power function, with different shape parameters, are shown in Figure 9. It is obvious that in both cases, with respect to the values of the shape parameter α) there are sufficient shifts in the distributions with respect to the basic version when $\lambda = 0$. The shifts are towards the case with $\lambda \to 1$. The corresponding **pdf**s, shown in Figure 10 reveal more distinguishable plots but

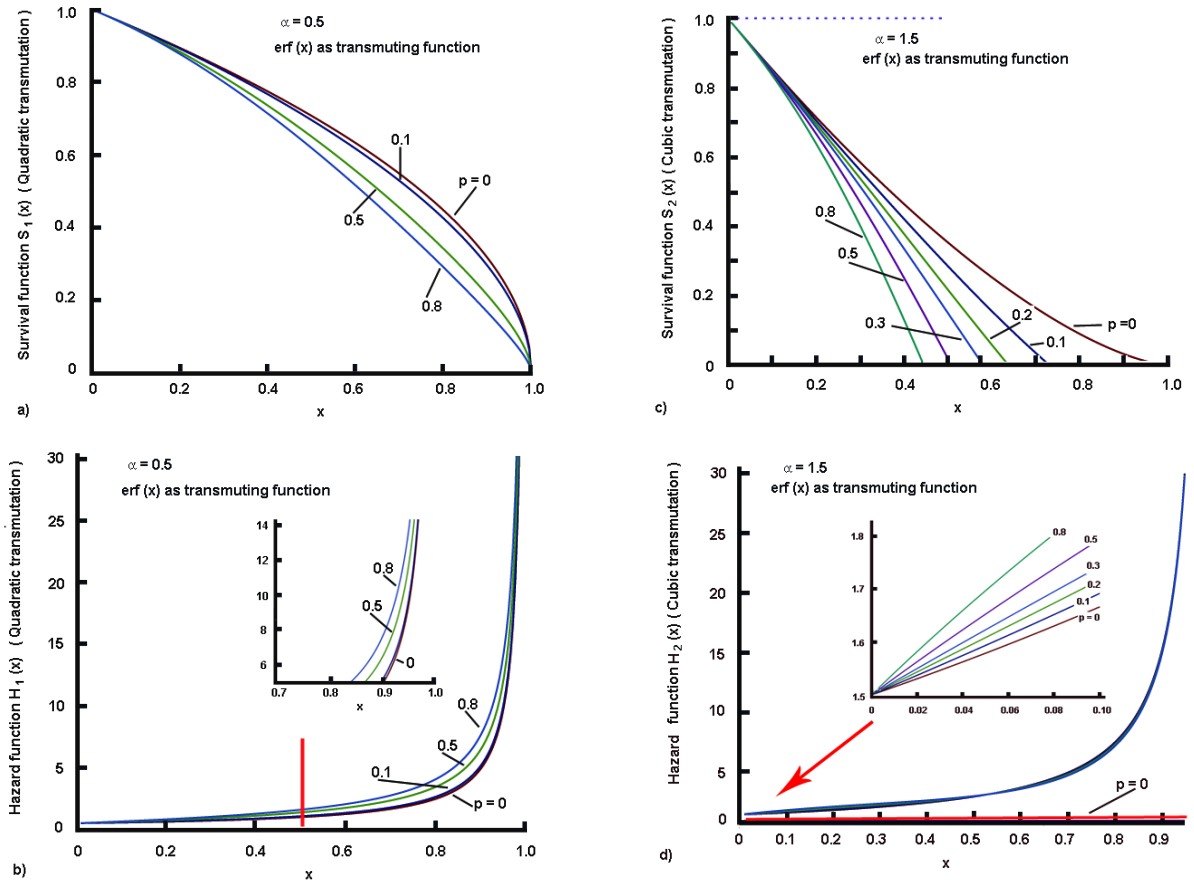

Figure 8. Survival and Hazard function with $erf(x)$ as transmutation parameter. Left column: Quadratic transmutation; Right column: Cubic transmutation

the shifts are again towards the case corresponding to $\lambda \to 1$.

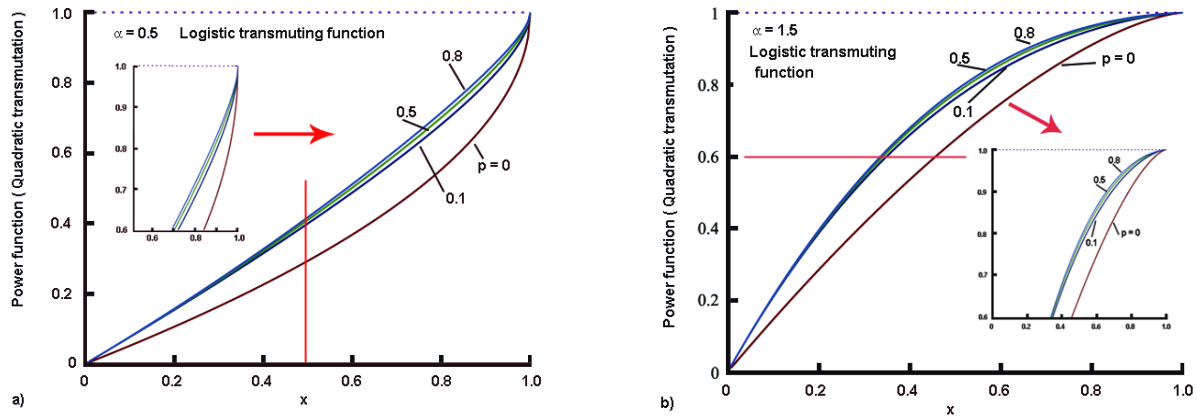

Figure 9. Two examples of distributions with variable function $V(x)$ (Standard Logistic Function) to the quadratic transmuted power function. Left: $\alpha = 0.5$; Right: $\alpha = 1.5$

Cubic transmutation

The cubic transmuted profiles ($k = 2$) of the cumulative power distribution in figure 11 have almost the same behaviour as the quadratic counterparts ($k = 1$) but now they are located too close and the effect on the the skewness and kurtosis is not so distinguished as in the case with $k = 1$. Only in the central zone, we can see some differences (see the insert).

Reliability analysis: Survival and Hazard functions of transmuted distributions

The survival function $S_k(x)$ of F_k and Hazard function $H_k(x)$ are shown in Figures 12 and 13.

We can see again that the effect of the cubic transmutation with the standard logistic function as transmuting function is practically negligible in contrast to the case when the error function is used.

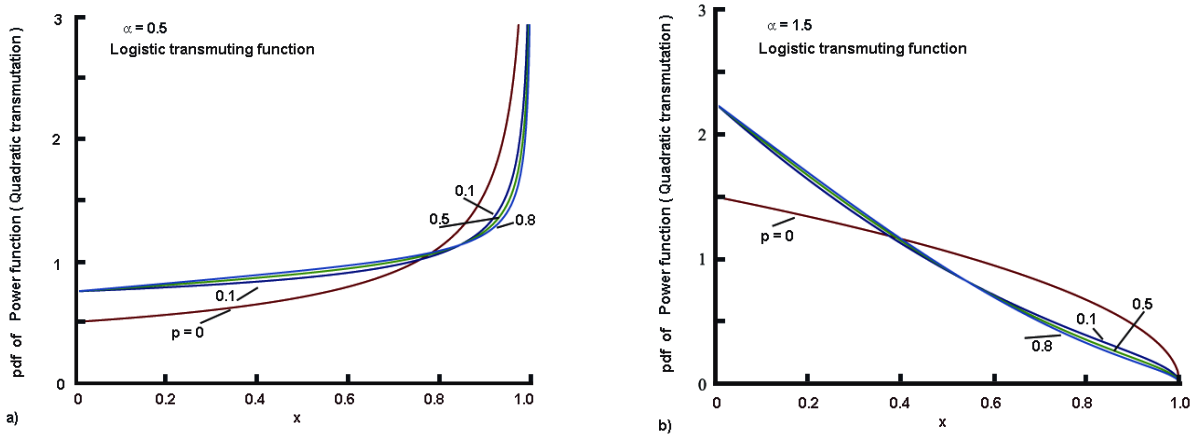

Figure 10. Two examples of *pdf*s with variable function $V(x)$ (Standard Logistic Function) to the quadratic transmuted power function. Left: $\alpha = 0.5$; Right: $\alpha = 1.5$

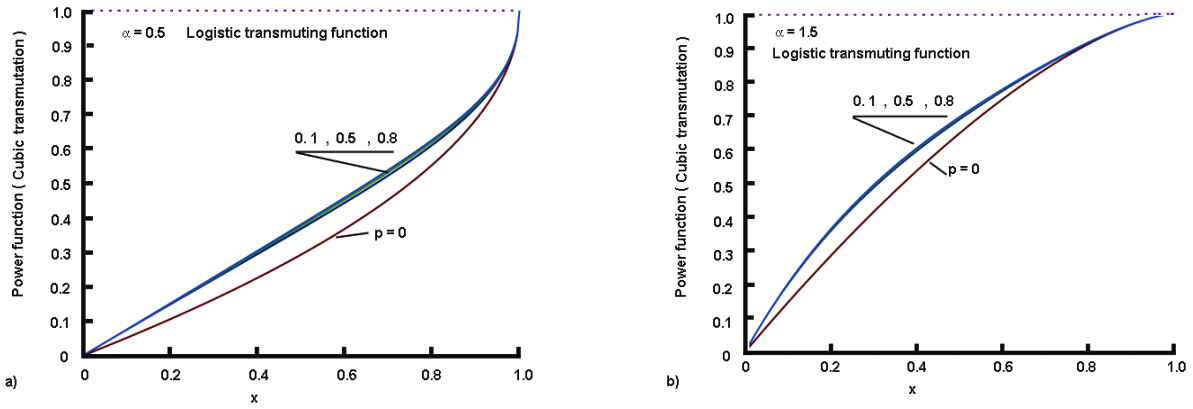

Figure 11. Two examples of *pdf*s with variable function $V(x)$ (Standard Logistic Function) to the cubic transmuted power function. Left: $\alpha = 0.5$; Right: $\alpha = 1.5$

Some briefs on the examples demonstrating the new concept

The idea developed here results in a new type of distribution which to a greater extent are similar to the mixed distribution [30, 31, 32], where the constructions of the cumulative distributions $C(x)$ as a combination of distribution functions $G_i(x)$ follow the rule [32, 33]

$$C(x) = \sum_{i=1}^{N} \omega_i G_i(x), \tag{28}$$

where $\omega_i > 0$ are mixture weights obeying the condition $\sum_{i=1}^{N} \omega_i = 1$. Moreover, it is not necessary that $G_i(x)$ belong to one and the same distribution family on have the same number of parameters [32, 33].
In the idea developed here, even though this aspect is not developed and draws future research. Moreover, this approach, to some extent, resembles the idea of transmutation (2) but bears in mind the significant differences between the two approaches. We have to stress the attention on the fact that in the approach developed here the weighting coefficients follow two main conditions: $\lambda \in [-1, 1]$ coming from the constructions of the transmutation theory, and they are dependent on the variable x , but their variations are within the range $[-1, 1]$. The numerical experiments reveal two basic issues, based on the experiments performed with the power function as a test distribution, namely:

- The quadratic transmutation provides more distinguishable distributions with both the error function and the standard logistic function as transmuting variable parameters.
- The increase in the transmutation rank, i.e. the application of the cubic transmutation, does not lead to significant changes in either the skewness or kurtosis of the new distributions. The shape parameter of the basic distribution has practically no effect on this.
- The error function is more suitable, as a variable transmuting parameter, than the standard logistic function, irrespective of the rank of transmutation, since it is allowing more distinguished new distributions to be generated.

These are comments relevant to the particular case of transmutations of the power functions. Some effects are strong and distinguishable, others not, to some extent. This cannot be considered discouraging because the next example will show how the new approach can be applied to another distribution.

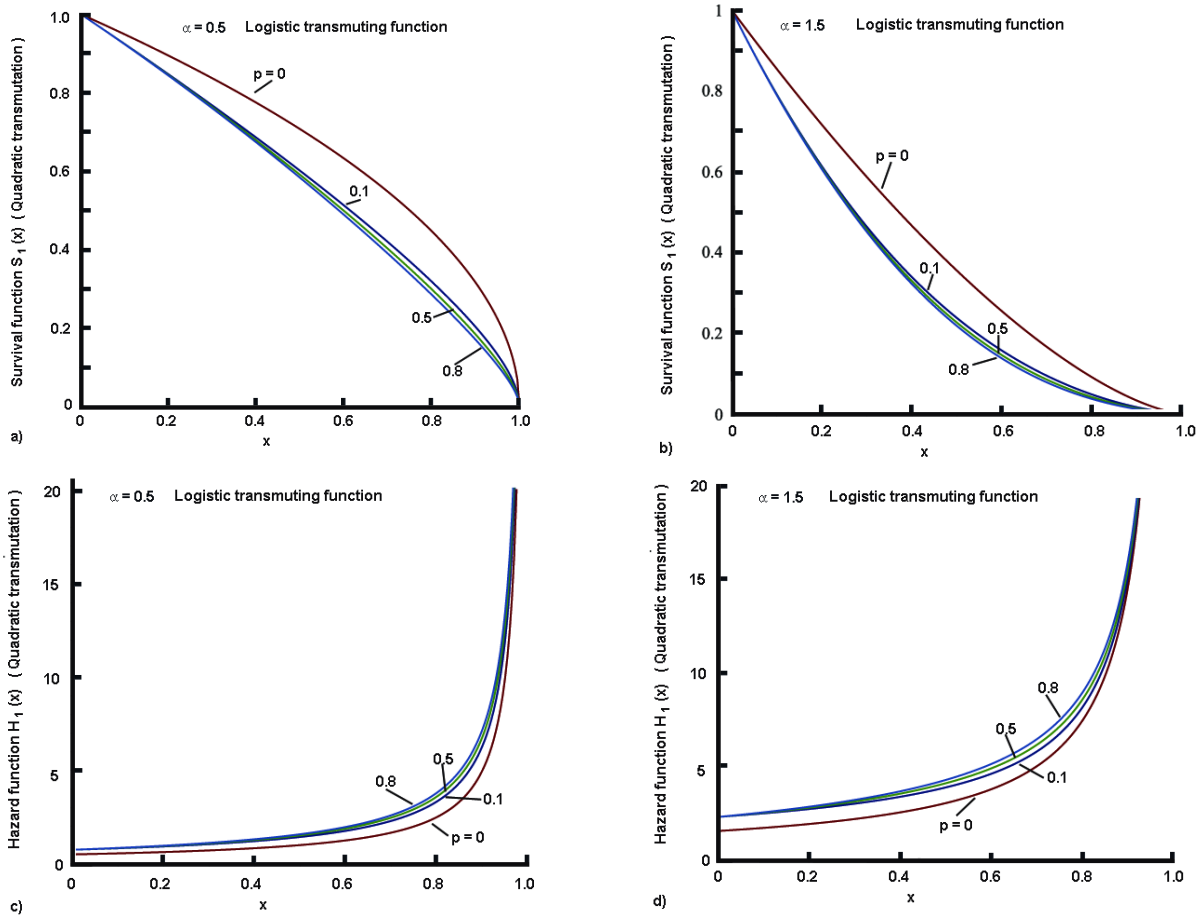

Figure 12. Survival and Hazard function with Standard Logistic Function as a variable transmutation parameter.Quadratic transmutations. Left column: $\alpha = 0.5$; Right column: $\alpha = 1.5$

7 Distributions with variable transmuting parameter: Additional example with the exponential distribution

Here we demonstrate how the quadratic transmutation, with error-function as transmuting parameter, can be applied to the exponential distribution [20, 22, 34]

$$G_{e1}(x) = 1 - \exp\left(-\frac{x}{\beta}\right), \quad x \in [0, \infty), \quad \lambda \in [0, 1], \tag{29}$$

with a quadratic transmuted *cdf*

$$F_{e1} = \left[1 - \exp\left(-\frac{x}{\beta}\right)\right]\left[1 + \lambda \exp\left(-\frac{x}{\beta}\right)\right]. \tag{30}$$

The effect of the rate parameter β on the development of the exponential distribution is shown in Figure 14. The effect of the *scale parameter* β, which may be termed as a *rate constant* of the exponential growth is stronger when $\beta < 1$ since we have $1/\beta \gg 1$ resulting in rapid saturation of the distribution. In contrast, for $\beta > 1$, the distributions are smoother. The following examples use $\beta = 0.5$ and $\beta = 1.5$, similar to the values of the shape parameter α of the power function. Moreover, $\beta = 1.5$ is used in the study of Rahman et al. [20] that allows comparing the results developed by the new approach.

Exponential distribution: Quadratic transmutation with fixed transmuting parameters

Examples of the classical transmutation approach with fixed values of λ are shown in Figure 15, thus demonstrating the effect the scale (rate) parameter β and the values of λ.

Exponential distribution: Quadratic transmutation with Error-function as a variable transmuting parameter

Now, applying the transmutation technology with the variable transmuting parameter we get flexible *cdf* and *pdf* shown in Figure 16. The generated distribution through the quadratic transmutations demonstrated the effect of the transmutation function which, to a greater extent, is similar to that of the discrete transmuting parameters. In contrast to the previous example with the power function, now we can

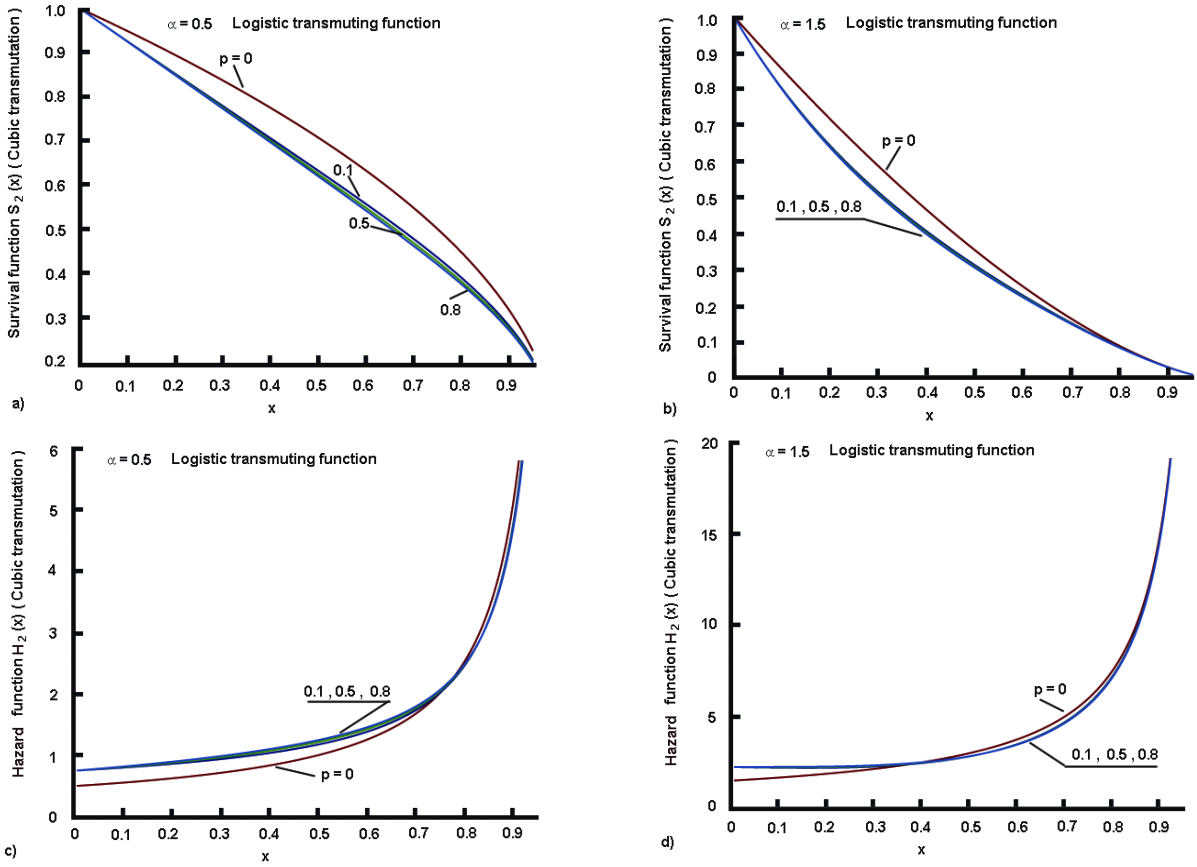

Figure 13. Survival and Hazard function with Standard Logistic Function as a variable transmutation parameter. Cubic transmutations. Left column: $\alpha = 0.5$; Right column: $\alpha = 1.5$

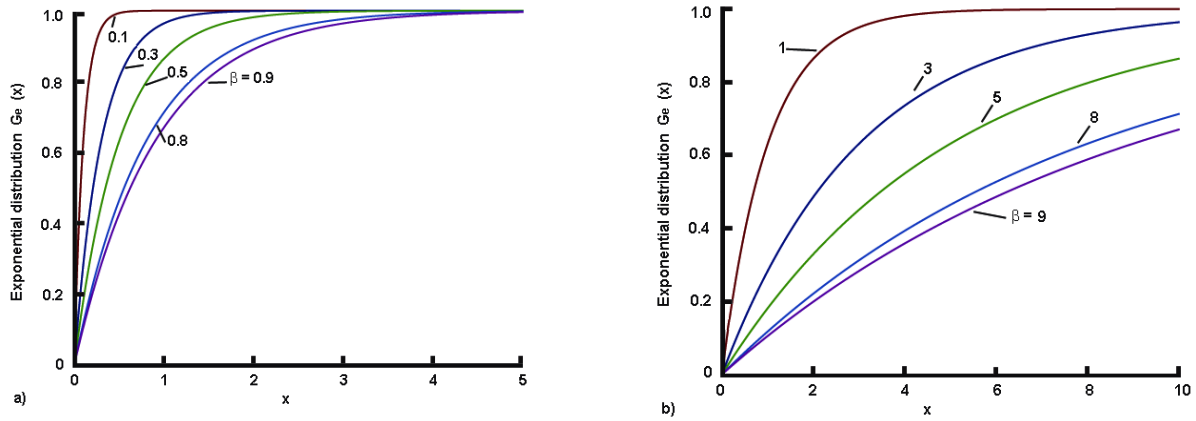

Figure 14. Two cases of basic exponential distribution: Left- with $\beta = 0.5$; Right- with $\beta = 1.5$

see that the transmuted profiles are well distinguished that could be attributed to both the rank of transmutation and the type of variable transmuting function chosen. Moreover, this can be related to the type of the basic exponential distribution which has an important control on its behaviour through the rate parameter β.

The Survival and the Hazard functions of the transmuted (quadratic) exponential distribution are shown in Figure 17.

8 Final comments and some emerging problems

This work conceived and explored tough examples of transmutations of distributions through a variable transmuting parameter (function) depending on the independent variable. The numerical experiments demonstrate the effect of the new approach is successful but at the same time formulate new problems and raise questions that should be answered through new studies, among them:

- The inverse (backward) problems are related to the determination of the rate parameter *p* because actually, the use of a variable transmuting function generates new basic distributions. This task is strongly dependent on the type of both the baseline distribution

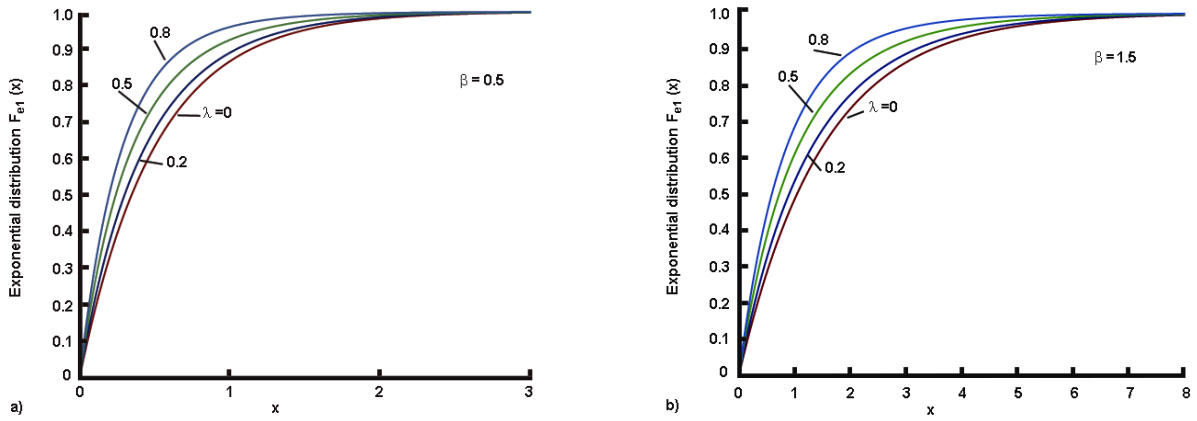

Figure 15. Two cases of quadratic transmutation of the exponential distribution (*cdf*) with fixed values of λ: Left- with β = 0.5; Right-with β = 1.5

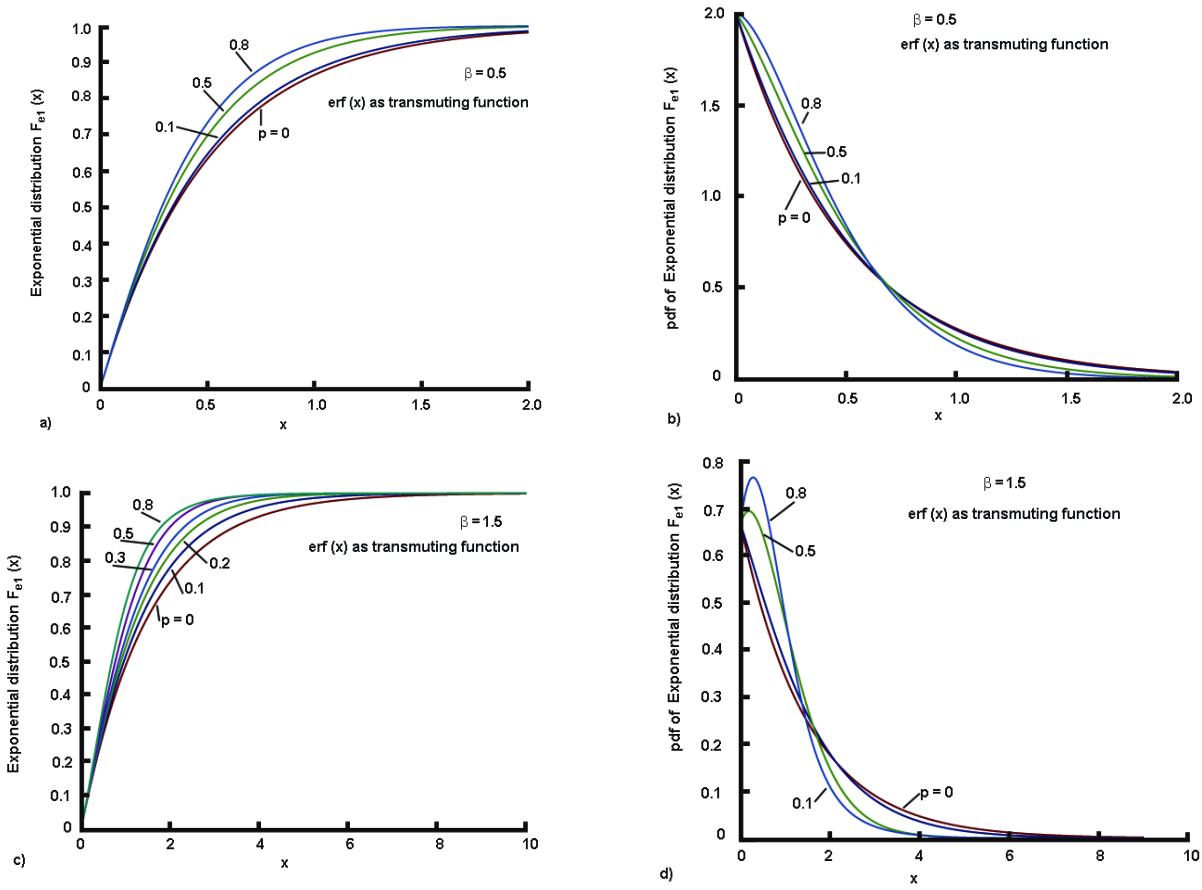

Figure 16. Cumulative and probability density functions of quadratic transmuted exponential distribution. Error-Function as a variable transmutation parameter: Left column: *cdf*s; Right column: *pdf*s

and the activation function and might be solved either analytically or numerically.

- Development of moments, quantile functions, random number generations, and many other related functions and parameters such as the ones well known from the cases when discrete transmuting parameters are applied. These are directions towards new studies beyond the scope of the present investigation.

- The new problems emerging in this study need the development of new analytical and numerical techniques for resolving the problem mentioned above and this draws new challenging areas for investigation.

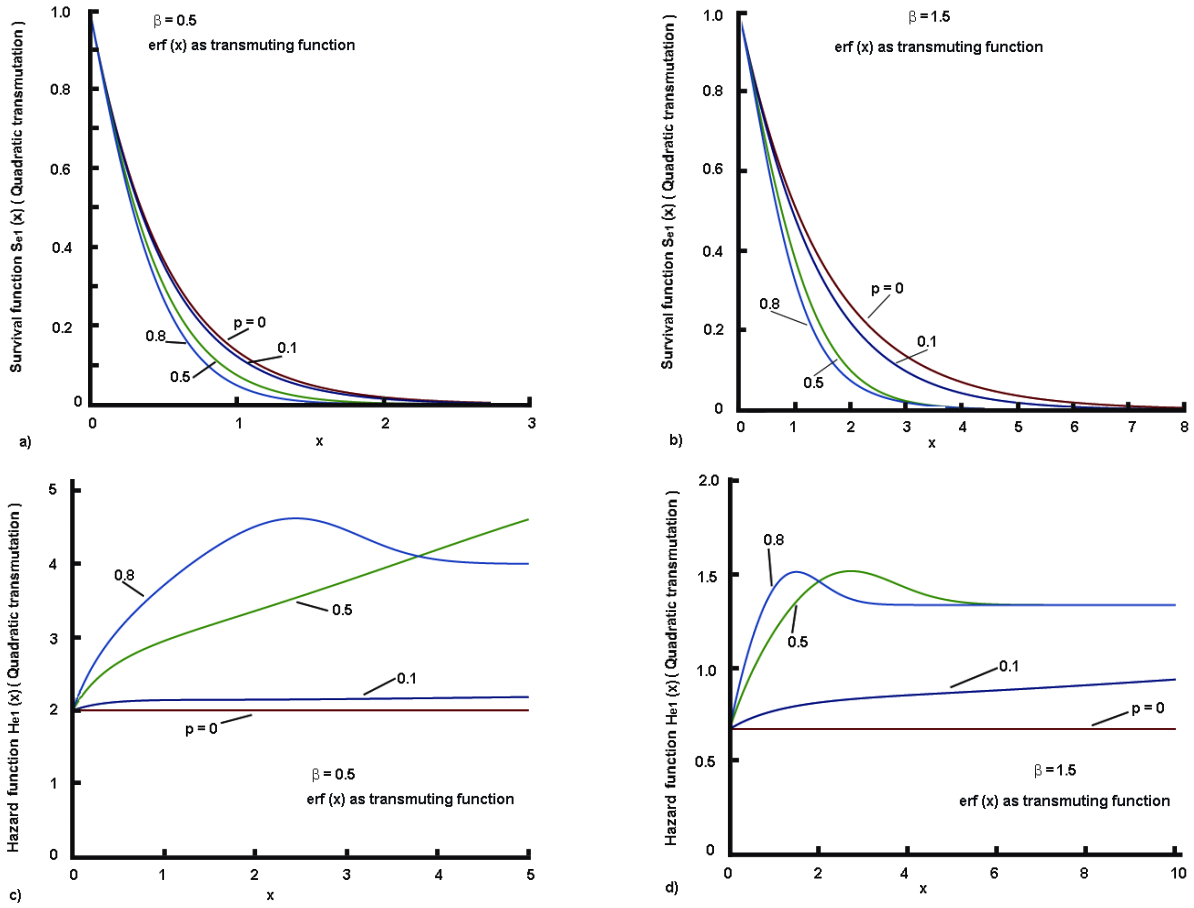

Figure 17. Survival and Hazard function of the quadratic transmuted exponential distribution. Error-Function as a variable transmutation parameter: Left column: $\beta = 0.5$; Right column: $\beta = 1.5$

9 Conclusions

A new concept in the transmutation of distributions applying variable transmuting (activation) function was conceived in this study. The idea of a variable transmuting parameter, dependent on the independent variable, was tested with the power distribution applying quadratic and cubic transmutations. This was performed through applications of two transmuting activation functions: the *error-function* and *standard logistic function*, and obeying the conditions imposed on the transmuting parameters imposed on it in the original concept of the transmutation mapping. Additional numerical experiments with the exponential distribution demonstrate the feasibility of the new approach and elucidate the fact that the effect of the transmutation strongly depends on the type of the function (distribution) to which it is applied. This is just the beginning and new tests with experimental data and available baseline distributions will allow elucidating the position of the distributions generated by the new concept among the well-know families of transformed functions. It is word remarking that the transmutation mapping can be applied not only to statistical distributions but to any other functions [35] thus allowing more flexibility in modelling of and approximate solutions.

Declarations

Consent for publication

Not applicable.

Conflicts of interest

The author declares that he has no known competing financial interests or personal relationships that could have appeared to influence the work reported in this paper.

Funding

The author declares that there is no funding source for the reported research.

Author's contributions

The research was carried out by the author and he accepts that the contributions and responsibilities belong to the author.

Acknowledgements

Not applicable.

References

[1] Dey, S., Kumar, D., Anis, M.Z., Nadarajah, S., & Okorie, I. A review of transmuted distributions. *Journal of the Indian Society for Probability and Statistics*, 22(1), 47-111, (2021). [CrossRef]
[2] Cordeiro, G.M., Ortega, E.M.M., & Popovic, B.V. The gamma-Lomax distribution. *Journal of Statistical computation and Simulation*, 85(2), 305-319, (2015). [CrossRef]
[3] Tahir, M.H., & Cordeiro, G.M. Compounding of distributions : a survey and new generalized classes. *Journal of Statistical Distributions and Applications*, 3(1) 1-35, (2016). [CrossRef]
[4] Afuecheta, E., Semeyutin, A., Chan, S., Nadarajah, S., & Ruiz, D.A.P. Compound distributions for financial returns. *Plos one*, 15(10), e0239652. [CrossRef]
[5] Al-Hussaini, E.K., & Ahsanullah, M. Exponentiated distributions. *Atlantis Studies in Probability and Statistics*, 21, (2015).
[6] Alexander, C. Cordeiro, G.M., Ortega, E.M., & Sarabia, J.M. Generalized beta-generated distributions. *Computational Statistics & Data Analysis*, 56(6), 1880-1897, (2012). [CrossRef]
[7] Alizadeh, M., Cordeiro, G.M., Brito, E.D., & Demetrio, C.G.B. The beta Marshal-Olkin family of distributions. *Journal of Statistical Distributions and Applications*, 2(1), 1-18, (2015). [CrossRef]
[8] Marshall, A.W., & Olkin, I. A new method for adding a parameter to a family of distributions with application to the exponential and Weibull families. *Biometrika*, 84(3), 641-652, (1997). [CrossRef]
[9] Patil, G.P., & Rao, C.R. Weighted distributions and size-biased sampling with applications to wildlife populations and human families. *Biometrics*, 34(2), 179-189, (1978). [CrossRef]
[10] Bakouch, H., Chesneau, C., & Enany, M. A weighted general family of distributions: Theory and practice. *Computational and Mathematical Methods*, 3(6), e1135, (2021). [CrossRef]
[11] Shaw W., & Buckley, I.R. The alchemy of probability distributions: beyond Gram-Charlier expansions, and a skew-kurtosis normal distribution from a rank transmutation map. Research Report. UCL discovery repository, *arXiv preprint: 0901.0434, Statistical Finance*), (2009). [CrossRef]
[12] Almalki, S.J., & Nadarajh, S. Modification of the Weibull distribution: a review. *Reliability Engineering & System Safety*, 124, 32-55, (2014). [CrossRef]
[13] Lai, M.T. Optimum number of minimal repairs for a system under increasing failure rate shock model with cumulative repair-cost limit. *International Journal of Reliability and Safety*, 7(2), 95-107, (2013).
[14] Elbatal, I. Transmuted modified inverse Weibull distribution: a generalization of the modified inverse Weibull probability distribution. *International Journal of Mathematical Archive*, 4(8), 117-129, (2013).
[15] Afify, A.Z., Nofal, Z.M., Yousuf, H.M., El Gebaly, Y.M., & Butt, N.S. The transmuted Weibull Lomax distribution: properties and application. *Pakistan Journal of Statistics and Operation Research*, 11, 135-152, (2015). [CrossRef]
[16] Granzotto, D.C.T., Louzada, F. & Balakrishnan N. Cubic rank transmuted distributions: inferential issues and applications. *Journal of statistical Computation and Simulation*, 87(14), 2760–2778, (2017). [CrossRef]
[17] Khan, M.S., & King,R. Transmuted modified Weibul distribution: a generalization of the modified Weibull probability distribution. *European Journal of pure and applied mathematics*, 6(1), 66-88, (2013).
[18] Okorie, I.E., Akpanta, A.C., Ohakwe, J., & Chikezie, D.C., The modified Power function distribution. *Cogent Mathematics*, 2017(4), 1219592, (2017). [CrossRef]
[19] Sakthivel, K.M., Rajitha, C.S., & Dhivakar, K. Two parameter cubic rank transmutation of Lindley distribution. *AIP Conference Proceedings* , 2261, 030086, (2020). [CrossRef]
[20] Rahman, M.M., Al-Zahrani, B., & Shahbaz, M.Q. A general transmuted family of distributions. *Pakistan Journal of Statistics and Operation Research*, 14(2), 451-469, (2018). [CrossRef]
[21] Ghosh, S., Kataria, K.K., & Vellaisamy, P. On transmuted generalized linear exponential distribution. *Communications in Statistics - Theory and Methods*, 50(9), 1978-2000, (2021). [CrossRef]
[22] Rahman, M.M., Al-Zahrani, B., Shahbaz, S.H., & Shahbaz, M.Q. Transmuted probability distributions: A review. *Pakistan Journal of Statistics and Operation Research*, 16(1), 83-94, (2020). [CrossRef]
[23] Celik, N. Some cubic rank transmuted distributions. *Journal of Applied Mathematics, Statistics and Informatics*, 14(2), 27-43, (2018). [CrossRef]
[24] Tian, Y., Tian, M., Zhu, Q. Transmuted Linear Exponential Distribution: A New Generalization of the Linear Exponential Distribution. *Communications in Statistics-Simulation and Computation*, 43(10), 2661-2677, (2014). [CrossRef]
[25] Alizadeh, M., Merovci, F., & Hamedani, G.G. Generalized transmuted family of distributions: properties and applications. *Hacettepe Journal of Mathematics and Statistics*, 46(4), 645-667, (2017). [CrossRef]
[26] Merovci, F., Alizadeh, M., & Hamedani, G.G. Another generalized transmuted family of distributions: properties and applications. *Austrian Journal of Statistics*, 45(3), 71-93, (2016). [CrossRef]
[27] Bourguignon, M., Gosh, I., & Cordeiro, G.M. General; results for transmuted family of distributions and new models. *Journal of Probability and Statistics*, 7208425, (2016). [CrossRef]
[28] Aryal, G.R., & Tsokos, C.P. On the transmuted extreme value distribution with application. *Nonlinear Analysis: Theory, Methods & Applications*, 71(12), e1401-e1407, (2009). [CrossRef]
[29] Aryal, G.R., & Tsokos, C.P. Transmuted Weibull distribution: A generalized of the Weibull probability distribution. *European Journal*

of pure and applied mathematics, 4(2), 89-102, (2011).
[30] Koopmans, L.H. Some simple singular and mixed probability distributions. *Some simple singular and mixed probability distributions*, 76(3), 297-299, (1969). [CrossRef]
[31] Karlis. D., & Xekalaki,E. Mixed poisson distributions. *International Statistical Review/Revue Internationale de Statistique*, 73(1), 35-58, (2005). [CrossRef]
[32] Fischer, S., Schumann, A., & Schulte, M. Characterisation of seasonal flood types according to timescales in mixed probability distributions. *Journal of Hydrology*, 539, 38-56, (2016). [CrossRef]
[33] McLachlan, G.J., & Peel, D. Finite mixture models. *John Wiley & Sons*, (2004).
[34] Owoloko, E.A., Oguntunde, P.E., & Adejumo, A.O. Performance rating of the transmuted exponential distribution: An analytical approach. *Springer Plus*, 4(1), 1-15, (2015). [CrossRef]
[35] Hristov, J. Integral-balance method with transmuted profiles: Concept, examples and emerging problems. *Journal of Computational and Applied Mathematics*, in press, (2022).

10 Appendix

The kurtosis (*Kurt*) is a measure of whether the data are heavy-tailed or light-tailed relative to a normal distribution and is given as

$$Kurt = \frac{\mu_4}{\sigma^4},$$

and the skewness ($\tilde{\mu}^3$) is a measure of the asymmetry of distribution and is given as

$$\tilde{\mu}^3 = \frac{\sum_i^N \left(X_i - \bar{X}\right)^3}{(N-1)\,\sigma^3}.$$

Mathematical Modelling and Numerical Simulation with Applications (MMNSA) (https://www.mmnsa.org)

Mathematical Modelling and Numerical Simulation with Applications, 2022, 2(2), 88–107

https://www.mmnsa.org
ISSN Online: 2791-8564 / Open Access
https://doi.org/10.53391/mmnsa.2022.008

RESEARCH PAPER

Asymptotic behavior and semi-analytic solution of a novel compartmental biological model

Muhammad Sinan[1,*,‡], Jinsong Leng[1,‡], Misbah Anjum[2,‡] and Mudassar Fiaz[3,‡]

[1]School of Mathematical Sciences, University of Electronic Science and Technology of China, Chengdu, 611731, People's Republic of China, [2]International School of Fundamental and Frontier Sciences, University of Electronic Science and Technology of China, Chengdu, 611731, People's Republic of China, [3]Department of Mathematics, COMSATS University Islamabad, Lahore Campus, Pakistan

*Corresponding Author
‡ 202124110102@std.uestc.edu.cn, sinanmathematics@gmail.com (Muhammad Sinan); lengjs@uestc.edu.cn (Jinsong Leng); anjummisbah33@gmail.com, 202124210103@std.uestc.edu.cn (Misbah Anjum); mudassarfiaz789@gmail.com (Mudassar Fiaz)

Abstract

This study proposes a novel mathematical model of COVID-19 and its qualitative properties. Asymptotic behavior of the proposed model with local and global stability analysis is investigated by considering the Lyapunov function. The mentioned model is globally stable around the disease-endemic equilibrium point conditionally. For a better understanding of the disease propagation with vaccination in the population, we split the population into five compartments: susceptible, exposed, infected, vaccinated, and recovered based on the fundamental Kermack-McKendrick model. He's homotopy perturbation technique is used for the semi-analytical solution of the suggested model. For the sake of justification, we present the numerical simulation with graphical results.

Key words: Local asymptotic stability; global asymptotic stability; Routh-Hurwitz criterion; COVID-19; infectious disease modeling
AMS 2020 Classification: 34L30; 92D30; 37N30; 37N25

1 Introduction

Most nations throughout the world have been afflicted by the COVID-19 outbreak, and their economy has suffered as a result. There have been several cases of infection, as well as the occurrence of subsequent infection waves that have resulted in a greater number of cases than the prior wave. Although various preventative techniques and other control measures have been used to restrict the disease's spread, it is still unknown when this lethal sickness will be eradicated from the community. COVID-19 is currently infecting and killing people in the majority of the world's countries. The total number of infected cases recorded till September 4, 2021, was 220917130, including 4571624 deaths, and 197441726 [1] people recovered from COVID-19 infection. Researchers, biologists, and medical professionals are constantly attempting to develop efficient vaccines, preventions, and treatment measures for coronavirus infection management. Because there are so many different strains of this sickness, researchers are working to develop a more effective vaccine for infection prevention. According to the literature, several study publications on the virus's infection reduction have been written and published from various perspectives. We have a lot of models if we speak out that connected study on coronavirus using mathematical models. Mathematical models are the only means to determine the infection's peak and the best strategy to manage it.

In [2], researchers studied COVID-19 using a mathematical model that included Susceptible S(t), Exposed E(t), Infected I(t), Quarantine Q(t), and Recovered R(t). The goals were to examine the stability and optimal management of the concerned mathematical model for both

➤ **Received:** 24.03.2022 ➤ **Revised:** 20.06.2022 ➤ **Accepted:** 21.06.2022 ➤ **Published:** 24.06.2022

local and global stability using a third additive compound matrix technique, as well as to produce threshold values using a next-generation approach. The author created a graphic representation of the anticipated outcomes which also used the homotopy perturbation approach for the solution and for each population of the underlying model with control variables utilizing optimal control methods based on Pontryagin's maximal Principle to control the spread of COVID-19 infection in a population. In [3], researchers implemented fractional calculus on a COVID-19 mathematical model and investigated local and global stability for the stabilization of the disease in a population with an approximate solution using the Laplace-Adomian decomposition method. In [4], the authors examined the global view of the coronavirus model to real data from Ghana, as well as its cost-effective analysis with environmental changes. In [5], the authors proposed a nonlinear predictive control model and its management for coronavirus infection. In [6], the authors modeled and explored the use of medication resistance in coronavirus infection. In [7], the authors investigated the spread of coronavirus infection in China, as well as its modeling and prediction. In order to investigate the impact of lockdown in reducing coronavirus spread [8], the author examined a system of five nonlinear fractional-order equations in the Caputo sense. The hypothesised coronavirus model under lockdown's solutions were shown to exist and to be distinct using the fixed-point theorems of Schauder and Banach, respectively. Ulam-Hyers and generalised Ulam-Hyers frames for stability analysis were established.

To simulate the transmission of disease, the authors [9] looked at the SIR model with a generic incidence rate function and a nonlinear recovery rate. The influence of the health system affects the nonlinear recovery rate. The authors also established the model solution's existence, uniqueness and boundedness. They looked into the model's many steady-state solutions, stability details, and reproductive number. The research demonstrates that the free steady state is unstable otherwise and locally stable when the reproduction number is smaller than unity. The backward bifurcation phenomenon is illustrated by the model. For the transmission dynamics of HIV epidemics, the authors [10] have developed a nonlinear SEI1I2R fractional order epidemic model. The generalised mean value theorem is used to determine the model's non-negative solution. In order to determine the disease status, we obtained the fundamental reproductive number R_0, which serves as a threshold parameter. Using the fractional Routh-Hurwitz stability criterion, the asymptotically stable outcomes of equilibria are explored. While this is going on, a suitable Lyapunov function is built to evaluate the global asymptotic stability of the disease-free and endemic equilibrium point. In order to increase the concept of propagation delay, this research [11, 12] focuses on a delayed epidemic model with information-dependent vaccination.

Researchers have delved deeply into the transmission of infectious diseases or concentrated on the differential model, which solely takes into account the traits of infectious diseases themselves. The dynamic study of infectious illnesses based on vaccination rates has not received much attention. The authors [13] looked at a population model of the novel COVID-19 under ABC fractional order derivatives, and they also demonstrated enough evidence for the solution's existence and uniqueness for the model under consideration. They also demonstrated that the model has at least one solution with a stable result. The author [14] showed in this work the potential of modelling the dynamics of SARS-CoV-2 infection as a helpful support tool for measuring the population's level of compliance with the GIM and projecting the impact of corrective measures. This book [15] helps with the preliminary results and is valuable to study in the field of mathematical modelling in public health biology or public health epidemiology. In [16], the author investigated COVID-19 epidemic has had a substantial influence on children and adolescents' mental health, which should be of great concern to policymakers and practitioners around the world. This [17, 18, 19, 20, 21, 22] work examines a new mathematical model for the dynamics of Hepatitis-B virus transmission in a fractional environment in light of asymptomatic carriers and vaccination classes. Because the authors took into account both the vaccination and asymptomatic caries, this new model is more advanced than the previous models proposed for the dynamics of the Hepatitis-B virus. In this study [23, 24], the dynamics of the COVID-19 epidemic in Pakistan were examined, and a mathematical model was developed. Its fundamental and essential mathematical aspects, such as the existence and positivity of the system and its solution, were then supplied. Using fractional stability techniques, the detailed stability results for disease-free and disease-endemic equilibrium points are examined on a local and global scale.

For the dynamics of the Zika virus [25, 26] with a mutation that results in defects in newborns, a mathematical model has been devised. The threshold quantity at risk-free equilibrium and the equilibrium for Zika infection were also computed by the authors. Both locally and internationally, the stability analysis at disease-free and disease-endemic equilibrium are computed. The authors [27, 28] examined a mathematical model with slow and quick exposed cases and its impact on the model dynamics to comprehend the TB infections in the KP area of Pakistan. They also researched the fundamental math needed to model the fractional-order model. The model's stability was then examined, and it was demonstrated that the TB model is both locally and globally asymptotically stable. The examination and analysis of the suggested drinking model must also be included by the authors, who also used stochastic system perturbation to determine the solution's existence and uniqueness as well as some drinking dynamics [29]. The authors have also come to some important conclusions on how to control drinking habits at all stages, from risky to moderate and moderate to non-consumer. A discrete-time Bazykin-Berezovskaya prey-predator model's complex dynamics were described in detail by the authors [30]. Additionally, they showed that the model has a single positive interior fixed point (FPP). They also concentrated on the analytical and numerical bifurcation analysis of the interior fixed point FPP due to its biological significance.

The scientists [31] looked at an SIR model for COVID-19 in Indonesia, taking into account parameters like immunisation, treatment, application of health protocols, and coronavirus burden. Additionally, they discovered that immunisation and the application of health practices significantly limit or stop the spread of COVID-19 in Indonesia. Similar to vaccination [32] and the application of health protocols, treatment can decrease or stop the pace of COVID-19 infection. However, its impact is not as great. This study [33] presents a novel strategy for combating the COVID-19 epidemic. Using actual data from the United Kingdom, a fractional order pandemic model is created to investigate the spread of COVID-19 with and without the Omicron form and its connection to heart attacks. In [34], an optimal control model has been developed in light of the potential controls that are thought to be successful. The World Health Organization's (WHO) basic principles, such as immunisation of people, rapid testing, and early treatment of infected individuals by COVID-19, have been used to consider the four control variables in the form of preventions. In [35], this study examines the mathematical modelling of COVID-19 transmission at the fractional-order level. Using nonlinear analysis, they demonstrate the model's existence and originality. The goal of this work [36] is to thoroughly study a mathematical model for computing the nonsingular fractional order derivative-based transmissibility of a novel coronavirus (COVID-19) disease. By using the Krasnoselskii and Banach fixed point theorems, the existence and uniqueness of the proposed model have been ensured. Additionally, some stability outcomes of the Ulam-type have been developed.

In [37], the researchers studied that there was a substantial but statistically minor rise in mental health symptoms before to and during the COVID-19 pandemic in 2020, according to a study that sampled mostly European and North American people. Depressive symptoms showed bigger and longer-lasting increases, compared to anxiety disorder symptoms and measures of general mental health

functioning, which showed lower changes. It will be critical to keep track of changes in mental health (especially depression) and ensure that proper therapeutic therapy is accessible. The total rise in mental health symptoms was most evident in the first two months after the WHO proclaimed a pandemic (March 2020), before declining and returning to pre-pandemic levels by mid-2020 for most symptom kinds. In [38], the authors study COVID–19 with quarantine, isolation, and environmental viral load. They fitted the COVID–19 model to real data and calculated the parameters.

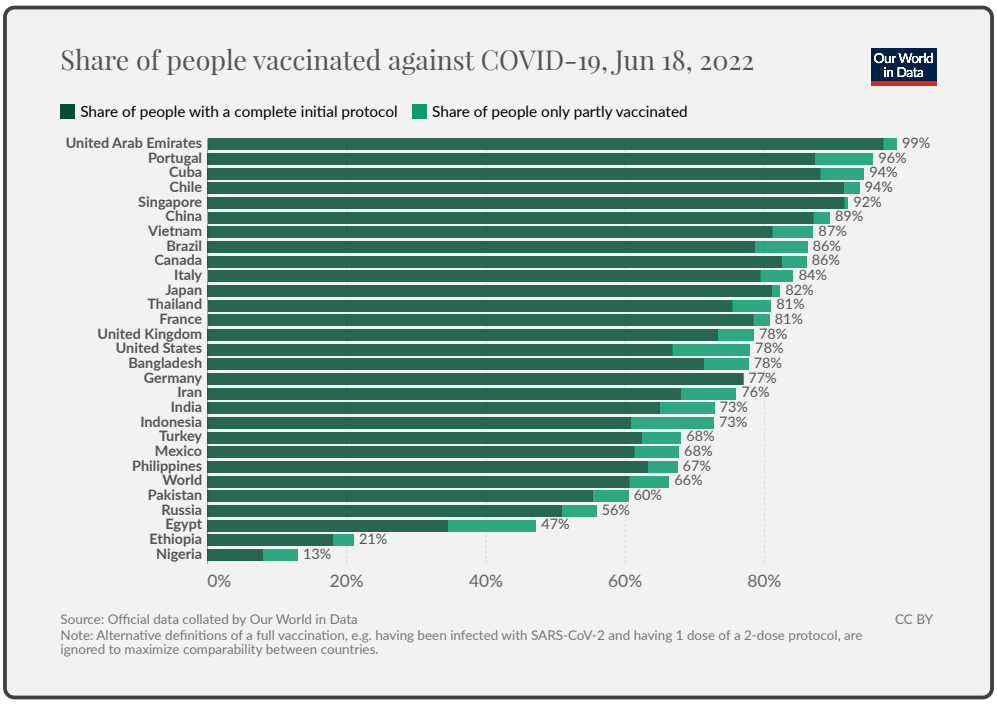

Figure 1. [39], The bar chart represents the vaccinated population with complete initial protocol and partly vaccinated for different countries

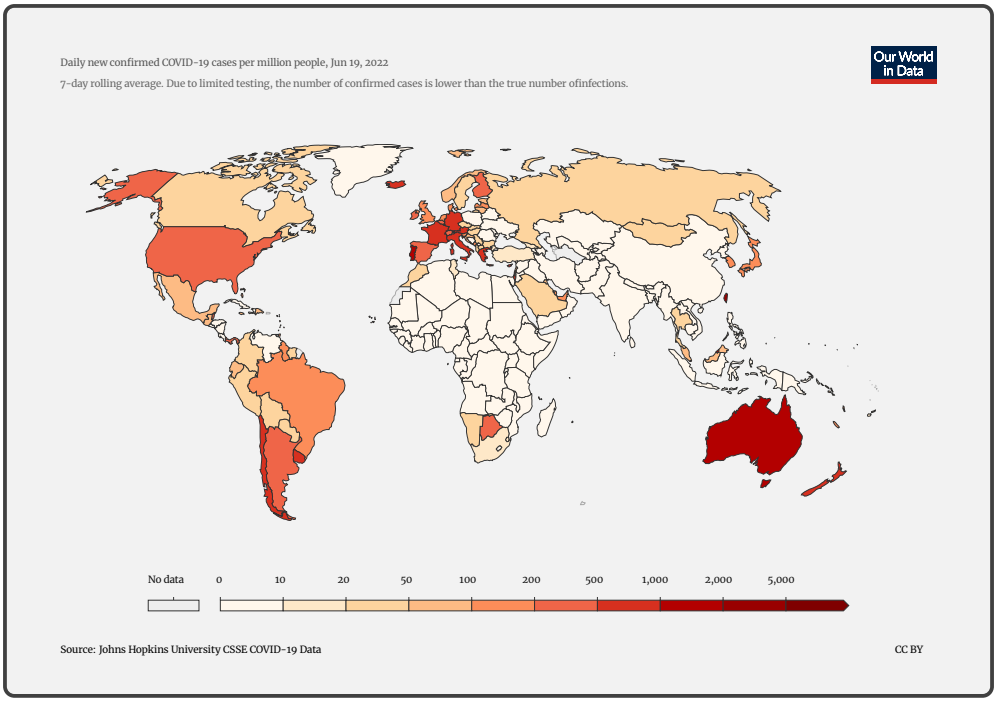

Figure 2. [39], The map of the world represents the confirmed cases of COVID–19

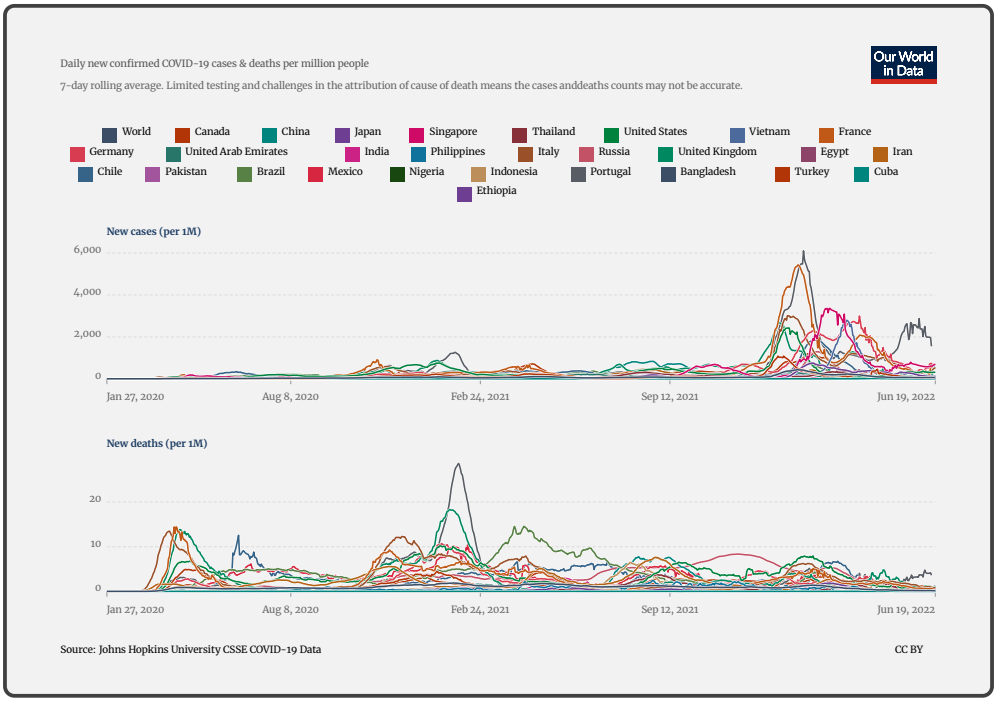

Figure 3. [39], The plots of confirmed and death cases per million people

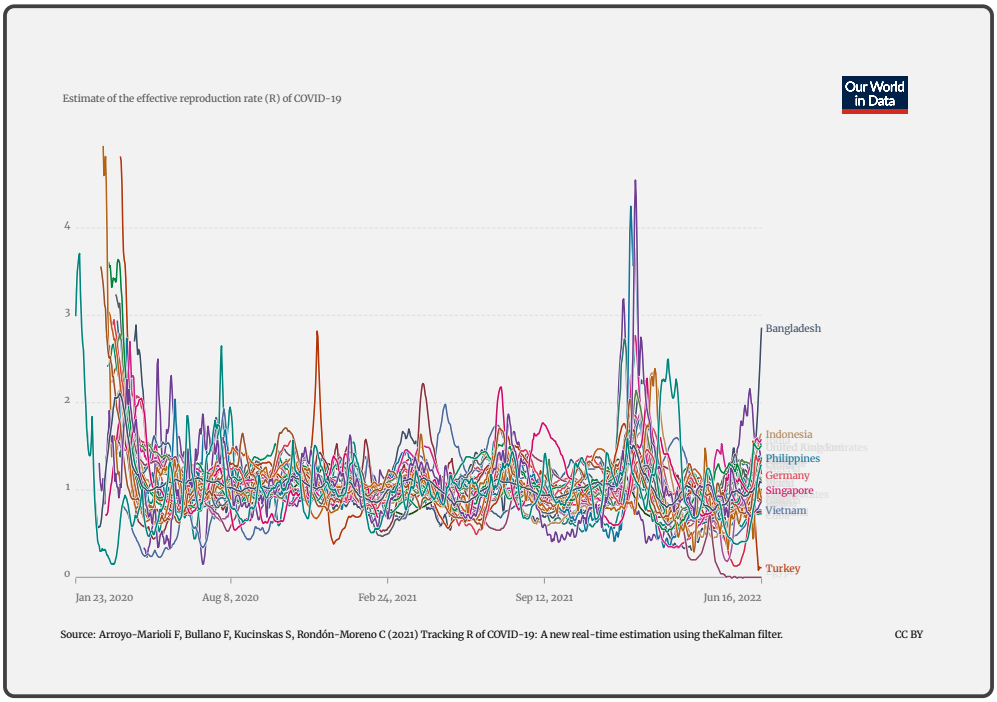

Figure 4. [39], The behaviour of basic reproduction number or reproductive rate R_0 of COVID−19 for different countries. The reproduction rate represents the average number of new infections caused by a single infected individual. If the rate is greater than 1, the infection is able to spread in the population. If it is below 1, the number of cases occurring in the population will gradually decrease to zero

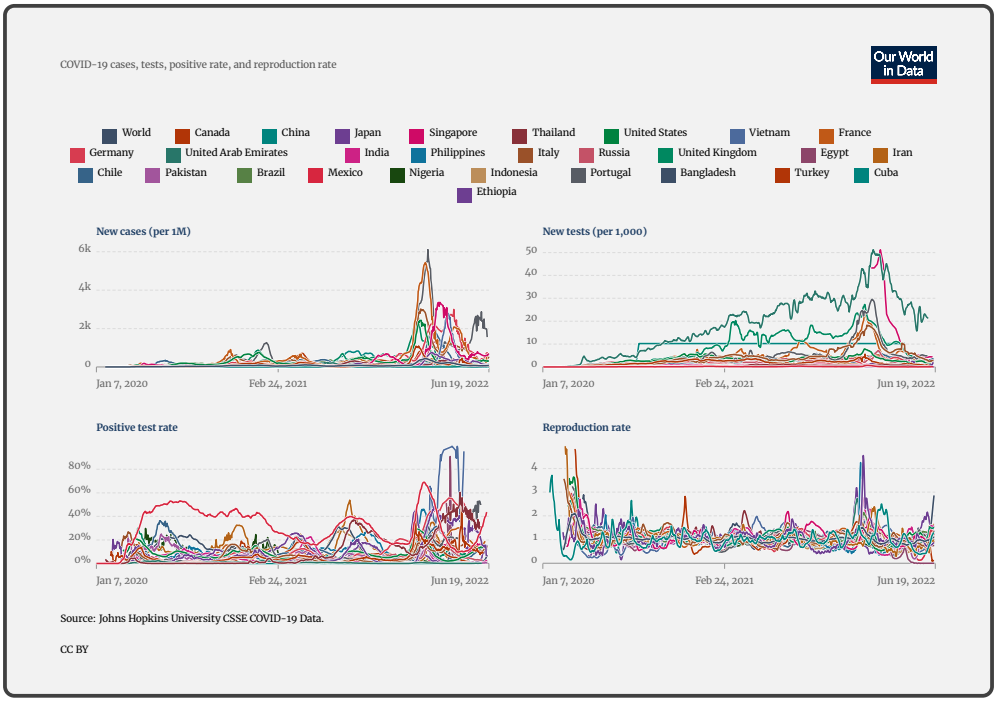

Figure 5. [39], Gallery of charts for new cases, new tests, positive test rate, and reproductive rate. 7-day rolling average. Due to limited testing, the number of confirmed cases is lower than the true number of infections. Comparisons across countries are affected by differences in testing policies and reporting methods

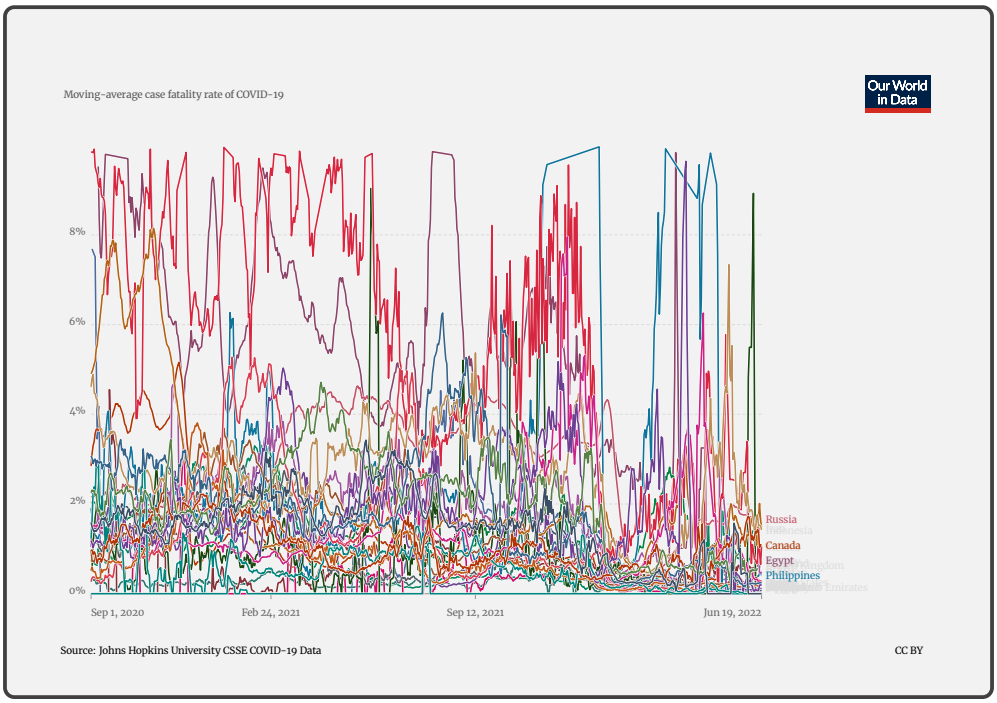

Figure 6. [39], The case fatality rate (CFR) is the ratio between confirmed deaths and confirmed cases. Our rolling-average CFR is calculated as the ratio between the 7-day average number of deaths and the 7-day average number of cases 10 days earlier.

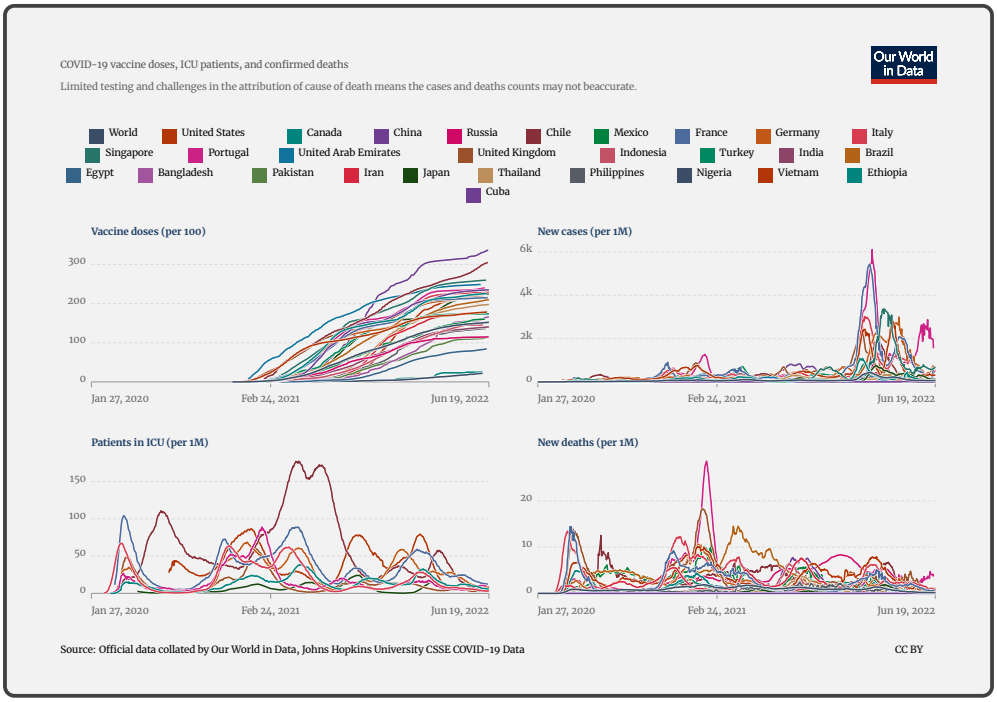

Figure 7. [39], Gallery of charts for vaccine doses, new cases, patients in ICU and New deaths

According to [40], immunization is a global success story in terms of health and development, saving millions of lives each year. Vaccines interact with your body's natural defenses to build protection, lowering your risk of contracting a disease. Your immune system reacts when you receive a vaccine. Vaccines for more than 20 life-threatening diseases are now available, allowing individuals of all ages to enjoy longer, healthier lives. Every year, vaccinations prevent 3.5-5 million fatalities from diseases such as diphtheria, tetanus, pertussis, influenza, and measles. Immunization is an indisputable human right and an important component of primary health care. It's also one of the most cost-effective health investments available. Vaccines are also essential for preventing and controlling outbreaks of infectious diseases. They are essential in the fight against antimicrobial resistance and support global health security. Despite significant advances, vaccine coverage has plateaued in recent years, and in 2020, it may potentially decline for the first time in a decade. Over the last two years, the COVID-19 pandemic and its aftermath have put pressure on health services, with 23 million children skipping vaccinations in 2020, 3.7 million more than in 2019, and the largest amount since 2009. Preliminary data from 2021 reveal continuous disruption, but on the plus side, nearly all nations had implemented COVID-19 immunization by the end of 2021, and one billion doses of COVID-19 vaccine had been supplied via COVAX by early 2022. In this paper, we investigate the asymptotic behaviour of the model locally and globally at disease–free and endemic equilibrium points. For the global stability, Lyapunov function is considered. We also use the homotopy perturbation method (HPM) to solve the non-linear dynamical system of COVID-19 semi-analytically. HPM approach was initially suggested by [41] and has since been used to solve differential and integral equations in both linear and nonlinear scenarios by [42]. In [43], the authors used the HPM to solve the nonlinear Kawahara partial differential equation semi–analytically. The HPM was used by the authors [44] to solve a set of partial differential equations. Without the use of linearization, transformation, discretization, or constrictive assumptions, the approach is used directly. We can get the conclusion that the HPM is very effective and powerful in locating analytical solutions for a variety of boundary value problems. In [45] to solve the system of rabies transmission dynamics, for resolving the generalised Zakharov equations, the HPM is suggested by the authors [46]. With potential unknown constants that can be found by imposing the boundary and initial conditions, the initial approximations can be freely chosen. For the mathematical study of obtaining the solution of a first-order in-homogeneous partial differential equation $u_x(x,y) + a(x,y)u_y(x,y) + b(x,y)g(u) = f(x,y)$, a new homotopy technique is proposed [47]. This new method is developed by combining the decomposition of a source function and the HPM.

COVID-19 mathematical model formulation

In this section, we modifying Susceptible, Infected, and Recovered (SIR) model [9, 31] for COVID-19 infection with the implementation of the vaccination class/compartment such that:

$$\begin{aligned} \frac{dS(t)}{dt} &= -\beta S(t)I(t), \\ \frac{dI(t)}{dt} &= \beta S(t)I(t) - \gamma I(t), \\ \frac{dI(t)}{dt} &= \gamma I(t). \end{aligned} \tag{1}$$

For mathematical modelling of the model, we provide the compartmental diagram below:

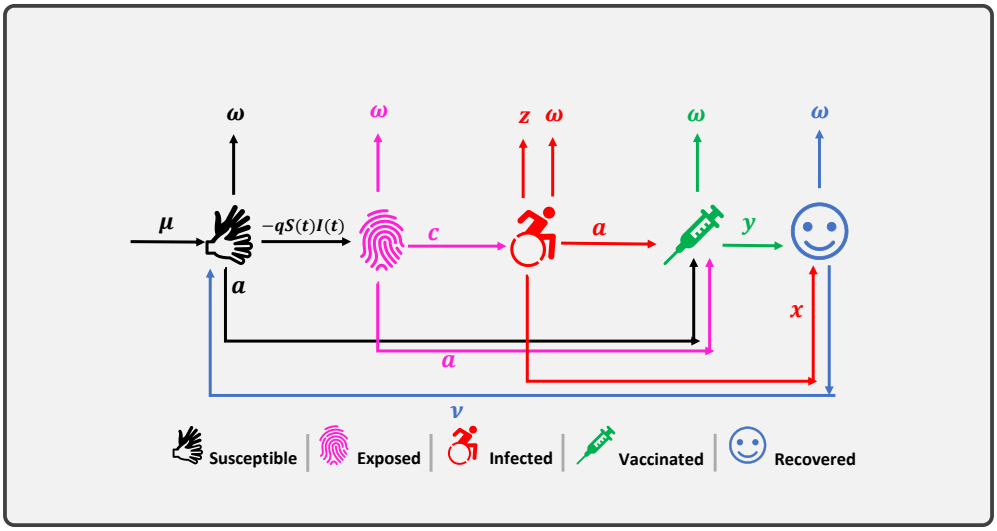

Figure 8. Compartmental diagram of COVID–19 model

Based on the compartmental diagram (8), the following model is proposed:

$$\left.\begin{aligned}
\frac{dS(t)}{dt} &= \mu - qS(t)I(t) - (\omega + a)S(t) + \nu R(t),\\
\frac{dE(t)}{dt} &= qS(t)I(t) - (c + \omega + a)E(t),\\
\frac{dI(t)}{dt} &= cE(t) - (a + \omega + x + z)I(t),\\
\frac{dV(t)}{dt} &= aI(t) - (\omega + y)V(t) + aE(t) + aS(t),\\
\frac{dR(t)}{dt} &= xI(t) + yV(t) - (\omega + \nu)R(t),
\end{aligned}\right\} \tag{2}$$

with $S(0) \geq 0$, $E(0) \geq 0$, $I(0) \geq 0$, $V(0) \geq 0$, and $R(0) \geq 0$. Also, here SEIVR represents Susceptible, Exposed, Infected, Vaccinated and Recovered compartments, respectively. Also, μ is the rate of recruitment, q is the rate of transmission, ω is the rate of natural death, a is the rate of vaccination, ν is the rate of loss of immunity, c is the rate of infection of Exposed population, x is the recovery rate of Infected population, z is the death rate of Infected population due to the disease, y is the immunity of vaccinated population.

More assumptions

In order to build a new model, we must make assumptions in order to simplify reality. The Kermack–McKendrick model's primary premise is that diseased people are likewise contagious. The overall population size remains constant. There are only two types of death in the population: natural death and death due to the disease. The population is open to accept new individuals from outside the existing population. The infected individuals can be recovered with hospitalization. The parameters of are non-negative and $N(t) = S(t) + E(t) + I(t) + V(t) + R(t)$ where $N(t)$ stands for the total population at the time t such that $t \in \Omega := [0, T]$ for $T > 0$.

2 Equilibrium points and their stability analysis

The disease–free equilibrium point is computed as:

$$E^0 = \left(S^0, 0, 0, V^0, R^0\right), \tag{3}$$

where,

$$\left.\begin{aligned}
S^0 &= \frac{\mu\left(\nu\omega + \nu y + \omega y + \omega^2\right)}{\nu\omega^2 + \omega^2 q + \omega^2 y + \omega^3 - a\nu y + \nu\omega q + \nu\omega y + \nu q y + \omega q y},\\
V^0 &= \frac{a\mu(\nu + \omega)}{\nu\omega^2 + \omega^2 q + \omega^2 y + \omega^3 - a\nu y + \nu\omega q + \nu\omega y + \nu q y + \omega q y},\\
R^0 &= \frac{a\mu y}{\nu\omega^2 + \omega^2 q + \omega^2 y + \omega^3 - a\nu y + \nu\omega q + \nu\omega y + \nu q y + \omega q y}.
\end{aligned}\right\} \tag{4}$$

The basic reproduction number at the disease-free equilibrium point for the model (2) is computed below:

$$R_0 = \frac{cqS^0}{(a+c+\omega)(a+\omega+x+z)}, \tag{5}$$

where,

$$S^0 = \frac{\mu\left(\nu\omega+\nu y+\omega y+\omega^2\right)}{\nu\omega^2+\omega^2 q+\omega^2 y+\omega^3-a\nu y+\nu\omega q+\nu\omega y+\nu q y+\omega q y}. \tag{6}$$

Theorem 1 *The COVID-19 model at the disease-free equilibrium point E^0 is locally asymptotically stable if $R_0 < 1$, otherwise unstable.*

Proof 1 *The Jacobian matrix of the model (2) is computed as:*

$$J(E^0) = \begin{bmatrix} -a-\omega & 0 & -qS^0 & 0 & \nu \\ 0 & -a-c-\omega & qS^0 & 0 & 0 \\ 0 & c & -a-\omega-x-z & 0 & 0 \\ a & a & a & -\omega-y & 0 \\ 0 & 0 & x & y & -\nu-\omega \end{bmatrix}. \tag{7}$$

After a little simplification using the row reduction process, then the matrix (7) takes the form:

$$J(E^0) = \begin{bmatrix} -a-\omega & 0 & -qS^0 & 0 & \nu \\ 0 & -a-c-\omega & qS^0 & 0 & 0 \\ 0 & 0 & cqS^0-(a+\omega+x+z)(a+c+\omega) & 0 & 0 \\ 0 & 0 & [a(a+\omega)-aqS^0](a+c+\omega)+qS^0a(a+\omega) & -(\omega+y)(a+\omega)(a+c+\omega) & 0 \\ 0 & 0 & x & y & -\nu-\omega \end{bmatrix}. \tag{8}$$

Clearly, we get all the eigenvalues such that $\lambda_1 = -a-\omega$, $\lambda_2 = -a-c-\omega$, $\lambda_3 = -\nu-\omega$, $\lambda_4 = -(\omega+y)(a+\omega)(a+c+\omega)$, and $\lambda_5 = cqS^0-(a+\omega+x+z)(a+c+\omega)$. As we see that the eigenvalues other than λ_5 are negative while $\lambda_5 < 0$ if $cqS^0-(a+\omega+x+z)(a+c+\omega) < 0$ implies that $cqS^0 < (a+\omega+x+z)(a+c+\omega)$ furthermore $cqS^0/(a+\omega+x+z)(a+c+\omega) < 1 \Rightarrow R_0 < 1$. Hence the model (2) is locally asymptotically stable around disease−free equilibrium point E_0 if $R_0 < 1$. This completes the proof.

Theorem 2 *The COVID-19 model at the disease-endemic equilibrium point E^* is locally asymptotically stable if $R_0 > 1$, otherwise unstable.*

Proof 2 *The Jacobian matrix of the model (2) is computed as:*

$$J(E^*) = \begin{bmatrix} -a-\omega-qI^* & 0 & -qS^* & 0 & \nu \\ qI^* & -a-c-\omega & qS^* & 0 & 0 \\ 0 & c & -a-\omega-x-z & 0 & 0 \\ a & a & a & -\omega-y & 0 \\ 0 & 0 & x & y & -\nu-\omega \end{bmatrix}. \tag{9}$$

Computing the characteristic equation of Jacobian matrix (9), such that:

$$\lambda^5 + a_1\lambda^4 + a_2\lambda^3 + a_3\lambda^2 + a_4\lambda + a_5, \tag{10}$$

where, the coefficients are the following:

$$
\begin{aligned}
a_1 &= (3a + c + \nu + 5\omega + x + y + z + I^*q)\,,\\
a_2 &= (2ac + 3a\nu + 12a\omega + c\nu + 4c\omega + 2ax + 3ay + 2az + cx + cy + cz + 4\nu\omega + \nu x + 4\omega x + \nu y + 4\omega y\\
&\quad + \nu z + 4\omega z + xy + yz + 3a^2 + 10\omega^2 + 2I^*aq + I^*cq - Scq + I^*\nu q + 4I^*\omega q + Iqx + Iqy + Iqz),\\
a_3 &= (a^2c + 3a^2\nu + 18a\omega^2 + 9a^2\omega + 6c\omega^2 + a^2x + 3a^2y + a^2z + 6\nu\omega^2 + 6\omega^2x\\
&\quad + 6\omega^2y + 6\omega^2z + a^3 + 10\omega^3 + 2ac\nu + 6ac\omega + acx + 2acy + acz + 9a\nu\omega + 3c\nu\omega + 2a\nu x\\
&\quad + 6a\omega x + 2a\nu y + 9a\omega y + 2a\nu z + c\nu x + 6a\omega z + 3c\omega x + c\nu y + 3c\omega y + c\nu z + 3c\omega z\\
&\quad + 2axy + 2ayz + cxy + 3\nu\omega x + cyz + 3\nu\omega y + 3\nu\omega z + \nu xy + 3\omega xy + \nu yz + 3\omega yz + I^*a^2q\\
&\quad + 6I^*\omega^2q + I^*\nu qx + 3I^*\omega qx + I^*\nu qy + 3I^*\omega qy + I^*\nu qz\\
&\quad + 3I^*\omega qz + I^*qxy + I^*qyz + I^*acq - Sacq + 2I^*a\nu q + 6I^*a\omega q + I^*c\nu q\\
&\quad + 3I^*c\omega q + I^*aqx + 2I^*aqy + I^*aqz + I^*cqx - Sc\nu q + I^*cqy - 3Sc\omega q + I^*cqz + 3I^*\nu\omega q - Scqy),\\
a_4 &= (a^3\nu + 12a\omega^3 + 2a^3\omega + 4c\omega^3 + a^3y + 4\nu\omega^3 + 4\omega^3x + 4\omega^3y + 4\omega^3z + 5\omega^4\\
&\quad + 9a^2\omega^2 + a^2\nu x + 6a\omega^2x + 2a^2\omega x + a^2\nu y + 9a\omega^2y + 6a^2\omega y + a^2\nu z + 6a\omega^2z + 3c\omega^2x\\
&\quad + 2a^2\omega z + 3c\omega^2y + 3c\omega^2z + a^2xy + a^2yz + 3\nu\omega^2x + 3\nu\omega^2y + 3\nu\omega^2z + 3\omega^2xy + 3\omega^2yz\\
&\quad + 4I^*\omega^3q + a^2c\nu + 6ac\omega^2 + 2a^2c\omega + a^2cy + 9a\nu\omega^2 + 6a^2\nu\omega + 3c\nu\omega^2 + 4ac\nu\omega\\
&\quad + ac\nu x + 2ac\omega x + ac\nu y + 4ac\omega y + ac\nu z + 2ac\omega z + acxy + 4a\nu\omega x + acyz + 4a\nu\omega y + 4a\nu\omega z + 2c\nu\omega x\\
&\quad + 2c\nu\omega y + 2c\nu\omega z + a\nu xy + 4a\omega xy + a\nu yz + c\nu xy + 4a\omega yz + 2c\omega xy + c\nu yz + 2c\omega yz + 2\nu\omega xy\\
&\quad + 2\nu\omega yz + I^*a^2\nu q + 6I^*a\omega^2q + 2I^*a^2\omega q + 3I^*c\omega^2q + I^*a^2qy\\
&\quad - 3Sc\omega^2q + 3I^*\nu\omega^2q + 3I^*\omega^2qx + 3I^*\omega^2qy + 3I^*\omega^2qz + I^*ac\nu q\\
&\quad + 2I^*ac\omega q - Sac\nu q + I^*acqy - 2Sac\omega q + 4I^*a\nu\omega q + 2I^*c\nu\omega q - Sacqy + I^*a\nu qx\\
&\quad + 2I^*a\omega qx + I^*a\nu qy + 4I^*a\omega qy + I^*a\nu qz + 2I^*a\omega qz + 2I^*c\omega qx + I^*c\nu qy\\
&\quad - 2Sc\nu\omega q + 2I^*c\omega qy + I^*c\nu qz + 2I^*c\omega qz + I^*aqxy + I^*aqyz + I^*cqxy - Sc\nu qy\\
&\quad - 2Sc\omega qy + 2I^*\nu\omega qx + I^*cqyz + 2I^*\nu\omega qy + 2I^*\nu\omega qz + I^*\nu qxy + 2I^*\omega qxy + I^*\nu qyz + 2I^*\omega qyz),\\
a_5 &= 3a\omega^4 + c\omega^4 + \nu\omega^4 + \omega^4x + \omega^4y + \omega^4z + \omega^5 + 3a^2\omega^3 + a^3\omega^2 + 2a\omega^3x + 3a\omega^3y\\
&\quad + a^3\omega y + 2a\omega^3z + c\omega^3x + c\omega^3y + c\omega^3z + \nu\omega^3x + \nu\omega^3y + \nu\omega^3z + \omega^3xy + \omega^3yz\\
&\quad + a^2c\omega^2 + 3a^2\nu\omega^2 + a^2\omega^2x + 3a^2\omega^2y + a^2\omega^2z + I^*\omega^4q + 2ac\omega^3 + 3a\nu\omega^3 + a^3\nu\omega + c\nu\omega^3\\
&\quad + 2I^*a\omega^3q + I^*c\omega^3q - Sc\omega^3q + I^*\nu\omega^3q + I^*\omega^3qx + 2ac\nu\omega^2 + a^2c\nu\omega + I^*\omega^3qy\\
&\quad + I^*\omega^3qz + ac\omega^2x + 2ac\omega^2y + a^2c\omega y + ac\omega^2z + 2a\nu\omega^2x + a^2\nu\omega x + 2a\nu\omega^2y + a^2\nu\omega y\\
&\quad + 2a\nu\omega^2z + c\nu\omega^2x + a^2\nu\omega z + c\nu\omega^2y + c\nu\omega^2z + 2a\omega^2xy + a^2\omega xy + 2a\omega^2yz + c\omega^2xy + a^2\omega yz\\
&\quad + c\omega^2yz + \nu\omega^2xy + \nu\omega^2yz + I^*a^2\omega^2q + ac\nu\omega x + ac\nu\omega y + ac\nu\omega z + ac\omega xy + ac\omega yz + a\nu\omega xy\\
&\quad + a\nu\omega yz + c\nu\omega xy + c\nu\omega yz + I^*ac\omega^2q - Sac\omega^2q + 2I^*a\nu\omega^2q + I^*a^2\nu\omega q\\
&\quad + I^*c\nu\omega^2q + I^*a\omega^2qx + 2I^*a\omega^2qy + I^*a^2\omega qy + I^*a\omega^2qz + I^*c\omega^2qx - Sc\nu\omega^2q\\
&\quad + I^*c\omega^2qy + I^*c\omega^2qz - Sc\omega^2qy + I^*\nu\omega^2qx + I^*\nu\omega^2qy + I^*\nu\omega^2qz\\
&\quad + I^*\omega^2qxy + I^*\omega^2qyz + I^*ac\nu\omega q - Sac\nu\omega q + I^*ac\omega qy - Sac\omega qy + I^*a\nu\omega qx\\
&\quad + I^*a\nu\omega qy + I^*a\nu\omega qz + I^*c\nu\omega qy + I^*c\nu\omega qz + I^*a\omega qxy + I^*a\omega qyz\\
&\quad + I^*c\omega qxy - Sc\nu\omega qy + I^*c\nu qyz + I^*c\omega qyz + I^*\nu\omega qxy + I^*\nu\omega qyz.
\end{aligned}
\tag{11}
$$

Apparently, for positive endemic equilibrium point E^* $(S^*, E^*, I^*, V^*, R^*)$ is locally asymptotically stable [48] if the following inequalities are satisfied

$$
det_1 = a_5 > 0,\quad det_2 = \begin{vmatrix} a_1 & 1 \\ a_3 & a_2 \end{vmatrix} > 0,\quad det_3 = \begin{vmatrix} a_1 & 1 & 0 \\ a_3 & a_2 & a_1 \\ 0 & a_4 & a_3 \end{vmatrix} > 0,\quad \text{and}\quad det_4 = \begin{vmatrix} a_1 & 1 & 0 & 0 \\ a_3 & a_2 & a_1 & 1 \\ a_5 & a_4 & a_3 & a_2 \\ 0 & 0 & a_5 & a_4 \end{vmatrix} > 0. \tag{12}
$$

Considering the coefficients (11) *of the characteristic equation* (10)*, the Routh–Hurwitz criterion [49] is satisfied because all of the coefficients are positive and inequalities* (12) *are satisfied. As a result, all the eigenvalues are negative or have negative real parts and $R_0 > 1$. Hence, the model is locally asymptotically stable around the disease-endemic equilibrium point, E^*.*

3 Global stability analysis

For the endemic Lyapunov function, $\{S, E, I, V, R\}$, $\dot{L} < 0$ is the endemic equilibrium E^*.

Theorem 3 *[10, 11, 15] If $R_0 > 1$, the endemic equilibrium point E^* of the model* (2) *is globally asymptotically stable otherwise unstable.*

Proof 3 *For proof, the Lyapunov function can be written as*

$$L(S^*, E^*, I^*, V^*, R^*) = \left(S - S^* - S^* \log \frac{S^*}{S}\right) + \left(E - E^* - E^* \log \frac{E^*}{E}\right) + \left(V - V^* - V^* \log \frac{V^*}{V}\right) + \left(I - I^* - I^* \log \frac{I^*}{I}\right) + \left(R - R^* - R^* \log \frac{R^*}{R}\right). \tag{13}$$

Therefore, applying the derivative respect to t on both sides yields

$$\frac{dL}{dt} = \left(\frac{S - S^*}{S}\right)\dot{S} + \left(\frac{E - E^*}{E}\right)\dot{E} + \left(\frac{I - I^*}{I}\right)\dot{I} + \left(\frac{V - V^*}{V}\right)\dot{V} + \left(\frac{R - R^*}{R}\right)\dot{R}, \tag{14}$$

which implies that

$$\left.\begin{aligned}\frac{dL}{dt} &= \left(\frac{S - S^*}{S}\right)(\mu - qS(t)I(t) - (\omega + a)S(t) + \nu R(t)) \\ &+ \left(\frac{E - E^*}{E}\right)(qS(t)I(t) - (c + \omega + a)E(t)) \\ &+ \left(\frac{I - I^*}{I}\right)(cE(t) - (a + \omega + x + z)I(t)) \\ &+ \left(\frac{V - IV^*}{V}\right)(aI(t) - (\omega + y)V(t) + aE(t) + aS(t)) \\ &+ \left(\frac{R - R^*}{R}\right)(xI(t) + yV(t) - (\omega + \nu)R(t)).\end{aligned}\right\} \tag{15}$$

Furthermore,

$$\left.\begin{aligned}\frac{dL}{dt} &= \mu - \frac{\mu S^*}{S} - \frac{qI}{S}(S - S^*)^2 + \frac{q}{S}I^*(S - S^*)^2 - \frac{(\omega + a)}{S}(S - S^*)^2 + \nu R - \nu R^* - \frac{VS^*R}{S} + \frac{VS^*R^*}{S} \\ &- \frac{qE^*I^*}{E} + qSI - qS^*I - \frac{qE^*I^*S^*}{E} - \frac{(c + \omega + a)}{E}(E - E^*)^2 + \frac{cI^*E}{I} - \frac{cE^*I^*}{I} \\ &+ cE - cE^* - (a + \omega + x + z)\frac{(I - I^*)^2}{I} + aI - aI^* - \frac{aVI^*}{V} - \frac{aV^*I^*}{V} - (\omega + y)\frac{(V - V^*)^2}{V} \\ &+ aE - aE^* - \frac{aV^*E}{V} - \frac{aE^*V^*}{V}.\end{aligned}\right\} \tag{16}$$

Now, Eq. (16) *can be written in the form of:*

$$\frac{dL}{dt} = \digamma - \alpha, \tag{17}$$

where,

$$\digamma = \mu + \frac{q}{S}I^*(S - S^*)^2 + \nu R + \frac{VS^*R^*}{S} + qSI + \frac{cI^*E}{I} + cE + aI + aE, \tag{18}$$

and

$$\left.\begin{aligned}\alpha &= -\frac{\mu S^*}{S} - \frac{qI}{S}(S - S^*)^2 - \frac{(\omega + a)}{S}(S - S^*)^2 - \nu R^* - \frac{VS^*R}{S} \\ &- \frac{qE^*I^*}{E} - qS^*I - \frac{qE^*I^*S^*}{E} - \frac{(c + \omega + a)}{E}(E - E^*)^2 - \frac{cE^*I^*}{I} \\ &- cE^* - (a + \omega + x + z)\frac{(I - I^*)^2}{I} - aI^* - \frac{aVI^*}{V} - \frac{aV^*I^*}{V} \\ &- (\omega + y)\frac{(V - V^*)^2}{V} - aE^* - \frac{aV^*E}{V} - \frac{aE^*V^*}{V}.\end{aligned}\right\} \tag{19}$$

Eventually, if $\digamma < \alpha$ *then* $\frac{dL}{dt} < 0$ *while using* $S = S^*, E = E^*, I = I^*, V = V^*$, *and* $R = R^*$, $0 = \digamma - \alpha$ *implies that* $\frac{dL}{dt} = 0$. *Also, for the suggested model* (2) *we are looking the largest compact invariant set* $\left\{(S^*, E^*, I^*, V^*, R^*) \in \Omega : \frac{dL}{dt} = 0\right\}$ *is the endemic equilibrium point* $E^* = (S^*, E^*, I^*, V^*, R^*)$ *of the considered model. Thus, the model* (2) *is stable in* Ω *if* $R_0 > 1$ *and* $\digamma < \alpha$.

4 Homotopy perturbation method

Consider a general type problem given by

$$A(\mu) - f(r) = 0, \quad r \in \Omega, \tag{20}$$

with the boundary conditions as

$$\beta\left(\mu, \frac{\partial \mu}{\partial n}\right) = 0, r \in \Gamma, \tag{21}$$

where A is a general differential operator, β is a boundary operator, $f(r)$ is a known analytic function, and Γ is the boundary of the domain Ω. The operator A is divided into linear part L and nonlinear part N. Therefore, (20) can be written as

$$L(\mu) + N(u) - f(r) = 0. \tag{22}$$

By HPM, we can construct a homotopy as

$$v(r, \mathbf{s}) : \Omega \times [0, 1] \to R, \tag{23}$$

satisfying

$$H(v, \mathbf{s}) = (1 - \mathbf{s})[L(v) - L(\mu)] + \mathbf{s}[A(v - f(r))] = 0, \tag{24}$$

which is also equivalent to

$$H(v, \mathbf{s}) = L(v) - L(\mu_0) + \mathbf{s}L(v_0) + \mathbf{s}[N(v) - f(r)] = 0, \tag{25}$$

where $\mathbf{s} \in [0;1]$ is an embedding parameter, and μ_0 is the initial approximation of the given equation that satisfies the boundary conditions; we have

$$\begin{aligned} H(v, 0) &= L(v) - L(\mu_0) = 0, \\ H(v, 1) &= A(v) - f(r) = 0. \end{aligned} \tag{26}$$

Keeping these points, we construct the required solution to equation (22) as

$$v = v_0 + \mathbf{s}^1 v_1 + \mathbf{s}^2 v_2 + \mathbf{s}^3 v_3 + \cdots. \tag{27}$$

Furthermore, by taking the limit as $p \to 1$ in the approximation equation (27), one has

$$\lim_{\mathbf{s}\to 1} v = \lim_{\mathbf{s}\to 1} v_0 + \mathbf{s}^1 v_1 + \mathbf{s}^2 v_2 + \mathbf{s}^3 v_3 + \cdots, \tag{28}$$

which yields

$$v = v_0 + v_1 + v_2 + v_3 + \cdots. \tag{29}$$

Equation (29) represents the semianalytic solution of the problem equation (20).

5 Approximate solution of the proposed COVID-19 model

Applying homotopy on the model (2)

$$\left.\begin{aligned} \mathcal{D}S(t) - \mathcal{D}S(0) &= \mathbf{s}[\mu - qS(t)I(t) - (\omega + a)S(t) + \nu R(t)], \\ \mathcal{D}E(t) - \mathcal{D}E(0) &= \mathbf{s}[qS(t)I(t) - (c + \omega + a)E(t)], \\ \mathcal{D}I(t) - \mathcal{D}I(0) &= \mathbf{s}[cE(t) - (a + \omega + x + z)I(t)], \\ \mathcal{D}V(t) - \mathcal{D}V(0) &= \mathbf{s}[aI(t) - (\omega + y)V(t) + aE(t) + aS(t)], \\ \mathcal{D}R(t) - \mathcal{D}R(0) &= \mathbf{s}[xI(t) + yV(t) - (\omega + \nu)R(t)]. \end{aligned}\right\} \tag{30}$$

Assume series solution to the model (2), such that

$$\left.\begin{aligned} S(t) &= S(0) + \mathbf{s}S_1(t) + \mathbf{s}^2 S_2(t) + \mathbf{s}^3 S_3(t) + \cdots, \\ E(t) &= E(0) + \mathbf{s}E_1(t) + \mathbf{s}^2 E_2(t) + \mathbf{s}^3 E_3(t) + \cdots, \\ I(t) &= I(0) + \mathbf{s}I_1(t) + \mathbf{s}^2 I_2(t) + \mathbf{s}^3 I_3(t) + \cdots, \\ V(t) &= V(0) + \mathbf{s}V_1(t) + \mathbf{s}^2 V_2(t) + \mathbf{s}^3 V_3(t) + \cdots, \\ R(t) &= R(0) + \mathbf{s}R_1(t) + \mathbf{s}^2 R_2(t) + \mathbf{s}^3 R_3(t) + \cdots. \end{aligned}\right\} \tag{31}$$

Now by comparison we get $\mathbf{s}^0, \mathbf{s}^1, \mathbf{s}^2, \cdots$ by using system of equations (31) in (30), we have:

Zeroth-order problem

$$\left.\begin{aligned}
\mathbf{s}^0 &:= \mathcal{D}S(0) = \mathcal{D}S_0,\\
\mathbf{s}^0 &:= \mathcal{D}E(0) = \mathcal{D}E_0,\\
\mathbf{s}^0 &:= \mathcal{D}I(0) = \mathcal{D}I_0,\\
\mathbf{s}^0 &:= \mathcal{D}V(0) = \mathcal{D}V_0,\\
\mathbf{s}^0 &:= \mathcal{D}R(0) = \mathcal{D}R_0.
\end{aligned}\right\} \tag{32}$$

First-order problem

$$\left.\begin{aligned}
\mathbf{s}^1 &:= \mathcal{D}S_1 = \mu - qS(0)I(0) - (\omega + a)S(0) + \nu R(0),\\
\mathbf{s}^1 &:= \mathcal{D}E_1 = qS(0)I(0) - (c + \omega + a)E(0),\\
\mathbf{s}^1 &:= \mathcal{D}I_1 = cE(0) - (a + \omega + x + z)I(0),\\
\mathbf{s}^1 &:= \mathcal{D}V_1 = aI(0) - (\omega + y)V(0) + aE(0) + aS(0),\\
\mathbf{s}^1 &:= \mathcal{D}R_1 = xI(0) + yV(0) - (\omega + \nu)R(0).
\end{aligned}\right\} \tag{33}$$

Second-order problem

$$\left.\begin{aligned}
\mathbf{s}^2 &:= \mathcal{D}S_2 = -qS_1(t)I_1(t) - (\omega + a)S_1(t) + \nu R_1(t),\\
\mathbf{s}^2 &:= \mathcal{D}E_2 = qS_1(t)I_1(t) - (c + \omega + a)E_1(t),\\
\mathbf{s}^2 &:= \mathcal{D}I_2 = cE_1(t) - (a + \omega + x + z)I_1(t),\\
\mathbf{s}^2 &:= \mathcal{D}V_2 = aI_1(t) - (\omega + y)V_1(t) + aE_1(t) + aS_1(t),\\
\mathbf{s}^2 &:= \mathcal{D}R_2 = xI_1(t) + yV_1(t) - (\omega + \nu)R_1(t).
\end{aligned}\right\} \tag{34}$$

Third-order problem

$$\left.\begin{aligned}
\mathbf{s}^3 &:= \mathcal{D}S_3 = -qS_2(t)I_2(t) - (\omega + a)S_2(t) + \nu R_2(t),\\
\mathbf{s}^3 &:= \mathcal{D}E_3 = qS_2(t)I_2(t) - (c + \omega + a)E_2(t),\\
\mathbf{s}^3 &:= \mathcal{D}I_3 = cE_2(t) - (a + \omega + x + z)I_2(t),\\
\mathbf{s}^3 &:= \mathcal{D}V_3 = aI_2(t) - (\omega + y)V_2(t) + aE_2(t) + aS_2(t),\\
\mathbf{s}^3 &:= \mathcal{D}R_3 = xI_2(t) + yV_2(t) - (\omega + \nu)R_2(t).\\
&\vdots
\end{aligned}\right\} \tag{35}$$

nth-order problem

$$\left.\begin{aligned}
\mathbf{s}^{(n+1)} &:= \mathcal{D}S_{(n+1)} = -qS_{(n)}(t)I_{(n)}(t) - (\omega + a)S_{(n)}(t) + \nu R_{(n)}(t),\\
\mathbf{s}^{(n+1)} &:= \mathcal{D}E_{(n+1)} = qS_{(n)}(t)I_{(n)}(t) - (c + \omega + a)E_{(n)}(t),\\
\mathbf{s}^{(n+1)} &:= \mathcal{D}I_{(n+1)} = cE_{(n)}(t) - (a + \omega + x + z)I_{(n)}(t),\\
\mathbf{s}^{(n+1)} &:= \mathcal{D}V_{(n+1)} = aI_{(n)}(t) - (\omega + y)V_{(n)}(t) + aE_{(n)}(t) + aS_{(n)}(t),\\
\mathbf{s}^{(n+1)} &:= \mathcal{D}R_{(n+1)} = xI_{(n)}(t) + yV_{(n)}(t) - (\omega + \nu)R_{(n)}(t).
\end{aligned}\right\} \tag{36}$$

Next, system of equations (33) becomes:

$$\left.\begin{aligned}
S_1(t) &= (\mu - qS_0I_0 - (\omega + a)S_0 + \nu R_0)t,\\
E_1(t) &= (qS_0I_0 - (c + \omega + a)E_0)t,\\
I_1(t) &= (cE_0 - (a + \omega + x + z)I_0)t,\\
V_1(t) &= (aI_0 - (\omega + y)V_0 + aE_0 + aS_0)t,\\
R_1(t) &= (xI_0 + yV_0 - (\omega + \nu)R_0)t.
\end{aligned}\right\} \tag{37}$$

Next, system of equations (34) becomes:

$$\left.\begin{aligned} S_2(t) &= (-q(E_0c - I_0(a+\omega+x+z))(\mu + R_0\nu - S_0(a+\omega) - I_0S_0q))t^3 \\ &\quad + (\nu(I_0x + V_0y - R_0(\nu+\omega)) - (a+\omega)(\mu + R_0\nu - S_0(a+\omega) - I_0S_0q))t^2, \\ E_2(t) &= (q(E_0c - I_0(a+\omega+x+z))(\mu + R_0\nu - S_0(a+\omega) - I_0S_0q))t^3 \\ &\quad + ((E_0(a+c+\omega) - I_0S_0q)(a+c+\omega))t^2, \\ I_2(t) &= (-(E_0c - I_0(a+\omega+x+z))(a+\omega+x+z) - c(E_0(a+c+\omega) - I_0S_0q))t^2, \\ V_2(t) &= (a(E_0c - I_0(a+\omega+x+z)) - a(E_0(a+c+\omega) - I_0S_0q) - (\omega+y)(E_0a \\ &\quad + I_0a + S_0a - V_0(\omega+y)) + a(\mu + R_0\nu - S_0(a+\omega) - I_0S_0q))t^2, \\ R_2(t) &= (x(E_0c - I_0(a+\omega+x+z)) - (\nu+\omega)(I_0x + V_0y - R_0(\nu+\omega)) \\ &\quad + y(E_0a + I_0a + S_0a - V_0(\omega+y)))t^2. \end{aligned}\right\} \tag{38}$$

Next, system of equations (35) becomes:

$$\left.\begin{aligned} S_3(t) &= (-q^2\alpha_5\alpha_2\alpha_3)t^6 + (q\alpha_1\alpha_2)t^5 + (q(a+\omega)\alpha_5\alpha_3)t^4 + (\nu(x\alpha_5 - (\nu+\omega)\alpha_4 \\ &\quad + y(E_0a + I_0a + S_0a - V_0(\omega+y))) - (a+\omega)\alpha_1)t^3, \end{aligned}\right\} \tag{39}$$

where,

$$\left.\begin{aligned} \alpha_1 &= \nu\alpha_4 - (a+\omega)\alpha_3, \\ \alpha_2 &= \alpha_5(a+\omega+x+z) + c(E_0(a+c+\omega) - I_0S_0q), \\ \alpha_3 &= \mu + R_0\nu - S_0(a+\omega) - I_0S_0q, \\ \alpha_4 &= I_0x + V_0y - R_0(\nu+\omega), \\ \alpha_5 &= E_0c - I_0(a+\omega+x+z). \end{aligned}\right\} \tag{40}$$

$$\begin{aligned} E_3(t) &= (q^2\kappa_3\kappa_2\kappa_1)t^6 + (-q(\nu(I_0x + V_0y - R_0(\nu+\omega)) - (a+\omega)\kappa_1)\kappa_2)t^5 \\ &\quad + (-q\kappa_3(a+c+\omega)\kappa_1)t^4 + (-\kappa_4(a+c+\omega)^2)t^3, \end{aligned} \tag{41}$$

where,

$$\left.\begin{aligned} \kappa_1 &= \mu + R_0\nu - S_0(a+\omega) - I_0S_0q, \\ \kappa_2 &= \kappa_3(a+\omega+x+z) + c\kappa_4, \\ \kappa_3 &= E_0c - I_0(a+\omega+x+z), \\ \kappa_4 &= E_0(a+c+\omega) - I_0S_0q. \end{aligned}\right\} \tag{42}$$

$$I_3(t) = (cq\tau_2(\mu + R_0\nu - S_0(a+\omega) - I_0S_0q))t^4 + ((\tau_2(a+\omega+x+z) + c\tau_1)(a+\omega+x+z) + c\tau_1(a+c+\omega))t^3, \tag{43}$$

where,

$$\left.\begin{aligned} \tau_1 &= E_0(a+c+\omega) - I_0S_0q, \\ \tau_2 &= E_0c - I_0(a+\omega+x+z). \end{aligned}\right\} \tag{44}$$

$$\begin{aligned} V_3(t) &= (a(\nu(I_0x + V_0y - R_0(\nu+\omega)) - (a+\omega)\phi_2) - a(\phi_3(a+\omega+x+z) + c\phi_1) \\ &\quad + (\omega+y)((\omega+y)(E_0a + I_0a + S_0a - V_0(\omega+y)) + a\phi_1 - a\phi_3 - a\phi_2) + a\phi_1(a+c+\omega))t^3, \end{aligned} \tag{45}$$

where,

$$\left.\begin{aligned} \phi_1 &= E_0(a+c+\omega) - I_0S_0q, \\ \phi_2 &= \mu + R_0\nu - S_0(a+\omega) - I_0S_0q, \\ \phi_3 &= E_0c - I_0(a+\omega+x+z). \end{aligned}\right\} \tag{46}$$

$$\begin{aligned} R_3(t) &= (-y((\omega+y)\sigma_2 + a\sigma_3 - a\sigma_1 - a(\mu + R_0\nu - S_0(a+\omega) - I_0S_0q)) - (\nu+\omega)(x\sigma_1 \\ &\quad - (\nu+\omega)(I_0x + V_0y - R_0(\nu+\omega)) + y\sigma_2) - x(\sigma_1(a+\omega+x+z) + c\sigma_3))t^3, \end{aligned} \tag{47}$$

where,

$$\left.\begin{aligned}\sigma_1 &= E_0c - I_0(a+\omega+x+z),\\ \sigma_2 &= E_0a + I_0a + S_0a - V_0(\omega+y),\\ \sigma_3 &= E_0(a+c+\omega) - I_0S_0q.\end{aligned}\right\} \tag{48}$$

The resultant solution to model (2) is obtained as:

$$\left.\begin{aligned}S(t) &= (-q^2\alpha_5\alpha_2\alpha_3)t^6 + (q\alpha_1\alpha_2)t^5 + (q(a+\omega)\alpha_5\alpha_3)t^4 + (\nu(x\alpha_5 - (\nu+\omega)\alpha_4\\ &\quad + y(E_0a + I_0a + S_0a - V_0(\omega+y))) - (a+\omega)\alpha_1 - q\alpha_5\alpha_3)t^3 + \alpha_1t^2 + \alpha_3t + S_0,\\ E(t) &= (q^2\kappa_3\kappa_2\kappa_1)t^6 + (-q(\nu(I_0x + V_0y - R_0(\nu+\omega)) - (a+\omega)\kappa_1)\kappa_2)t^5 + (-q\kappa_3(a+c+\omega)\kappa_1)t^4\\ &\quad + (q\kappa_3\kappa_1 - \kappa_4(a+c+\omega)^2)t^3 + (\kappa_4(a+c+\omega))t^2 + (I_0S_0q - \kappa_5)t + E_0,\\ I(t) &= (cq\tau_1(\mu + R_0\nu - S_0(a+\omega) - I_0S_0q))t^4 + ((\tau_1(a+\omega+x+z) + c\tau_2)(a+\omega+x+z)\\ &\quad + c\tau_2(a+c+\omega))t^3 + (-\tau_1(a+\omega+x+z) - c\tau_2)t^2 + \tau_1t + I_0,\\ V(t) &= (a(\nu(I_0x + V_0y - R_0(\nu+\omega)) - (a+\omega)\phi_3) - a(\phi_4(a+\omega+x+z) + c\phi_1)\\ &\quad + (\omega+y)((\omega+y)\phi_2 + a\phi_1 - a\phi_4 - a\phi_3) + a\phi_1(a+c+\omega))t^3 + (a\phi_4 - a\phi_1\\ &\quad - (\omega+y)\phi_2 + a\phi_3)t^2 + \phi_2t + V_0,\\ R(t) &= (-y((\omega+y)\sigma_4 + a\sigma_1 - a\sigma_3 - a(\mu + R_0\nu - S_0(a+\omega) - I_0S_0q)) - (\nu+\omega)\sigma_2\\ &\quad - x(\sigma_3(a+\omega+x+z) + c\sigma_1))t^3 + \sigma_2t^2 + \sigma_5t + R_0.\end{aligned}\right\} \tag{49}$$

Furthermore, we present the following plots based on solution (49) in the graphical justification such that:

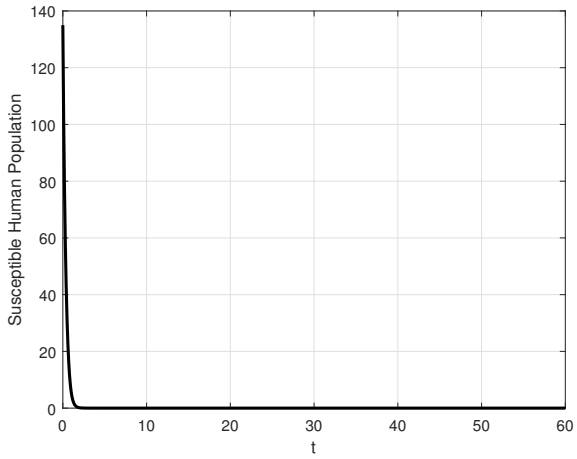

Figure 9. The plot shows the numerical simulation of susceptible human population, $S(t)$.

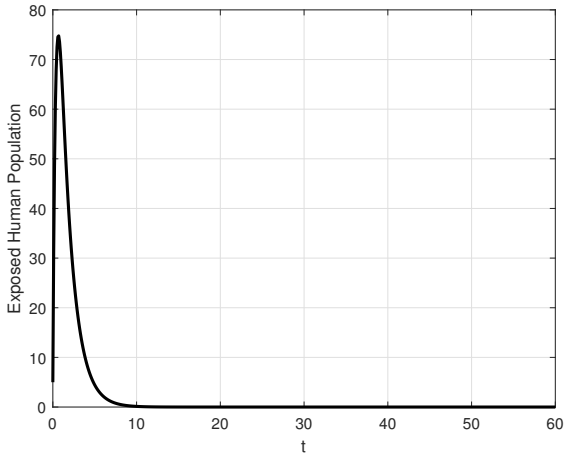

Figure 10. The plot shows the numerical simulation of exposed human population, $E(t)$.

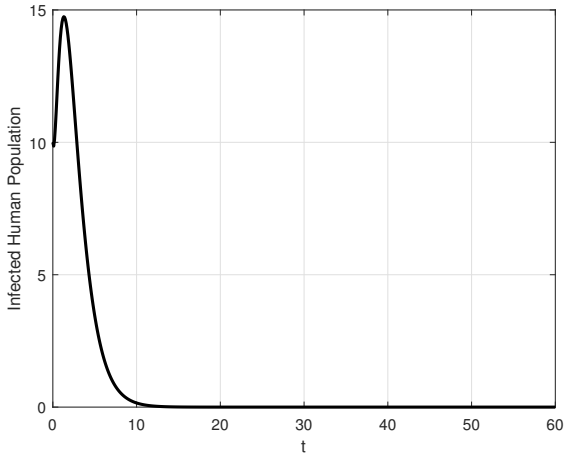

Figure 11. The plot shows the numerical simulation of infected human population, $I(t)$.

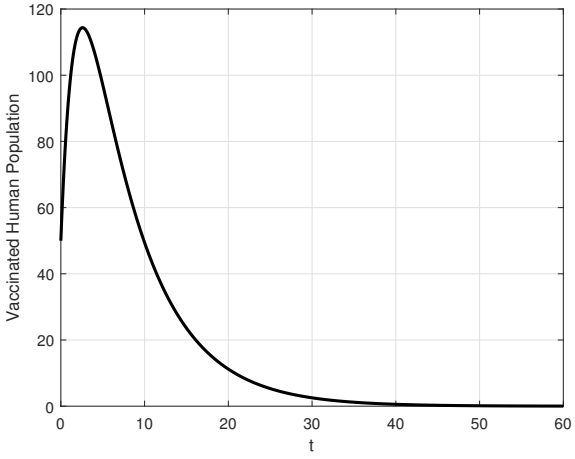

Figure 12. The plot shows the numerical simulation of vaccinated human population, $V(t)$.

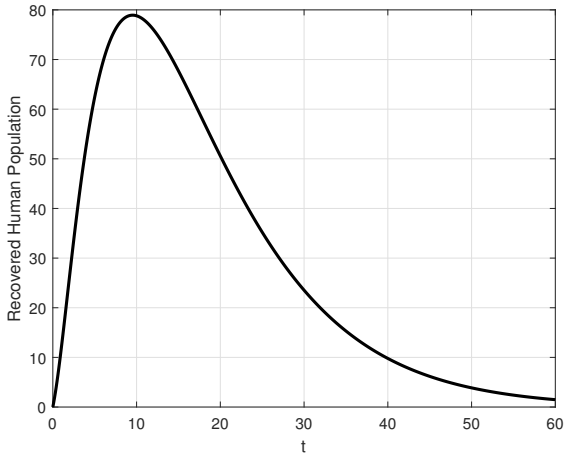

Figure 13. The plot shows the numerical simulation of recovered human population, $R(t)$.

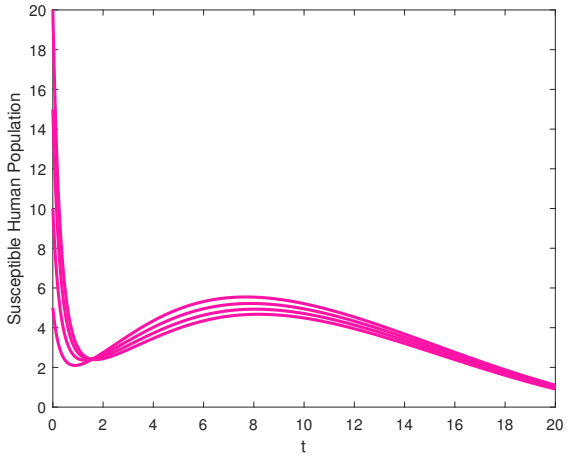

Figure 14. The plot shows the numerical simulation of susceptible human population, $R(t)$ with asymptotic stability graphically.

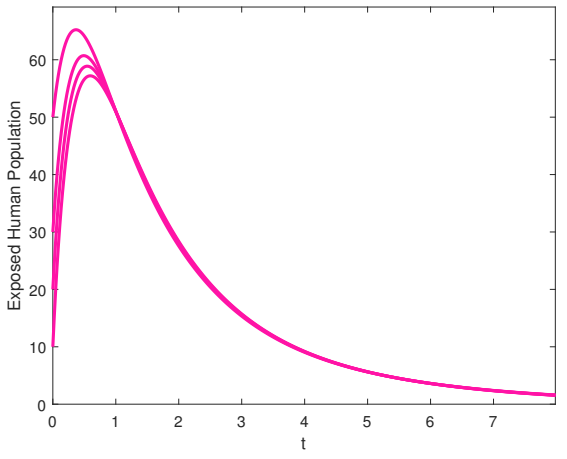

Figure 15. The plot shows the numerical simulation of exposed human population, $E(t)$ with asymptotic stability graphically.

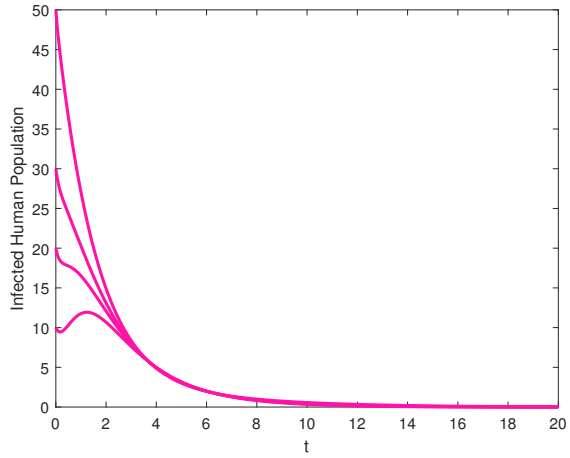

Figure 16. The plot shows the numerical simulation of infected human population, $I(t)$ with asymptotic stability graphically.

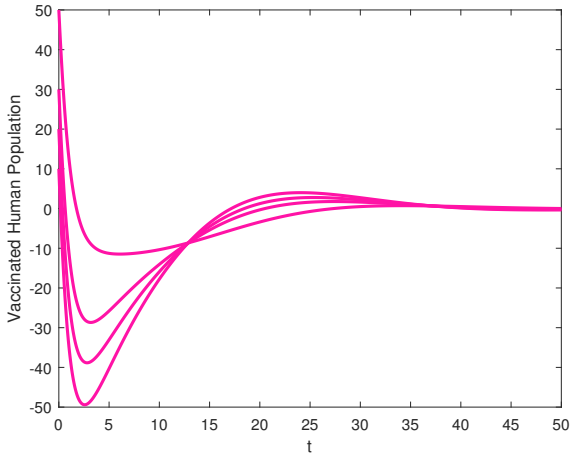

Figure 17. The plot shows the numerical simulation of vaccinated human population, $V(t)$ with asymptotic stability graphically.

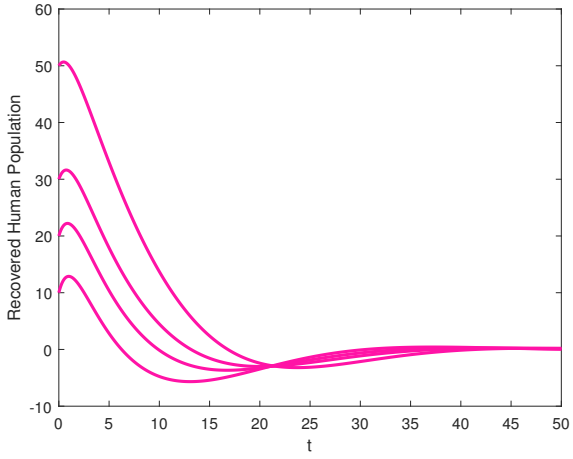

Figure 18. The plot shows the numerical simulation of recovered human population, $R(t)$ with asymptotic stability graphically.

Table 1. Table of description and initial condition of compartment of population

Symbol of Compartment	Description of Compartment	Initial Condition
$S(t)$	Susceptible Human Population	$N-(E+I+V+R)$
$E(t)$	Exposed Human Population	10
$I(t)$	Infected Human Population	20
$V(t)$	Vaccinated Human Population	30
$R(t)$	Recovered Human Population	0
N	Total Population	200

Table 2. Table of description and values of parameters

Symbol	Description of Parameter	Unit	Value
ω	Natural Death Rate	day^{-1}	$\frac{1}{67.7\times 365}$
μ	Recruitment Rate	day^{-1}	$\omega \times N$
q	Transmission rate	day^{-1}	0.2784
a	Vaccination Rate	day^{-1}	0.5
ν	Lose of Immunity in Recovered Population	day^{-1}	0.1
c	Rate of Infection of Exposed Population	day^{-1}	0.23
x	Recovery Rate of Infected Population	day^{-1}	0.05
y	Recovery Rate of Vaccinated Population	day^{-1}	0.15
z	Death Rate of Infected Population due to COVID−19 Infection	day^{-1}	0.32

6 Results and discussion

We discuss the outcomes of the stability analysis of COVID−19 at both disease-free and endemic equilibrium points, the spread of the infection is asymptotically stable locally and globally under certain conditions such that $F < \alpha$. For global stability analysis the Lyapunov function is used at disease free and endemic equilibrium points. The Lyapunov function is negative is $F < \alpha$ so it means that the spread of infection will be stable and will not be spread in the population so it cannot lead to a pandemic. After the recent invention of the vaccination, we implemented the vaccinated individuals compartment $V(t)$ also the Figure (12) which is the graphical behaviour. We discuss the outcomes of the Homotopy Perturbation Method by applying it to the COVID−19 model, (2). In Figure (9), the dynamics of susceptible human population ion has been shown in which the population decreases with time due to the large transmission b and vaccination a rates. In Figure (10), the plot shows the dynamics of the Exposed Human population in which the population increased in the first week while then decreased asymptotically. In Figure (11), in the first two weeks, the prevalence increased due to the higher rate of transmission and infectivity, and then the disease disappeared from the population thus the prevalence decreasing to zero. In Figures (12) and (13), the dynamics of the Vaccinated and Recovered populations have been shown. While the Figures (14), (15), (16), (17), and (18) give the asymptotically stable behaviour of Susceptible, Exposed, Infected, Vaccinated, and Recovered Populations, respectively by varying the initial conditions for each class of the model (2).

7 Conclusion

In this paper, we studied the stability of the COVID−19 model which is locally and globally asymptotically stable around the disease-free and endemic equilibrium points by having negative eigenvalues at both disease-free and endemic equilibrium points satisfying Routh−Hurwitz criterion. Global stability is investigated with the help of Lyapunov function. The disease is locally asymptotically stable at disease−free equilibrium point if $R_0 < 1$ while unstable if $R_0 > 1$ likewise, at endemic−equilibrium point if $R_0 > 1$ while unstable if $R_0 < 1$. Looking for the behaviour of the vaccination in population, it has a positive impact on population and ability to protect the population from re−infection and future pandemics. Individual vaccination, rapid diagnosis, and possibly early treatment are the most effective ways to prevent coronavirus infection in the community. As is generally known, the COVID-19 infection has caused significant damage to human society, with many developing countries experiencing significant financial losses. As a result, adequate individual vaccines and infection control should be a priority for less developed countries in order to sustain their populations and economies. On analyzing the semi-analytic solution of the COVID−19 models using the homotopy perturbation method, we have obtained that the homotopy perturbation method is efficient, powerful, and more accurate and is capable of obtaining a semi-analytic solution that is both linear and non−linear as well. This method can be applied to ordinary differential equations in integer-order and fractional orders too, partial differential equations, and boundary value problems. The said method can be applied to the system of many differential equations and higher-order problems. In all scenarios, the solution can be obtained semi-analytically and more accurately.

Declarations

Consent for publication

Not applicable.

Conflicts of interest

The authors declare that they have no known competing financial interests or personal relationships that could have appeared to influence the work reported in this paper.

Author's contributions

M.S.: Writing-Original draft preparation, Validation, Conceptualization, Methodology, Software. J.L.: Supervision, Validation, Conceptualization, Methodology, Investigation, Software. M.A.: Writing-Original draft preparation, Methodology. M.F.: Visualization, Methodology, Writing–Reviewing and Editing. All authors discussed the results and contributed to the final manuscript.

Acknowledgements

Not applicable.

References

[1] https://www.worldometers.info/coronavirus/, Coronavirus cases. Access Date: 20.06.2022
[2] Sinan, M., Ali, A., Shah, K., Assiri, T.A., & Nofal, T.A. Stability analysis and optimal control of COVID-19 pandemic SEIQR fractional mathematical model with harmonic mean type incidence rate and treatment. *Results in Physics*, 22, 103873, (2021). [CrossRef]
[3] Ali, A., Khan, M.Y., Sinan, M., Allehiany, F.M., Mahmoud, E.E., Abdel-Aty, A.H., & Ali, G. Theoretical and numerical analysis of novel COVID-19 via fractional order mathematical model. *Results in physics*, 20, 103676, (2021). [CrossRef]
[4] Asamoah, J.K.K., Owusu, M.A., Jin, Z., Oduro, F.T., Abidemi, A., & Gyasi, E.O. Global stability and cost-effectiveness analysis of COVID-19 considering the impact of the environment: using data from Ghana. *Chaos, Solitons & Fractals*, 140, 110103, (2020). [CrossRef]
[5] Péni, T., Csutak, B., Szederkényi, G., & Röst, G. Nonlinear model predictive control with logic constraints for COVID-19 management. *Nonlinear Dynamics*, 102(4), 1965-1986, (2020). [CrossRef]
[6] Matouk, A.E. Complex dynamics in susceptible-infected models for COVID-19 with multi-drug resistance. *Chaos, Solitons & Fractals*, 140, 110257, (2020). [CrossRef]
[7] Sun, D., Duan, L., Xiong, J., & Wang, D. Modeling and forecasting the spread tendency of the COVID-19 in China. *Advances in Difference Equations*, 2020(1), 1-16, (2020). [CrossRef]
[8] Ahmed, I., Baba, I.A., Yusuf, A., Kumam, P., & Kumam, W. Analysis of Caputo fractional-order model for COVID-19 with lockdown. *Advances in difference equations*, 2020(1), 1-14, (2020). [CrossRef]
[9] Alqahtani, R.T. Mathematical model of SIR epidemic system (COVID-19) with fractional derivative: stability and numerical analysis. *Advances in Difference Equations*, 2021(1), 1-16, (2021). [CrossRef]
[10] Naik, P.A., Zu, J., & Owolabi, K.M. Global dynamics of a fractional order model for the transmission of HIV epidemic with optimal control. *Chaos, Solitons & Fractals*, 138, 109826, (2020). [CrossRef]
[11] Zhu, L., Zhou, X., Li, Y., & Zhu, Y. Stability and bifurcation analysis on a delayed epidemic model with information-dependent vaccination. *Physica scripta*, 94(12), 125202, (2019). [CrossRef]
[12] Allegretti, S., Bulai, I.M., Marino, R., Menandro, M.A., & Parisi, K. Vaccination effect conjoint to fraction of avoided contacts for a Sars-Cov-2 mathematical model. *Mathematical Modelling and Numerical Simulation with Applications*, 1(2), 56-66, (2021). [CrossRef]
[13] Shah, K., Abdeljawad, T., Mahariq, I., & Jarad, F. Qualitative analysis of a mathematical model in the time of COVID-19. *BioMed Research International*, 2020, (2020). [CrossRef]
[14] Pais, R.J., & Taveira, N. Predicting the evolution and control of the COVID-19 pandemic in Portugal. *F1000Research*, 9, (2020). [CrossRef]
[15] Martcheva, M. *An introduction to mathematical epidemiology* (Vol. 61, pp. 9-31). New York: Springer, (2015).
[16] Samji, H., Wu, J., Ladak, A., Vossen, C., Stewart, E., Dove, N., ... & Snell, G. Mental health impacts of the COVID-19 pandemic on children and youth–a systematic review. *Child and adolescent mental health*, 27(2), 173-189, (2022). [CrossRef]
[17] Li, X.P., Gul, N., Khan, M.A., Bilal, R., Ali, A., Alshahrani, M.Y., ... & Islam, S. A new Hepatitis B model in light of asymptomatic carriers and vaccination study through Atangana–Baleanu derivative. *Results in Physics*, 29, 104603, (2021). [CrossRef]
[18] Din, A., & Li, Y. Stationary distribution extinction and optimal control for the stochastic hepatitis B epidemic model with partial immunity. *Physica Scripta*, 96(7), 074005, (2021). [CrossRef]
[19] Din, A., & Li, Y. Lévy noise impact on a stochastic hepatitis B epidemic model under real statistical data and its fractal–fractional Atangana–Baleanu order model. *Physica Scripta*, 96(12), 124008, (2021). [CrossRef]
[20] Din, A., Li, Y., Khan, F.M., Khan, Z.U., & Liu, P. On Analysis of fractional order mathematical model of Hepatitis B using Atangana–Baleanu Caputo (ABC) derivative. *Fractals*, 30(01), 2240017, (2022). [CrossRef]
[21] Din, A., Li, Y., Yusuf, A., & Ali, A.I. Caputo type fractional operator applied to Hepatitis B system. *Fractals*, 30(01), 2240023, (2022). [CrossRef]
[22] Din, A., & Abidin, M.Z. Analysis of fractional-order vaccinated Hepatitis-B epidemic model with Mittag-Leffler kernels. *Mathematical Modelling and Numerical Simulation with Applications*, 2(2), 59-72, (2022). [CrossRef]
[23] Ali, A., Alshammari, F.S., Islam, S., Khan, M.A., & Ullah, S. Modeling and analysis of the dynamics of novel coronavirus (COVID-19) with Caputo fractional derivative. *Results in Physics*, 20, 103669, (2021). [CrossRef]
[24] Daşbaşı, B. Stability analysis of an incommensurate fractional-order SIR model. *Mathematical Modelling and Numerical Simulation with Applications*, 1(1), 44-55, (2021). [CrossRef]
[25] Ali, A., Islam, S., Khan, M.R., Rasheed, S., Allehiany, F.M., Baili, J., ... & Ahmad, H. Dynamics of a fractional order Zika virus model with mutant. *Alexandria Engineering Journal*, 61(6), 4821-4836, (2022). [CrossRef]
[26] Ali, A., Iqbal, Q., Asamoah, J.K.K., & Islam, S. Mathematical modeling for the transmission potential of Zika virus with optimal control strategies. *The European Physical Journal Plus*, 137(1), 1-30, (2022). [CrossRef]
[27] Zhang, X.H., Ali, A., Khan, M.A., Alshahrani, M.Y., Muhammad, T., & Islam, S. Mathematical analysis of the TB model with treatment via Caputo-type fractional derivative. *Discrete Dynamics in Nature and Society*, 2021, (2021). [CrossRef]
[28] Faniran, T., Ali, A., Adewole, M.O., Adebo, B., & Akanni, O.O. Asymptotic behavior of tuberculosis between smokers and non-smokers. *Partial Differential Equations in Applied Mathematics*, 5, 100244, (2022). [CrossRef]
[29] Din, A., & Li, Y. The extinction and persistence of a stochastic model of drinking alcohol. *Results in Physics*, 28, 104649, (2021). [CrossRef]

[30] Naik, P.A., Eskandari, Z., Yavuz, M., & Zu, J. Complex dynamics of a discrete-time Bazykin–Berezovskaya prey-predator model with a strong Allee effect. *Journal of Computational and Applied Mathematics*, 413, 114401, (2022). [CrossRef]
[31] Abdy, M., Side, S., Annas, S., Nur, W., & Sanusi, W. An SIR epidemic model for COVID-19 spread with fuzzy parameter: the case of Indonesia. *Advances in difference equations*, 2021(1), 1-17, (2021). [CrossRef]
[32] Yavuz, M., Coşar, F.Ö., Günay, F., & Özdemir, F.N. A new mathematical modeling of the COVID-19 pandemic including the vaccination campaign. *Open Journal of Modelling and Simulation*, 9(3), 299-321, (2021). [CrossRef]
[33] Özköse, F., Yavuz, M., Şenel, M.T., & Habbireeh, R. Fractional order modelling of omicron SARS-CoV-2 variant containing heart attack effect using real data from the United Kingdom. *Chaos, Solitons & Fractals*, 157, 111954, (2022). [CrossRef]
[34] Shen, Z.H., Chu, Y.M., Khan, M.A., Muhammad, S., Al-Hartomy, O.A., & Higazy, M. Mathematical modeling and optimal control of the COVID-19 dynamics. *Results in Physics*, 31, 105028, (2021). [CrossRef]
[35] Ahmad, S., Ullah, A., Al-Mdallal, Q.M., Khan, H., Shah, K., & Khan, A. Fractional order mathematical modeling of COVID-19 transmission. *Chaos, Solitons & Fractals*, 139, 110256, (2020). [CrossRef]
[36] Abdo, M.S., Shah, K., Wahash, H.A., & Panchal, S.K. On a comprehensive model of the novel coronavirus (COVID-19) under Mittag-Leffler derivative. *Chaos, Solitons & Fractals*, 135, 109867, (2020). [CrossRef]
[37] Robinson, E., Sutin, A.R., Daly, M., & Jones, A. A systematic review and meta-analysis of longitudinal cohort studies comparing mental health before versus during the COVID-19 pandemic in 2020. *Journal of affective disorders*, 296, 567-576, (2022). [CrossRef]
[38] Oud, M.A.A., Ali, A., Alrabaiah, H., Ullah, S., Khan, M.A., & Islam, S. A fractional order mathematical model for COVID-19 dynamics with quarantine, isolation, and environmental viral load. *Advances in Difference Equations*, 2021(1), 1-19, (2021). [CrossRef]
[39] Mathieu, E., et al. A global database of COVID-19 vaccinations. *Nature Human Behaviour*, 5(7), 947-953, (2021). [CrossRef]
[40] https://www.who.int/ Access Date: 20.06.2022
[41] He, J.H. Homotopy perturbation technique. *Computer methods in applied mechanics and engineering*, 178(3-4), 257-262, (1999). [CrossRef]
[42] He, J.H. Comparison of homotopy perturbation method and homotopy analysis method. *Applied Mathematics and Computation*, 156(2), 527-539, (2004). [CrossRef]
[43] Sinan, M., Shah, K., Khan, Z.A., Al-Mdallal, Q., & Rihan, F. On Semianalytical Study of Fractional-Order Kawahara Partial Differential Equation with the Homotopy Perturbation Method. *Journal of Mathematics*, 2021, (2021). [CrossRef]
[44] Mohyud-Din, S.T., & Noor, M.A. Homotopy perturbation method for solving partial differential equations. *Zeitschrift für Naturforschung A*, 64(3-4), 157-170, (2009). [CrossRef]
[45] Sinan, M. Analytic approximate solution of rabies transmission dynamics using homotopy perturbation method. *Matrix Science Mathematics (MSMK)*, 4(1), 01-05, (2020). [CrossRef]
[46] Zedan, H.A., & El Adrous, E. The application of the homotopy perturbation method and the homotopy analysis method to the generalized Zakharov equations. *In Abstract and Applied Analysis*, 2012, (2012). [CrossRef]
[47] Demir, A., Erman, S., Özgür, B., & Korkmaz, E. Analysis of the new homotopy perturbation method for linear and nonlinear problems. *Boundary Value Problems*, 2013(1), 1-11, (2013). [CrossRef]
[48] Zhang, Z., ur Rahman, G., Gómez-Aguilar, J.F., & Torres-Jiménez, J. Dynamical aspects of a delayed epidemic model with subdivision of susceptible population and control strategies. *Chaos, Solitons & Fractals*, 160, 112194, (2022). [CrossRef]
[49] Wang, Z., Nie, X., & Liao, M. Stability Analysis of a Fractional-Order SEIR-KS Computer Virus-Spreading Model with Two Delays. *Journal of Mathematics*, 2021, (2021). [CrossRef]

Mathematical Modelling and Numerical Simulation with Applications (MMNSA) (https://www.mmnsa.org)

Mathematical Modelling and Numerical Simulation with Applications, 2022, 2(2), 108–116

https://www.mmnsa.org
ISSN Online: 2791-8564 / Open Access
https://doi.org/10.53391/mmnsa.2022.009

RESEARCH PAPER

An optimal control strategy and Grünwald-Letnikov finite-difference numerical scheme for the fractional-order COVID-19 model

Ihtisham Ul Haq[1,‡,*], Nigar Ali[1,‡] and Kottakkaran Sooppy Nisar[2,‡]

[1]Department of Mathematics, University of Malakand, Chakdara Dir (L), 18000, Khyber Pakhtunkhwa, Pakistan,
[2]Department of Mathematics, College of Arts and Science, Prince Sattam bin Abdulaziz University, Saudi Arabia

*Corresponding Author
‡ihtisham0095@gmail.com (Ihtisham Ul Haq); nigaruom@gmail.com (Nigar Ali); n.soopy@psau.edu.sa (Kottakkaran Sooppy Nisar)

Abstract

In this article, a mathematical model of the COVID-19 pandemic with control parameters is introduced. The main objective of this study is to determine the most effective model for predicting the transmission dynamic of COVID-19 using a deterministic model with control variables. For this purpose, we introduce three control variables to reduce the number of infected and asymptomatic or undiagnosed populations in the considered model. Existence and necessary optimal conditions are also established. The Grünwald-Letnikov non-standard weighted average finite difference method (GL-NWAFDM) is developed for solving the proposed optimal control system. Further, we prove the stability of the considered numerical method. Graphical representations and analysis are presented to verify the theoretical results.

Key words: Caputo fractional derivative; optimal control strategy; Grünwald-Letnikov numerical method; stability analysis
AMS 2020 Classification: 92B05; 49K10; 49J15; 65L03; 65L20

1 Introduction

COVID-19 pandemic can be considered as a dangerous infectious disease in the whole world, see [1]. It is transmitted to humans primarily through tiny droplets, or contact with contaminated surfaces. Mathematical modelling of epidemic diseases is very helpful for control strategies to a disease. Recently, a number of interesting papers have been developed regarding the modelling of the coronavirus, see for example [2, 3, 4, 5, 6, 7, 8, 9].

It has recently come to light that Fractional Differential Equations (FDE) can be successfully applied in mathematical modelling in various fields, including epidemics [10]. Fractional Calculus (FC) is a branch of mathematical analysis that deals with the study of fractional-order of derivatives and integral. A dynamical system using fractional-order derivative (FOD) in modeling helps define efficiency, usefulness, and memory as essential properties in many biological mechanisms [11, 12, 13, 14, 15, 16].

Optimal control (OC) theory is a branch of mathematical optimization. It involves investigating the control strategies for a dynamic system in a short time, such as minimizing or maximizing an objective function. Recently, OC theory has been used successfully in many fields, including robotics, aerospace, economics, finance, and management sciences [17, 18, 19]. Especially, the study of epidemiological models is closely related to the study of OC, as vaccination [20], resource allocation [21] and educational campaigns [22]. Caputo and Riemann–Liouville fractional derivatives [23, 24, 25, 26, 27] are the most important definitions of FD. Al-Mekhlafi and Sweilam established important numerical results for FOC [28, 29, 30].

An important contribution to this work is the development of numerical schemes providing approximate solutions for the fractional-order control problems (FOCPs). We discuss the COVID-19 model in [31] with changed fractional operator and parameters. This model was

➤ **Received:** 17.04.2022 ➤ **Revised:** 13.06.2022 ➤ **Accepted:** 20.06.2022 ➤ **Published:** 26.06.2022

modified with three controls $\mathscr{U}_l$,$\mathscr{U}_q$, and $\mathscr{U}_s$, to decrease the number of the infected, quarantine, and self-isolation. Finally, the numerical simulation is represented in the proposed system.

2 Basic definitions

Definition 1 *We define the Caputo fractional order derivative of the function $\mathscr{P}(t)$ [32]:*

$$ {}_0^C\mathscr{D}_t^{\alpha}[\mathscr{P}(t)] = \frac{1}{\Gamma(\mathscr{K}-\alpha)}\int_0^t (t-\eta)^{\mathscr{K}-\alpha-1}\,\mathscr{P}(t)^{(\mathscr{K})}(\eta)d\eta, \tag{1}$$

where, $\mathscr{K} = [\alpha]+1$ and $[\alpha]$ represents the integral parts of α.

Definition 2 *The discretization of Fractional derivative by the Grünwald–Letnikov approach [33]*

$$ {}_0^C\mathscr{D}_t^{\alpha}[\mathscr{P}(t)]\,|_{t=t^{\mathscr{K}}} = \frac{1}{\Delta t^{\alpha}}\left(\mathscr{P}_{\mathscr{K}+1} - \sum_{i=1}^{\mathscr{K}+1}\mathscr{U}_i\mathscr{P}_{\mathscr{K}+1-i} - \mathscr{Y}_{\mathscr{K}+1}\mathscr{P}_0\right), \tag{2}$$

where, $\mathscr{K} = 1,2,\ldots,\mathscr{N}_{\mathscr{K}}$, and the coordinate of each mesh point is $t^{\mathscr{K}} = \mathscr{K}\Delta t$, $\Delta t = \frac{\mathcal{T}_f}{\mathscr{N}_{\mathscr{K}}}$, $\mathscr{U}_i = (-1)^{i-1}\binom{\alpha}{i}$, $\mathscr{U}_1 = \alpha$, $\mathscr{Y}_i = \frac{i^{\alpha}}{\Gamma(1-\alpha)}$ and $i = 1,2,3,\ldots,\mathscr{K}+1$.

Additionally, Let us assume that $0 < \mathscr{U}_{i+1} < \mathscr{U}_i < \ldots < \mathscr{U}_1 = \alpha < 1$, $0 < \mathscr{Y}_{i+1} < \mathscr{Y}_i < \ldots < \mathscr{Y}_1 = \frac{1}{\Gamma(1-\alpha)}$.

Definition 3 *Let a function $\mathscr{P} : \mathscr{R}^+ \to \mathscr{R}$, the fractional integral is defined by*

$$ {}_0\mathscr{I}_t^{\alpha}\mathscr{P}(t) = \frac{1}{\Gamma(\alpha)}\int_0^t (t-\eta)^{\alpha-1}\,\mathscr{P}(\eta)d\eta,$$

where, $\mathscr{K} = [\alpha]+1$ and $[\alpha]$ represents the integral parts of α.

3 Mathematical model formulation

In this section, we discuss the mathematical model that consists of four compartments of the population which includes susceptible individuals $\mathbb{S}$, asymptomatic infectious $\mathbb{I}$, unreported symptomatic infectious $\mathbb{U}$, and reported symptomatic infectious $\mathbb{R}$. This model was developed in [31]. We modified the model with control variables and then represented it by a system of Caputo fractional derivative:

$$\begin{cases} {}_0^C\mathscr{D}_t^{\alpha}[\mathbb{S}] = -(1-\mathscr{U}_l)\,\mathscr{J}(t)\mathbb{S}(t)\left[\mathbb{I}(t)+\mathbb{U}(t)\right] - \mathscr{U}_q\mathbb{S} + \mathscr{U}_s\mathbb{U}, \\ {}_0^C\mathscr{D}_t^{\alpha}[\mathbb{I}] = (1-\mathscr{U}_l)\,\mathscr{J}(t)\mathbb{S}(t)\left[\mathbb{I}(t)+\mathbb{U}(t)\right] - \beta\mathbb{I}(t), \\ {}_0^C\mathscr{D}_t^{\alpha}[\mathbb{R}] = \beta_1\mathbb{I}(t) - \mu\mathbb{R}(t) + \mathscr{U}_q\mathbb{S}, \\ {}_0^C\mathscr{D}_t^{\alpha}[\mathbb{U}] = \beta_2\mathbb{I}(t) - \mu\mathbb{U}(t) - \mathscr{U}_s\mathbb{U}, \end{cases} \tag{3}$$

with the initial conditions $\mathbb{S}(t_0) = \mathbb{S}_0, \mathbb{I}(t_0) = \mathbb{I}_0, \mathbb{R}(t_0) = 0, \mathbb{U}(t_0) \geq 0$, where the function $\mathscr{U}_s$, $\mathscr{U}_q$, $\mathscr{U}_l$, are self isolation strategies, quarantine and states lock down, respectively. Table 1 represents the variables and Table 2 shows the descriptions of the model parameters.

Table 1. The variables of system (3)

Variable	Interpretation
$\mathbb{S}$	Susceptible individuals
$\mathbb{I}$	Asymptomatic Infection population
$\mathbb{R}$	Reported symptomatic infected population
$\mathbb{U}$	Unreported symptomatic infected population

Table 2. The parameters of system (3)

Parameter	Biological interpretations
t_0	The time when the epidemic began
$\mathbb{S}_0$	Number of susceptible individuals at time t_0
$\mathbb{I}_0$	Number of infected individuals at time t_0
$\mathbb{U}_0$	Number of unreported individuates at time t_0
$\mathbb{R}_0$	Number of reported individuates at time t_0
$\mathscr{J}$	Rate of transmission at time t_0
$\frac{1}{\beta}$	Represents the average time during which asymptomatic infectious become asymptomatic
β_1	Rate at which asymptomatic infectious become reported symptomatic
β_2	Rate at which asymptomatic infectious become unreported symptomatic
$\frac{1}{\mu}$	Average time symptomatic infectious have symptoms

We follow the basic reproduction number ($\mathscr{R}_0$) of the model (3) is given in [31].

$$\mathscr{R}_0 = \left(\frac{\mathscr{J}_0\mathbb{S}_0}{\beta_1+\beta_2}\right)\left(1+\frac{\beta_2}{\mu}\right) = \frac{\mathscr{J}_0\mathbb{S}_0(\mu+\beta_2)}{\mu(\beta_1+\beta_2)}. \tag{4}$$

The disease will decrease if $\mathscr{R}_0 < 1$. The disease will spread if $\mathscr{R}_0 > 1$ because every infection causes more than one new infection, see [31]. In this study, we consider $\mathscr{R}_0 > 1$.

4 Existence of the optimal control problem

In this section, we apply the optimal control theory to maximise the number of recovering people while lowering the number of infected individuals at the lowest possible cost and with the fewest possible unreported symptomatic infected population. Finally, we compute the numerical solution of the system and discuss the best control techniques using GL-NWAFDM.

Theorem 1 *We consider the optimal control system (3). There exists an OC* $\left(\mathscr{U}_l^*, \mathscr{U}_q^*, \mathscr{U}_s^*\right) \in \mathcal{U}$ *such as*

$$\mathcal{J}\left(\mathscr{U}_l^*, \mathscr{U}_q^*, \mathscr{U}_s^*\right) = \min_{\mathscr{U}_l,\mathscr{U}_q,\mathscr{U}_s\in\mathcal{U}} \mathcal{J}\left(\mathscr{U}_l, \mathscr{U}_q, \mathscr{U}_s\right). \tag{5}$$

Proof 1 *The existence of the OC can be investigated by using a result in [34]. The existence of the optimal control problem can be accomplished by checking the following steps:*

i. The corresponding state variables and the set of controls are nonempty. For this, we use a derived result of an existence in [35] to prove that the state variables and set of controls are nonempty. Let $\mathcal{Y}_j^{'} = \mathcal{F}_{\mathcal{X}_i}(t, \mathcal{Y}_1, \mathcal{Y}_2, \mathcal{Y}_3, \mathcal{Y}_4)$, where $(\mathcal{Y}_1, \mathcal{Y}_2, \mathcal{Y}_3, \mathcal{Y}_4) = (\mathbb{S}, \mathbb{I}, \mathbb{U}, \mathbb{R})$. Let $\mathscr{U}_l, \mathscr{U}_q$ and $\mathcal{U}_s$ for some constants and $\mathcal{Y}_1, \mathcal{Y}_2, \mathcal{Y}_3$ and $\mathcal{Y}_4$ are continuous, then $\mathcal{F}_{\mathbb{S}}, \mathcal{F}_{\mathbb{I}}, \mathcal{F}_{\mathbb{U}}$ and $\mathcal{F}_{\mathbb{R}}$ are also continuous. Therefore, the state variables and set of controls are nonempty.

ii. Next, the control space $\mathcal{U} = \{(\mathscr{U}_l, \mathscr{U}_q, \mathscr{U}_s)/(\mathscr{U}_l, \mathscr{U}_q, \mathscr{U}_s)$ is measurable, $0 \le \mathscr{U}_{\min} \le \mathscr{U}_l \le \mathscr{U}_{\max} \le 1, 0 \le \mathscr{U}_{\min} \le \mathscr{U}_q \le \mathscr{U}_{\max} \le 1$,and $0 \le \mathscr{U}_{\min} \le \mathscr{U}_s \le \mathscr{U}_{\max} \le 1, t \in [0, \mathcal{T}_f - 1]\}$ is closed and convex.

iii. The right hand sides of the problem equations are bounded above by a sum of bounded state and controls and can be written as a linear function of $\mathscr{U}_l, \mathscr{U}_q$ and $\mathscr{U}_s$.

iv. The integrand in the objective functional, $\mathbb{I}(t) + \mathbb{U}(t) + \frac{\eta_1\mathscr{U}_l^2(t)}{2} + \frac{\eta_2\mathscr{U}_q^2(t)}{2} + \frac{\eta_3\mathscr{U}_s^2(t)}{2}$ is convex on $\mathcal{U}$.

v. Finally, we show that there exists constants $\gamma_1, \gamma_2, \gamma_3, \gamma_4$ and γ such that $\mathbb{I}(t)+\mathbb{U}(t)+\frac{\eta_1\mathscr{U}_l^2(t)}{2}+\frac{\eta_2\mathscr{U}_q^2(t)}{2}+\frac{\eta_3\mathscr{U}_s^2(t)}{2}$ satisfies $\mathbb{I}(t)+\mathbb{U}(t)+\frac{\eta_1\mathscr{U}_l^2(t)}{2}+\frac{\eta_2\mathscr{U}_q^2(t)}{2}+\frac{\eta_3\mathscr{U}_s^2(t)}{2} \ge \gamma_1+\gamma_2\left|\mathscr{U}_l\right|^\gamma+\gamma_3\left|\mathscr{U}_q\right|^\gamma+\gamma_4\left|\mathscr{U}_s\right|^\gamma$. The state variables bounded, let $\gamma_1 = \inf_{t\in[0,\mathcal{T}_f]}\left(\mathbb{I}(t)+\mathbb{U}(t)\right)$, $\gamma_2 = \frac{\eta_1}{2}, \gamma_3 = \frac{\eta_2}{2}, \gamma_4 = \frac{\eta_3}{2}$ and $\gamma = 2$ then it follows $\mathbb{I}(t) + \mathbb{U}(t) + \frac{\eta_1\mathscr{U}_l^2(t)}{2} + \frac{\eta_2\mathscr{U}_q^2(t)}{2} + \frac{\eta_3\mathscr{U}_s^2(t)}{2} \ge \gamma_1+\gamma_2\left|\mathscr{U}_l\right|^\gamma+\gamma_3\left|\mathscr{U}_q\right|^\gamma+\gamma_4\left|\mathscr{U}_s\right|^\gamma$.

Hence, from Fleming et al. [34], the results indicate that there is an optimal control. Now, let system (3) in $\mathbb{R}^6$

$$\mathcal{U} = \left\{(\mathscr{U}_l(.), \mathscr{U}_q(.), \mathscr{U}_s(.)), 0 \le \mathscr{U}_l(.), \mathscr{U}_q(.), \mathscr{U}_s(.) \le 1, \forall t \in [0, \mathcal{T}_f]\right\},$$

where $\mathscr{U}_l, \mathscr{U}_q, \mathscr{U}_s$ are Lebesgue measurable on $[0, 1]$. We define the objective functional as:

$$\mathcal{J}(\mathscr{U}_l, \mathscr{U}_q, \mathscr{U}_s) = \int_0^{\mathcal{T}_f}\left(\mathbb{I}(t) + \mathbb{U}(t) + \frac{\eta_1\mathscr{U}_l^2(t)}{2} + \frac{\eta_2\mathscr{U}_q^2(t)}{2} + \frac{\eta_3\mathscr{U}_s^2(t)}{2}\right)dt. \tag{6}$$

The next step is to evaluate $\mathscr{U}_l, \mathscr{U}_q, \mathscr{U}_s$ as:

$$\mathcal{J}(\mathscr{U}_l, \mathscr{U}_q, \mathscr{U}_s) = \int_0^{\mathcal{T}_f}\mathcal{F}(\mathbb{S}, \mathbb{I}, \mathbb{R}, \mathbb{U}, \mathscr{U}_l, \mathscr{U}_q, \mathscr{U}_s, t)dt \tag{7}$$

is minimum, subject to restrictions

$${}_0^cD_t^\alpha\mathbb{W}_j = \chi_i, \tag{8}$$

where

$$\chi_i = \chi_i(\mathbb{S}, \mathbb{I}, \mathbb{R}, \mathbb{U}, \mathscr{U}_l, \mathscr{U}_q, \mathscr{U}_s, t), \qquad i = 1, \ldots, 4,$$

$$\mathbb{W}_j = \{\mathbb{S}, \mathbb{I}, \mathbb{R}, \mathbb{U}, \qquad j = 1, \ldots, 4\},$$

and the initial conditions satisfying

$$\mathbb{W}_1(t_0) = \mathbb{S}_0, \quad \mathbb{W}_2(t_0) = \mathbb{I}_0, \quad \mathbb{W}_3(t_0) = \mathbb{R}_0, \quad \mathbb{W}_4(t_0) = \mathbb{U}_0.$$

We use the fractional order case of the Pontryagin maximum principle, this fractional form is given by Agrawal in [26]. Functional modified as:

$$\bar{\mathcal{J}} = \int_0^{\mathcal{T}_f} \left[\mathcal{H}\left(\mathbb{S}, \mathbb{I}, \mathbb{R}, \mathbb{U}, \mathscr{U}_l, \mathscr{U}_q, \mathscr{U}_s, t\right) - \sum_{i=1}^{4} \mathscr{B}_i \chi_i \left(\mathbb{S}, \mathbb{I}, \mathbb{R}, \mathbb{U}, \mathscr{U}_l, \mathscr{U}_q, \mathscr{U}_s, t\right) \right] dt. \tag{9}$$

We define the Hamiltonian as:

$$\mathcal{H}\left(\mathbb{S}, \mathbb{I}, \mathbb{R}, \mathbb{U}, \mathscr{U}_l, \mathscr{U}_q, \mathscr{U}_s, t\right) = \mathscr{F}\left(\mathbb{S}, \mathbb{I}, \mathbb{R}, \mathbb{U}, \mathscr{U}_l, \mathscr{U}_q, \mathscr{U}_s, \mathscr{B}_i, t\right) + \sum_{i=1}^{4} \mathscr{B}_i \chi_i \left(\mathbb{S}, \mathbb{I}, \mathbb{R}, \mathbb{U}, \mathscr{U}_l, \mathscr{U}_q, \mathscr{U}_s, t\right). \tag{10}$$

We have got the necessary conditions from (9) and (10):

$${}_0^C D_t^{\alpha} \mathscr{B}_i = \frac{\partial \mathcal{H}}{\partial \mathscr{M}_i}, \quad i = 1, \ldots, 4, \tag{11}$$

where $\mathscr{M}_i = \{\mathbb{S}, \mathbb{I}, \mathbb{R}, \mathbb{U}, \mathscr{U}_l, \mathscr{U}_q, \mathscr{U}_s, \mathscr{B}_i, t, i = 1, \ldots, 4\}$,

$$0 = \frac{\partial \mathcal{H}}{\partial \mathscr{U}_{\mathscr{K}}}, \quad \mathscr{K} = l, q, s, \tag{12}$$

$${}_0^C D_t^{\alpha} \mathscr{M}_i = \frac{\partial \mathcal{H}}{\partial \mathscr{B}_i}, \quad i = 1, \ldots, 4, \tag{13}$$

with

$$\mathscr{B}_i(\mathcal{T}_f) = 0, \quad i = 1, \ldots, 4. \tag{14}$$

For more information, see [36].

Theorem 2 *The optimal control variables $\mathscr{U}_l, \mathscr{U}_q, \mathscr{U}_s$, with the corresponding solutions $\mathbb{S}^*, \mathbb{I}^*, \mathbb{R}^*, \mathbb{U}^*$ that minimize $\mathcal{J}(\mathscr{U}_l, \mathscr{U}_q, \mathscr{U}_s)$. There are also adjacent variables $\mathscr{B}_i, i = 1, \ldots, 4$ satisfying the following:*

- Adjoint equations:

$$\begin{aligned}
{}_0^C \mathscr{D}_t^{\alpha}[\mathscr{B}_1] &= -\left(\left(1 - \mathscr{U}_l^*\right) \mathscr{J}\left[\mathbb{I}^* + \mathbb{U}^*\right]\right)\left(\mathscr{B}_1 + \mathscr{B}_2\right) - \mathscr{B}_1 \mathscr{U}_q^* - \mathscr{B}_3 \mathscr{U}_q^*, && (15)\\
{}_0^C \mathscr{D}_t^{\alpha}]\mathscr{B}_2] &= -1 + \left(1 - \mathscr{U}_l^*\right) \mathscr{J}\mathbb{S}^*\left(\mathscr{B}_1 - \mathscr{B}_2\right) + \mathscr{B}_2 \beta - \mathscr{B}_3 \beta_1 - \mathscr{B}_4 \beta_2, && (16)\\
{}_0^C \mathscr{D}_t^{\alpha}[\mathscr{B}_3] &= \mathscr{B}_3 \mu, && (17)\\
{}_0^C \mathscr{D}_t^{\alpha}[\mathscr{B}_4] &= -1 + \left(1 - \mathscr{U}_l^*\right) \mathscr{J}\mathbb{S}^*\left(\mathscr{B}_1 - \mathscr{B}_2\right) - \mathscr{U}_s^* \mathscr{B}_1 + \mathscr{B}_4\left(\mu - \mathscr{U}_s^*\right). && (18)
\end{aligned}$$

- The transversality conditions:

$$\mathscr{B}_i(\mathcal{T}_f) = 0, \quad i = 1, \ldots, 4. \tag{19}$$

- Optimality conditions:

$$\mathcal{H}\left(\mathbb{S}, \mathbb{I}, \mathbb{R}, \mathbb{U}, \mathscr{U}_l, \mathscr{U}_q, \mathscr{U}_s, \mathscr{B}_i, t\right) = \min_{0 \le \mathscr{U}_p, \mathscr{U}_{ap}, \mathscr{U}_{cp} \le 1} \mathcal{H}\left(\mathbb{S}, \mathbb{I}, \mathbb{R}, \mathbb{U}, \mathscr{U}_l, \mathscr{U}_q, \mathscr{U}_s, \mathscr{B}_i, t\right). \tag{20}$$

Further,

$$\mathscr{U}_l = \min\left\{1, \max\left\{0, \frac{\mathscr{J}\mathbb{S}^*\left[\mathbb{I}^* + \mathbb{U}^*\right]\left(\mathscr{B}_1 - \mathscr{B}_2\right)}{\eta_1}\right\}\right\}, \tag{21}$$

$$\mathscr{U}_q = \min\left\{1, \max\left\{0, \frac{\mathbb{S}^*\left(\mathscr{B}_1 - \mathscr{B}_3\right)}{\eta_2}\right\}\right\}, \tag{22}$$

$$\mathscr{U}_s = \min\left\{1, \max\left\{0, \frac{\mathbb{U}^*\left(\mathscr{B}_4 - \mathscr{B}_2\right)}{\eta_3}\right\}\right\}. \tag{23}$$

Proof 2 *Eq. (15) to Eq. (19) can be obtained from (11), where*

$$\mathcal{H}^* = \mathscr{B}_{10}\,{}_0^c\mathscr{D}_t^\alpha\mathbb{S}^* + \mathscr{B}_{20}\,{}_0^c\mathscr{D}_t^\alpha\mathbb{I}^* + \mathscr{B}_{30}\,{}_0^c\mathscr{D}_t^\alpha\mathbb{R}^* + \mathscr{B}_{40}\,{}_0^c\mathscr{D}_t^\alpha\mathbb{U}^* + \mathbb{I}^* + \mathbb{R}^* + \mathbb{U}^* + \frac{\eta_1\mathscr{U}_l^2(t)}{2} + \frac{\eta_2\mathscr{U}_q^2(t)}{2} + \frac{\eta_3\mathscr{U}_s^2(t)}{2}$$

is the Hamiltonian. The conditions $\mathscr{B}_i(\mathcal{T}_f) = 0, i = 1, ..., 4$, hold. Now, using Eq. (20), we claim Eq. (21) to Eq. (23). Now, the state equations derived:

$$
\begin{aligned}
{}_0^c\mathscr{D}_t^\alpha[\mathbb{S}] &= -(1-\mathscr{U}_l^*)\,\mathscr{J}(t)\mathbb{S}^*(t)\left[\mathbb{I}^*(t)+\mathbb{U}^*(t)\right] - \mathscr{U}_q^*\mathbb{S}^* + \mathscr{U}_s^*\mathbb{U}^*, && (24)\\
{}_0^c\mathscr{D}_t^\alpha[\mathbb{I}] &= (1-\mathscr{U}_l^*)\,\mathscr{J}(t)\mathbb{S}(t)^*\left[\mathbb{I}^*(t)+\mathbb{U}^*(t)\right] - \beta\mathbb{I}^*(t), && (25)\\
{}_0^c\mathscr{D}_t^\alpha[\mathbb{R}] &= \beta_1\mathbb{I}^*(t) - \mu\mathbb{R}^*(t) + \mathscr{U}_q^*\mathbb{S}^*, && (26)\\
{}_0^c\mathscr{D}_t^\alpha[\mathbb{U}] &= \beta_2\mathbb{I}^*(t) - \mu\mathbb{U}^*(t) - \mathscr{U}_s^*\mathbb{U}^*. && (27)
\end{aligned}
$$

5 Procedure for solving control system

In this part of the paper, we develop a numerical scheme called GL-NWAFDM. Several results about this numerical scheme were discussed in [37, 38, 39]. The stability and efficiency of this method depend on the weight factor $0 \le \Omega \le 1$. Before, applying the GL-NWAFDM to the consider model, we first discrete the Caputo fractional derivative (2) by replacing $\triangle t$ by $\Psi(t)$, where

$$\Psi(\triangle t) = \triangle(t) + O(\triangle(t)^2), \quad 0 < \Psi(\triangle t) < 1, \quad \triangle(t) \to 0.$$

Then, the discretization for equations (24) to (27), where $\mathscr{K} = 0, 1, 2, ..., \mathcal{N}$, using GL-NWAFDM can be written as

$$
\begin{aligned}
\mathbb{S}^{\mathscr{K}+1*} - \sum_{i=1}^{\mathscr{K}+1}\mu_i\mathbb{S}^{\mathscr{K}+1-i*} - \mathscr{Y}_{\mathscr{K}+1}\mathbb{S}^{0*} \;=\; & \Omega\Psi(\triangle t)^\alpha\left(-(1-\mathscr{U}_l^*)\,\mathscr{J}\mathbb{S}^{\mathscr{K}+1*}\left[\mathbb{I}^{\mathscr{K}+1*}+\mathbb{U}^{\mathscr{K}+1*}\right] - \mathscr{U}_q^{\mathscr{K}+1*}\mathbb{S}^{\mathscr{K}+1*} + \mathscr{U}_s^{\mathscr{K}+1*}\mathbb{U}^{\mathscr{K}+1*}\right)\\
& + (1-\Omega)\,\Psi(\triangle t)^\alpha\left(-\left(1-\mathscr{U}_l^{\mathscr{K}*}\right)\mathscr{J}\mathbb{S}^{\mathscr{K}*}\left[\mathbb{I}^{\mathscr{K}*}+\mathbb{U}^{\mathscr{K}*}\right] + \left(-\mathscr{U}_q^{\mathscr{K}*}\mathbb{S}^{\mathscr{K}*} + \mathscr{U}_s^{\mathscr{K}*}\mathbb{U}^{\mathscr{K}*}\right)\right),
\end{aligned}
$$

$$
\begin{aligned}
\mathbb{I}^{\mathscr{K}+1*} - \sum_{i=1}^{\mathscr{K}+1*}u_i\mathbb{I}^{\mathscr{K}+1-i*} - \mathscr{Y}_{\mathscr{K}+1}\mathbb{I}^{0*} \;=\; & \Omega\Psi(\triangle t)^\alpha\left(\left(1-\mathscr{U}_l^{\mathscr{K}+1*}\right)\mathscr{J}\mathbb{S}^{\mathscr{K}+1*}\left[\mathbb{I}^{\mathscr{K}+1*}+\mathbb{U}^{\mathscr{K}+1*}\right] - \beta\mathbb{I}^{\mathscr{K}+1*}\right)\\
& + (1-\Omega)\,\Psi(\triangle t)^\alpha\left(\left(1-\mathscr{U}_l^{\mathscr{K}*}\right)\mathscr{J}\mathbb{S}^{\mathscr{K}*}\left[\mathbb{I}^{\mathscr{K}*}+\mathbb{U}^{\mathscr{K}*}\right] - \beta\mathbb{I}^{\mathscr{K}*}\right),
\end{aligned}
$$

$$
\begin{aligned}
\mathbb{R}^{\mathscr{K}+1*} - \sum_{i=1}^{\mathscr{K}+1}u_i\mathbb{R}^{\mathscr{K}+1-i*} - \mathscr{Y}_{\mathscr{K}+1}\mathbb{1}\mathbb{R}^{0*} \;=\; & \Omega\Psi(\triangle t)^\alpha\left(\beta_1\mathbb{I}^{\mathscr{K}+1*} - \mu\mathbb{R}^{\mathscr{K}+1*} + \mathscr{U}_q^{\mathscr{K}+1*}\mathbb{S}^{\mathscr{K}+1*}\right)\\
& + (1-\Omega)\,\Psi(\triangle t)^\alpha\left(\beta_1\mathbb{I}^{\mathscr{K}*} - \mu\mathbb{R}^{\mathscr{K}*} + \mathscr{U}_q^{\mathscr{K}*}\mathbb{S}^{\mathscr{K}*}\right),
\end{aligned}
$$

$$
\begin{aligned}
\mathbb{U}^{\mathscr{K}+1*} - \sum_{i=1}^{\mathscr{K}+1}u_i\mathbb{U}^{\mathscr{K}+1-i*} - \mathscr{Y}_{\mathscr{K}+1}\mathbb{U}^{0*} \;=\; & \Omega\Psi(\triangle t)^\alpha\left(\beta_2\mathbb{I}^{\mathscr{K}+1*} - \mu\mathbb{U}^{\mathscr{K}+1*} - \mathscr{U}_s^{\mathscr{K}+1*}\mathbb{U}^{\mathscr{K}+1*}\right)\\
& + (1-\Omega)\,\Psi(\triangle t)^\alpha\left(\beta_2\mathbb{I}^{\mathscr{K}*} - \mu\mathbb{U}^{\mathscr{K}*} - \mathscr{U}_s^{\mathscr{K}*}\mathbb{U}^{\mathscr{K}*}\right).
\end{aligned}
$$

We observe that this method is partially implicit for $\Omega \in [0, 1]$ and fully implicit for $\Omega = 1$ and explicit when $\Omega = 0$.

6 Stability of the developed numerical scheme

This section is devoted to describe that the GL-NWAFDM is unconditionally stable in implicit cases ($0 < \Omega < 1$). The stability of the numerical scheme is checked when ($\Omega \neq 0$), for this need, we take the test problem of the linear fractional differential equation:

$${}_0^c\mathscr{D}_t^\alpha\mathscr{X}(t) = P\mathscr{X}(t)t > 0, 0 < \alpha \le 1, P < 0. \tag{28}$$

Let the approximate solution of this equation is $\mathscr{X}(t_\mathscr{K}) = \mathscr{X}_\mathscr{K} = \mathscr{Z}_\mathscr{K}$, then applying the GL-NWAFDM, we rewrite Eq. (28) as

$$\mathscr{Z}^{\mathscr{K}+1} - \sum_{i=1}^{\mathscr{K}+1}\mu_i\mathscr{Z}^{\mathscr{K}+1-i} - \mathscr{Y}_{\mathscr{K}+1}\mathscr{Z}^0 = \Psi(\triangle t)^\alpha\left(\Omega P\mathscr{Z}^{\mathscr{K}+1} + (1-\Psi)\,P\mathscr{Z}^\mathscr{K}\right).$$

Then, we have

$$\mathscr{Z}^{\mathscr{K}+1} = \frac{1}{(1-\Psi(\triangle t)^\alpha\Omega P)}\left(\sum_{i=1}^{\mathscr{K}+1}\mu_i\mathscr{Z}^{\mathscr{K}+1-i} + \mathscr{Y}_{\mathscr{K}+1}\mathscr{Z}^0 + (1-\Psi)\Omega(\triangle t)^\alpha P\mathscr{Z}^\mathscr{K}\right), \qquad \mathscr{K} \ge 1,$$

we have $\frac{1}{(1-\Psi(\triangle t)^\alpha\Omega P)} < 1$, therefore, $\mathscr{Z}^1 \le \mathscr{Z}^0$, $\mathscr{Z}^{\mathscr{K}+1} \le \mathscr{Z}^\mathscr{K} \le \mathscr{Z}^{\mathscr{K}-1} \le ... \le \mathscr{Z}^0$. Hence, the proposed numerical method is stable.

7 Graphical representation and discussion

In this part of the paper, we have presented the graphical representation of the system (3) with and without control variables. Gl-NWAFDM is used in the previous section to get the approximate solution of the modified model with the given initial conditions and parameters values: $\mathbb{S}(0) = 100$, $\mathbb{I}(0) = 900$, $\mathbb{R}(0) = 100$, $\mathbb{U}(0) = 900$ and different values of fractional parameter with $\beta_1 = 0.98$, $\beta_2 = 0.87$, $\mu = 0.432$, $\mathscr{F} = 0.218$ and $\beta = 0.098$.

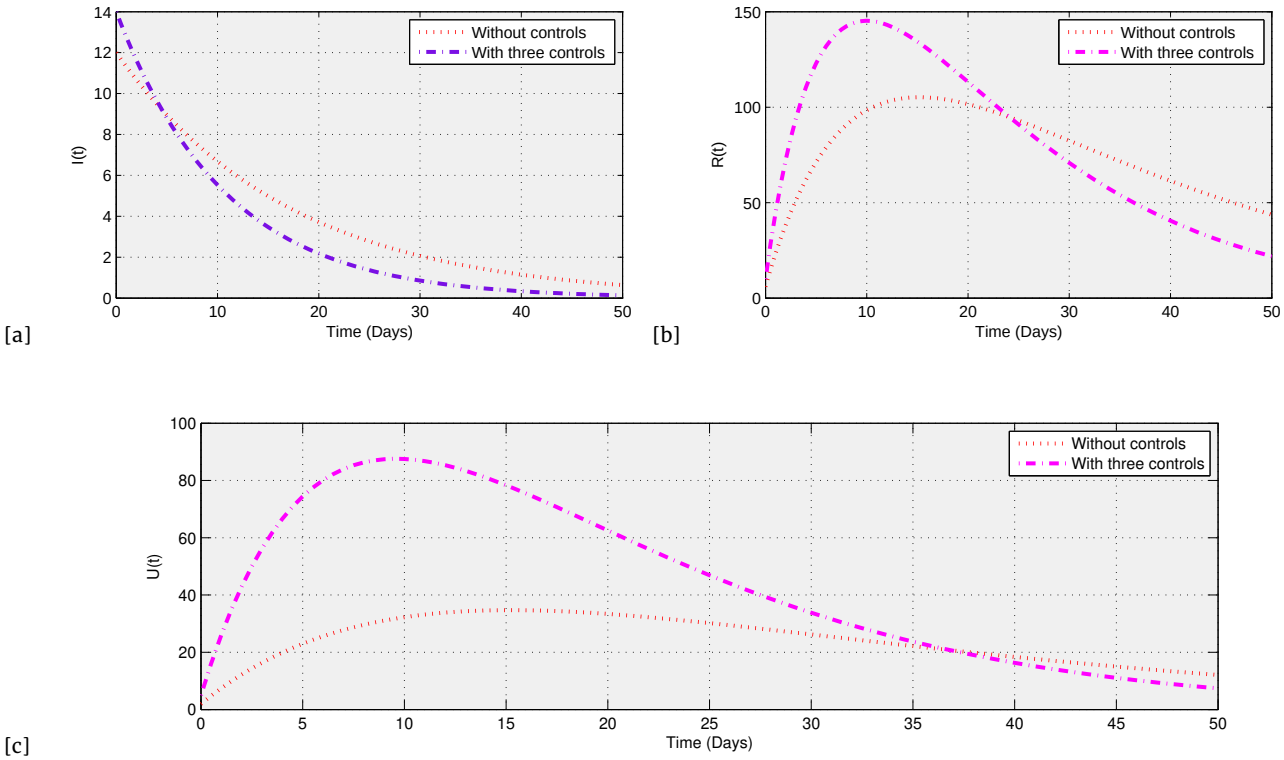

Figure 1. Simulations of $\mathbb{I}$,$\mathbb{R}$,and $\mathbb{U}$ at $\alpha = 0.85$ with and without controls

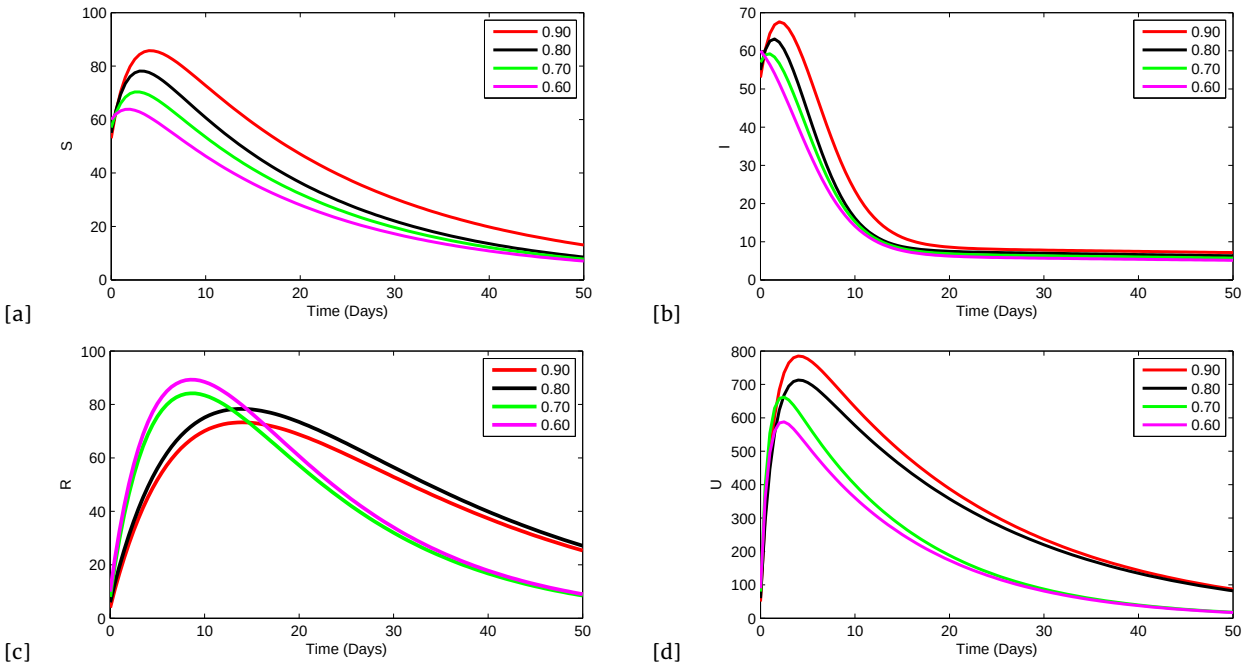

Figure 2. Numerical simulations of optimal control system with $\Omega = 10.23$ for $\alpha = 0.90, 0.80, 0.70$ and 0.60.

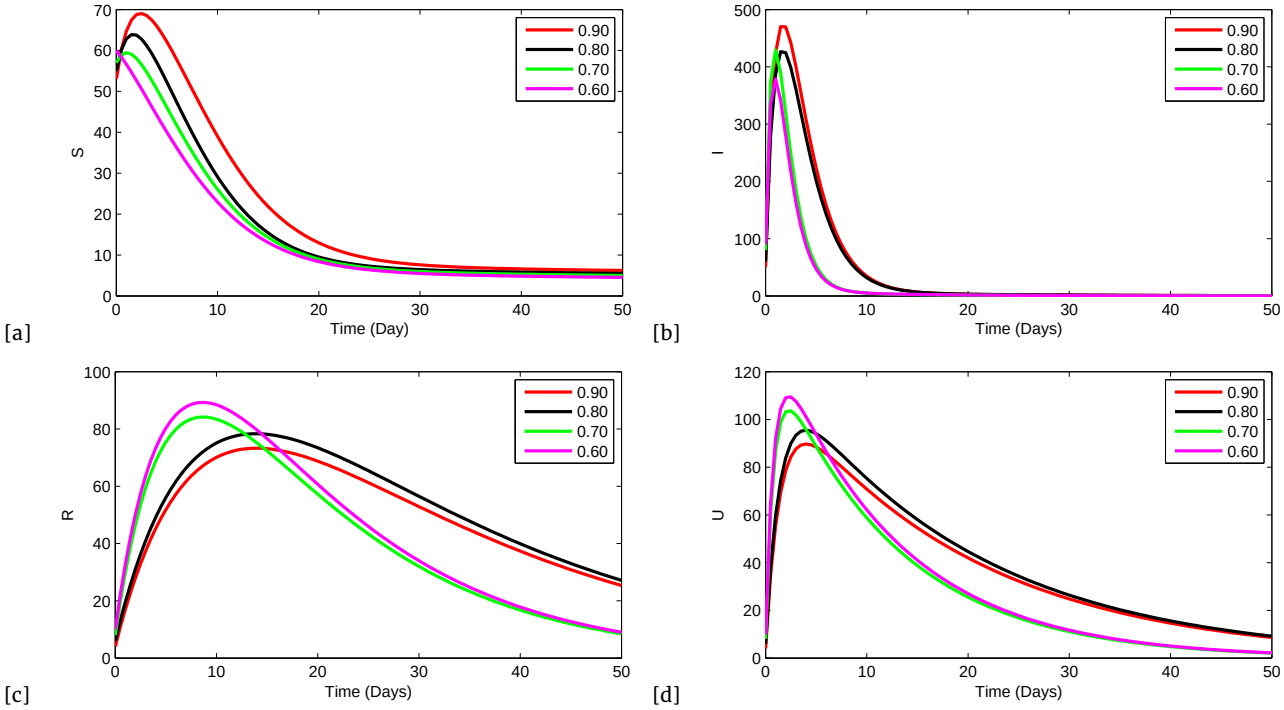

Figure 3. Numerical simulations of optimal control system with $\Omega = 11.32$ for $\alpha = 0.90, 0.80, 0.70$ and 0.60.

These figures show the efficiency and effectiveness of three control variables for the COVID-19 model. We have noted that the results obtained if $\Omega = 11.32$ were fully implicit. Moreover, for the control case best result is given at $\alpha = 0.6$. The dynamic of the solutions in the control case is shown in Figs. 2 and 3 by using various values of α and $\mathcal{T}_h$. These figures show that the approximate solutions of $\mathbb{S}$, $\mathbb{I}$, $\mathbb{R}$, $\mathbb{U}$ are unconditionally stable at $\Omega = 11.32$. Fig. 3 shows that the peak values of each infected category of the population decreases significantly when fractional order decreases. $\mathbb{U}$ (Un-reported infected) starts with a decreasing slope and later changes the peak but with a small number of infected individuals. This describes that these classes can have a huge impact on the development of the reported infected graph.

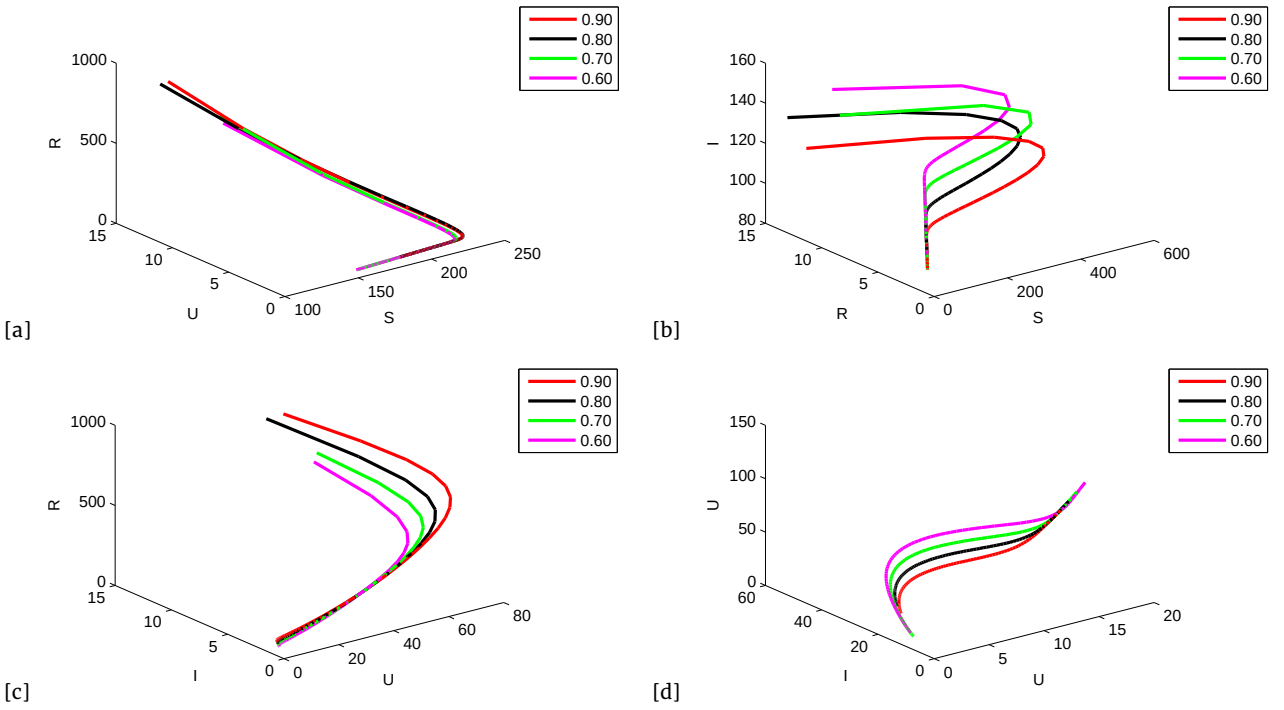

Figure 4. Numerical simulations of $\mathbb{I}$ with respect to $\mathbb{S}$, $\mathbb{R}$, and $\mathbb{U}$ with three controls variables for $\alpha = 0.90, 0.80, 0.70$ and 0.60.

8 Conclusion

In this work, we have presented a novel coronavirus model with the combination of optimal control and fractional-order derivatives to increase the model complexity and to improve the model dynamics. We have added three control variables to health care such as, $\mathscr{U}_q$, $\mathscr{U}_s$, $\mathscr{U}_l$, (Quarantine, Self isolation, Lockdown). These OC variables have been used to decrease the number of the asymptotically infected and unreported infected as we can see in Figs. 2 and 3. For this need, we have derived the necessary optimality conditions. GL-NWAFDM has been developed to obtain the approximate solution of the proposed model. This numerical method depends on the values of the factor ω. Further, we have also proved the stability of the Gl-NWAFDM. Finally, graphical representations have been presented to support our theoretical results. We have concluded that the fractional optimality systems can be solved effectively by using the Gl-NWAFDM.

Declarations

Consent for publication

Not applicable.

Conflicts of interest

The authors declare that they have no conflict of interests.

Funding

This research received no specific grant from any funding agency in the public, commercial, or not-for-profit sectors.

Author's contributions

I.U.H.: Conceptualization, Methodology, Software, investigation, Writing - Original Draft, Data Curation, Formal Analysis. N.A.: Writing-Review & Editing, Supervision, Formal Analysis. K.S.N.: Software, Validation, Writing-Review & Editing, Project Administration. All authors discussed the results and contributed to the final manuscript.

Acknowledgements

Not applicable.

References

[1] Bashier, H., Khader, Y., Al-Souri, R., & Abu-Khader, I. A Novel Coronavirus Outbreak: A Teaching Case-Study. *The Pan African Medical Journal*, 36(11), (2020).
[2] Ndaïrou, F., Area, I., Nieto, J.J., & Torres, D.F. Mathematical modeling of COVID-19 transmission dynamics with a case study of Wuhan. *Chaos, Solitons & Fractals*, 135, 109846, (2020). [CrossRef]
[3] Khan, M.A., & Atangana, A. Modeling the dynamics of novel coronavirus (2019-nCov) with fractional derivative. *Alexandria Engineering Journal*, 59(4), 2379-2389, (2020). [CrossRef]
[4] Machado, J.A., & Lopes, A.M. Rare and extreme events: the case of COVID-19 pandemic. *Nonlinear dynamics*, 100(3), 2953-2972, (2020). [CrossRef]
[5] Chen, T.M., Rui, J., Wang, Q.P., Zhao, Z.Y., Cui, J.A., & Yin, L. A mathematical model for simulating the phase-based transmissibility of a novel coronavirus. *Infectious diseases of poverty*, 9(1), 1-8, (2020). [CrossRef]
[6] Ivorra, B., Ferrández, M.R., Vela-Pérez, M., & Ramos, A.M. Mathematical modeling of the spread of the coronavirus disease 2019 (COVID-19) taking into account the undetected infections. The case of China. *Communications in nonlinear science and numerical simulation*, 88, 105303, (2020). [CrossRef]
[7] Naik, P.A., Yavuz, M., Qureshi, S., Zu, J., & Townley, S. Modeling and analysis of COVID-19 epidemics with treatment in fractional derivatives using real data from Pakistan. *The European Physical Journal Plus*, 135(10), 1-42, (2020). [CrossRef]
[8] Allegretti, S., Bulai, I.M., Marino, R., Menandro, M.A., & Parisi, K. Vaccination effect conjoint to fraction of avoided contacts for a Sars-Cov-2 mathematical model. *Mathematical Modelling and Numerical Simulation with Applications*, 1(2), 56-66, (2021). [CrossRef]
[9] Özköse, F., Yavuz, M., Şenel, M.T., & Habbireeh, R. Fractional order modelling of omicron SARS-CoV-2 variant containing heart attack effect using real data from the United Kingdom. *Chaos, Solitons & Fractals*, 157, 111954, (2022). [CrossRef]
[10] Dietz, K., & Heesterbeek, J.A.P. Bernoulli was ahead of modern epidemiology. *Nature*, 408(6812), 513-514, (2000). [CrossRef]
[11] Khan, H., Gómez-Aguilar, J.F., Alkhazzan, A., & Khan, A. A fractional order HIV-TB coinfection model with nonsingular Mittag-Leffler Law. *Mathematical Methods in the Applied Sciences*, 43(6), 3786-3806, (2020). [CrossRef]
[12] Sweilam, N.H., Al-Mekhlafi, S.M., & Hassan, A.N. Numerical treatment for solving the fractional two-group influenza model. *Progress in Fractional Differentiation and Applications*, 4, 1-15, (2018).
[13] Kumar, S., Ghosh, S., Lotayif, M. S., & Samet, B. A model for describing the velocity of a particle in Brownian motion by Robotnov function based fractional operator. *Alexandria Engineering Journal*, 59(3), 1435-1449, (2020). [CrossRef]
[14] Rihan, F.A., Baleanu, D., Lakshmanan, S., & Rakkiyappan, R. On fractional SIRC model with salmonella bacterial infection. *Abstract and Applied Analysis*, (2014). [CrossRef]
[15] Hammouch, Z., Yavuz, M., & Özdemir, N. Numerical solutions and synchronization of a variable-order fractional chaotic system. *Mathematical Modelling and Numerical Simulation with Applications*, 1(1), 11-23, (2021). [CrossRef]

[16] Özköse, F., Şenel, M.T., & Habbireeh, R. Fractional-order mathematical modelling of cancer cells-cancer stem cells-immune system interaction with chemotherapy. *Mathematical Modelling and Numerical Simulation with Applications*, 1(2), 67-83, (2021). [CrossRef]
[17] Kostylenko, O., Rodrigues, H.S., & Torres, D.F. The risk of contagion spreading and its optimal control in the economy. *arXiv preprint arXiv:1812.06975*, (2018). [CrossRef]
[18] Lemos-Paião, A.P., Silva, C.J., Torres, D.F., & Venturino, E. Optimal control of aquatic diseases: A case study of Yemen's cholera outbreak. *Journal of Optimization Theory and Applications*, 185(3), 1008-1030, (2020). [CrossRef]
[19] Ammi, M.R.S., & Torres, D.F. Optimal control of a nonlocal thermistor problem with ABC fractional time derivatives. *Computers & Mathematics with Applications*, 78(5), 1507-1516, (2019). [CrossRef]
[20] Brandeau, M.L., Zaric, G.S., & Richter, A. Resource allocation for control of infectious diseases in multiple independent populations: beyond cost-effectiveness analysis. *Journal of health economics*, 22(4), 575-598, (2003). [CrossRef]
[21] Ball, F., & Becker, N.G. Control of transmission with two types of infection. *Mathematical biosciences*, 200(2), 170-187, (2006). [CrossRef]
[22] Castilho, C. Optimal control of an epidemic through educational campaigns. *Electronic Journal of Differential Equations (EJDE)[electronic only]*, 2006, Paper-No, (2006).
[23] Rihan, F.A., Lakshmanan, S., & Maurer, H. Optimal control of tumour-immune model with time-delay and immuno-chemotherapy. *Applied Mathematics and Computation*, 353, 147-165, (2019). [CrossRef]
[24] Sweilam, N., Rihan, F., & Seham, A.M. A fractional-order delay differential model with optimal control for cancer treatment based on synergy between anti-angiogenic and immune cell therapies. *Discrete & Continuous Dynamical Systems-S*, 13(9), 2403, (2020). [CrossRef]
[25] Zaky, M.A., & Machado, J.T. On the formulation and numerical simulation of distributed-order fractional optimal control problems. *Communications in Nonlinear Science and Numerical Simulation*, 52, 177-189, (2017). [CrossRef]
[26] Agrawal, O.P. A formulation and a numerical scheme for fractional optimal control problems. *IFAC Proceedings Volumes*, 39(11), 68-72, (2006). [CrossRef]
[27] Agrawal, O.P., Defterli, O., & Baleanu, D. Fractional optimal control problems with several state and control variables. *Journal of Vibration and Control*, 16(13), 1967-1976, (2010). [CrossRef]
[28] Sweilam, N.H., Al-Mekhlafi, S.M., & Baleanu, D. Optimal control for a fractional tuberculosis infection model including the impact of diabetes and resistant strains. *Journal of advanced research*, 17, 125-137, (2019). [CrossRef]
[29] Sweilam, N.H., Al-Mekhlafi, S.M., Alshomrani, A.S., & Baleanu, D. Comparative study for optimal control nonlinear variable-order fractional tumor model. *Chaos, Solitons & Fractals*, 136, 109810, (2020). [CrossRef]
[30] Sweilam, N.H., & AL–Mekhlafi, S.M. Optimal control for a time delay multi-strain tuberculosis fractional model: a numerical approach. *IMA Journal of Mathematical Control and Information*, 36(1), 317-340, (2019). [CrossRef]
[31] Liu, Z., Magal, P., Seydi, O., & Webb, G. Predicting the cumulative number of cases for the COVID-19 epidemic in China from early data. *arXiv preprint arXiv:2002.12298*, (2020). [CrossRef]
[32] Lakshmikantham, V., & Vatsala, A.S. Basic theory of fractional differential equations. *Nonlinear Analysis: Theory, Methods & Applications*, 69(8), 2677-2682, (2008). [CrossRef]
[33] Arenas, A.J., Gonzalez-Parra, G., & Chen-Charpentier, B.M. Construction of nonstandard finite difference schemes for the SI and SIR epidemic models of fractional order. *Mathematics and Computers in Simulation*, 121, 48-63, (2016). [CrossRef]
[34] Heimann, B., Fleming, W.H., Rishel, R.W., Deterministic and Stochastic Optimal Control. New York-Heidelberg-Berlin. Springer-Verlag. 1975. XIII, 222 S, DM 60, 60. *Zeitschrift Angewandte Mathematik und Mechanik*, 59(9), 494-494, (1979). [CrossRef]
[35] Kouidere, A., Youssoufi, L.E., Ferjouchia, H., Balatif, O., & Rachik, M. Optimal control of mathematical modeling of the spread of the COVID-19 pandemic with highlighting the negative impact of quarantine on diabetics people with cost-effectiveness. *Chaos, Solitons & Fractals*, 145, 110777, (2021). [CrossRef]
[36] Sweilam, N.H., Al-Ajami, T.M., & Hoppe, R.H. Numerical solution of some types of fractional optimal control problems. *The Scientific World Journal*, 2013, (2013). [CrossRef]
[37] Scherer, R., Kalla, S.L., Tang, Y., & Huang, J. The Grünwald–Letnikov method for fractional differential equations. *Computers & Mathematics with Applications*, 62(3), 902-917, (2011). [CrossRef]
[38] Li, L., & Wang, D. Numerical stability of Grünwald–Letnikov method for time fractional delay differential equations. *BIT Numerical Mathematics*, 1-33, (2021). [CrossRef]
[39] Chakraborty, M., Maiti, D., Konar, A., & Janarthanan, R. A study of the grunwald-letnikov definition for minimizing the effects of random noise on fractional order differential equations. In *2008 4th International Conference on Information and Automation for Sustainability*, 449-456, IEEE, (2008). [CrossRef]

Mathematical Modelling and Numerical Simulation with Applications, 2022, 2(2), 117–126

https://www.mmnsa.org
ISSN Online: 2791-8564 / Open Access
https://doi.org/10.53391/mmnsa.2022.010

RESEARCH PAPER

Some integral inequalities via new family of preinvex functions

Muhammad Tariq[1,*,‡], Soubhagya Kumar Sahoo[2,‡], Hijaz Ahmad[3,‡], Asif Ali Shaikh[1,‡], Bibhakar Kodamasingh[2,‡] and Dawood Khan[4,‡]

[1]Department of Basic Sciences and Related Studies, Mehran University of Engineering and Technology, Jamshoro 76062, Pakistan, [2]Department of Mathematics, Institute of Technical Education and Research, Siksha 'O' Anusandhan University, Bhubaneswar 751030, Odisha, India, [3]Section of Mathematics, International Telematic University Uninettuno, Corso Vittorio Emanuele II, 39, 00186 Roma, Italy, [4]Department of Mathematics, University of Balochistan, 87300 Pakistan

*Corresponding Author
[‡]captaintariq2187@gmail.com (Muhammad Tariq); soubhagyalulu@gmail.com (Soubhagya Kumar Sahoo); hijaz555@gmail.com (Hijaz Ahmad); asif.shaikh@faculty.muet.edu.pk (Asif Ali Shaikh); bibhakarkodamasingh@soa.ac.in (Bibhakar Kodamasingh); dawooddawood601@gmail.com (Dawood Khan)

Abstract

The main objective of this work is to introduce and define the concept of $s-$type $m-$preinvex function and derive the new sort of Hermite–Hadamard inequality via the newly discussed idea. Furthermore, to enhance the quality of paper, we prove two new lemmas and we attain some extensions of Hermite–Hadamard-type inequality in the manner of newly explored definition for these lemmas. The concepts and tools of this paper may invigorate and revitalize for additional research in this mesmerizing and absorbing field of mathematics.

Key words: Preinvex function; $s-$type preinvexity; $s-$type $m-$preinvexity; Hermite–Hadamard inequality
AMS 2020 Classification: 26A51; 26A33; 26D07; 26D10; 26D15

1 Introduction

The theory of convexity has assumed a key part and has gotten exceptional consideration by numerous scientists in the improvement of different fields of pure and applied sciences. It all started with the book by Hardy, Littlewood and Pólya [1], where the term convexity was used. This theory presents us with a characteristic and general system to examine a wide class of irrelevant issues. Because of its importance, the ideas of convex sets and convex functions have been generalized in various ways utilizing novel and creative ideas. The convex function is a class of significant functions popularly accepted in mathematical analysis. This class represents prominent parts of the theory of inequality. Moreover, convex functions have been widely utilized in many research fields such as optimization, engineering, physics, financial activities, etc. In optimization, the concept of generalized convexity along with inequality theory is often used. The Hermite-Hadamard integral inequalities containing convex functions are an intense research topic for many mathematicians because of their relevance and efficiency in use. Convex functions have a very strong association with integral inequalities. As of late, several mathematicians have explored the close relationship and correlated work on symmetry and convexity. It is also explained that while working on any one of the concepts, it tends to be applied to the other one too. Many familiar and relevant inequalities are modifications of convex functions. In literature, there are some well-known inequalities such as Hermite-Hadamard inequality and Jensen inequality that interpret the geometrical meaning of convex functions (see [2, 3, 4, 5, 6, 7, 8, 9, 10]) and the references cited therein.

➤ **Received:** 24.04.2022 ➤ **Revised:** 29.06.2022 ➤ **Accepted:** 30.06.2022 ➤ **Published:** 30.06.2022

In [11], G. Toader introduced the class of $m-$convex functions. Soon after this many mathematicians like Latif [12] and Kalsoom [13] worked on the investigation of $m-$preinvexity.
Hanson [14] presented another new class of convex functions called invex functions, with the plan to generalize the legitimacy of the sufficiency of the Kuhn-Tucker conditions in nonlinear programming. Weir and Mond [15] introduced the preinvex function, which is an important extension of the convex function and it helped in handling numerous critical problems. It is realized that every convex function is a preinvex function but the converse is not true.

2 Preliminaries

Here, we remember several known definitions.

Definition 1 (see [16]) *Let $\Psi : \mathbb{A} \times \mathbb{A} \neq \emptyset \to \mathbb{R}$, then $\mathbb{A}$ is an invex w.r.t $\zeta(.,.)$ if $\nu + \delta\zeta(\mu,\nu) \in \mathbb{A}$, for every $\mu, \nu \in \mathbb{A}$ and $\delta \in [0,1]$.*

Note that, $\mathbb{A}$ is also called $\zeta-$connected set.
The above definition collapses to classical convexity if $\zeta(\mu,\nu) = \mu - \nu$. Therefore, every convex set is an invex but the converse is not true in general, (see [16] and [17]).

Definition 2 (see [15]) *The function $\Psi : \mathbb{A} \neq \emptyset \to \mathbb{R}$ on an invex set is called preinvex w.r.t ζ if*

$$\Psi(\nu + \delta\zeta(\mu,\nu)) \leq \delta\Psi(\mu) + (1-\delta)\Psi(\nu), \quad \forall \mu, \nu \in \mathbb{A}, \ \delta \in [0,1].$$

Definition 3 (see [18]) *A set $\mathbb{A} \subseteq \mathbb{R}^n$ is said to be $m-$invex w.r.t $\zeta : \mathbb{A} \times \mathbb{A} \times (0,1] \to \mathbb{R}^n$ for some fixed $m \in (0,1]$, if*

$$m\nu + \delta\zeta(\mu,\nu,m) \in \mathbb{A},$$

holds for every $\mu, \nu \in \mathbb{A}$, $m \in (0,1]$ and $\delta \in [0,1]$.

Definition 4 *[13] A $\Psi : \mathbb{A} \to \mathbb{R}$ is called generalized $m-$preinvex w.r.t $\zeta : \mathbb{A} \times \mathbb{A} \times (0,1] \to \mathbb{R}^n$ for fixed $m \in (0,1]$, if*

$$\Psi(m\nu + \delta\zeta(\mu,\nu,m)) \leq \delta\Psi(\mu) + m(1-\delta)\Psi(\nu), \tag{1}$$

holds for every $\mu, \nu \in \mathbb{A}$, $\delta \in [0,1]$.

Definition 5 (see [19]) *A nonnegative function $\Psi : \mathbb{A} \to \mathbb{R}$ is called $s-$type convex function if $\mu, \nu \in \mathbb{A}$, $s \in [0,1]$ and $\delta \in [0,1]$, if*

$$\Psi(\delta\mu + (1-\delta)\nu) \leq [1 - (s(1-\delta))]\Psi(\mu) + [1 - s\delta]\Psi(\nu). \tag{2}$$

We also want the following hypothesis regarding the function ζ which is due to Mohan and Neogy [20].
Condition-C: Let $\mathbb{A} \subset \mathbb{R}^n$ be an open invex subset w.r.t $\zeta : \mathbb{A} \times \mathbb{A} \to \mathbb{R}$. For any $\mu, \nu \in \mathbb{A}$ and $\delta \in [0,1]$

$$\begin{aligned} \zeta(\nu, \nu + \delta\zeta(\mu,\nu)) &= -\delta\zeta(\mu,\nu) \\ \zeta(\mu, \nu + \delta\zeta(\mu,\nu)) &= (1-\delta)\zeta(\mu,\nu). \end{aligned} \tag{3}$$

For any $\mu, \nu \in \mathbb{A}$ and $\delta_1, \delta_2 \in [0,1]$ from condition C, we have

$$\zeta(\nu + \delta_2\zeta(\mu,\nu), \nu + \delta_1\zeta(\mu,\nu)) = (\delta_2 - \delta_1)\zeta(\mu,\nu).$$

Extended condition-C ([21]): For any $\mu, \nu \in \mathbb{A}$, $\delta \in [0,1]$ and $\mathbb{A} \subset \mathbb{R}^n$ be an open $m-$invex subset with respect to $\zeta : \mathbb{A} \times \mathbb{X} \times (0,1] \to \mathbb{R}$. Then we have

$$\begin{aligned} \zeta(\nu, m\nu + \delta\zeta(\mu,\nu,m), m) &= -\delta\zeta(\mu,\nu,m) \\ \zeta(\mu, m\nu + \delta\zeta(\mu,\nu,m), m) &= (1-\delta)\zeta(\mu,\nu,m) \\ \zeta(\mu,\nu,m) &= -\zeta(\nu,\mu,m). \end{aligned}$$

3 Generalized preinvex function

In this part, we are to define and explore a new class of preinvex functions namely $s-$type $m-$preinvex function.

Definition 6 *Let $\mathbb{A} \subset \mathbb{R}$ be a nonempty $m-$invex set w.r.t $\zeta : \mathbb{A} \times \mathbb{A} \times (0,1] \to \mathbb{R}$. Then the function $\Psi : \mathbb{A} \to \mathbb{R}$ is called $s-$type $m-$preinvex, if*

$$\Psi(m\nu + \delta\zeta(\mu,\nu,m)) \leq [1 - (s(1-\delta))]\Psi(\mu) + m[1 - s\delta]\Psi(\nu), \tag{4}$$

holds $\forall \mu, \nu \in \mathbb{A}$, $s \in [0,1]$, $m \in (0,1]$ and $\delta \in [0,1]$.

Remark 1 *(i) If $s = m = 1$, then the above definition collapses to preinvex function [15].*
(ii) If $m = 1$ and $\zeta(\mu,\nu,m) = \mu - m\nu$, then the above definition collapses to $s-$type convex function [19].
(iii) If $s = m = 1$ and $\zeta(\mu,\nu,m) = \mu - m\nu$, then the above definition collapses to convex function [3].

4 Hermite–Hadamard type inequality via generalized preinvex function

Here, we are to explore the new sort of H-H inequality via $s-$type m-preinvex function.

Theorem 1 *Let $\mathbb{A}^\circ \subseteq \mathbb{R}$ be an open invex subset w.r.t $\zeta : \mathbb{A}^\circ \times \mathbb{A}^\circ \to \mathbb{R}$ and $\mu, \nu \in \mathbb{A}^\circ$ with $m\nu + \zeta(\mu, \nu, m) \leq \nu$. Suppose $\Psi : [m\nu + \zeta(\mu, \nu, m), \nu] \to (0, \infty)$ is $s-$type m-preinvex function, $\Psi \in L[m\nu + \zeta(\mu, \nu, m), \nu]$ for all $m \in (0, 1]$ and satisfies Condition–C then*

$$\frac{2}{2-s}\Psi\left(m\nu + \frac{1}{2}\zeta(\mu, \nu, m)\right) \leq \frac{1}{\zeta(\mu, \nu, m)}\left[\int_{m\nu}^{m\nu+\zeta(\mu,\nu,m)} \Psi(x)dx + m\int_{\frac{m\nu+\zeta(\mu,\nu,m)}{m}}^{\nu} \Psi(x)dx\right] \leq (2-s)\left[\Psi(\mu) + m\Psi(\nu)\right].$$

Proof Since $\mu, \nu \in \mathbb{A}^\circ$ and $\mathbb{A}^\circ$ is an invex set with respect to ζ, for every $m \in (0, 1]$ and $\delta \in [0, 1]$, we have $m\nu + \delta\zeta(\mu, \nu, m) \in \mathbb{A}^\circ$. For the left side, using the Definition 6, put $\delta = \frac{1}{2}$,

$$\Psi(my + \delta\zeta(x, y, m)) \leq [1 - (s(1-\delta))]\Psi(x) + m[1 - (s\delta)]\Psi(y)$$
$$\Psi(my + \frac{1}{2}\zeta(x, y, m)) \leq \left[1 - (\frac{s}{2})\right]\left[\Psi(x) + m\Psi(y)\right],$$

put $x = m\nu + \delta\zeta(\mu, \nu, m)$ and $my = m\nu + (1-\delta)\zeta(\mu, \nu, m)$ in the above inequality So we obtain

$$\Psi(my + \frac{1}{2}\zeta(x, y, m)) = \Psi(m\nu + (1-\delta)\zeta(\mu, \nu, m) + \frac{1}{2}\zeta(m\nu + \delta\zeta(\mu, \nu, m), m\nu + (1-\delta)\zeta(\mu, \nu, m), m)). \tag{5}$$

Now by using Condition C, we have

$$\zeta(m\nu + \delta\zeta(\mu, \nu, m), m\nu + (1-\delta)\zeta(\mu, \nu, m)) = (\delta - 1 + \delta)\zeta(\mu, \nu, m)$$

$$\zeta(m\nu + \delta\zeta(\mu, \nu, m), m\nu + (1-\delta)\zeta(\mu, \nu, m)) = (2\delta - 1)\zeta(\mu, \nu, m).$$

Now we put the value of ζ in (5), then as a result, we get

$$\Psi(my + \frac{1}{2}\zeta(x, y, m)) = \Psi(m\nu + (1-\delta)\zeta(\mu, \nu, m) + \frac{1}{2}(2\delta - 1)\zeta(\mu, \nu, m))$$

$$\Psi(my + \frac{1}{2}\zeta(x, y, m)) = \Psi(m\nu + (1 - \delta + \delta - \frac{1}{2})\zeta(\mu, \nu, m))$$

$$\Psi(my + \frac{1}{2}\zeta(x, y, m)) = \Psi(m\nu + \frac{1}{2}\zeta(\mu, \nu, m)).$$

Thus,

$$\begin{aligned}
&\Psi(m\nu + \frac{1}{2}\zeta(\mu, \nu, m)) \\
&\leq \left[1 - (\frac{s}{2})\right]\left[\int_0^1 \Psi(m\nu + \delta\zeta(\mu, \nu, m))d\delta + m\int_0^1 \Psi(\nu + \frac{(1-\delta)}{m}\zeta(\mu, \nu, m))d\delta\right] \\
&\leq \left[1 - (\frac{s}{2})\right]\frac{1}{\zeta(\mu, \nu, m)}\left[\int_{m\nu}^{m\nu+\zeta(\mu,\nu,m)} \Psi(x)dx + m\int_{\frac{m\nu+\zeta(\mu,\nu,m)}{m}}^{\nu} \Psi(x)dx\right].
\end{aligned}$$

For the right side of the inequality and from the property of $s-$type $m-$preinvexity, we have

$$\begin{aligned}
&\frac{1}{\zeta(\mu, \nu, m)}\left[\int_{m\nu}^{m\nu+\zeta(\mu,\nu,m)} \Psi(x)dx + m\int_{\frac{m\nu+\zeta(\mu,\nu,m)}{m}}^{\nu} \Psi(x)dx\right] \\
&\leq \left[\int_0^1 \Psi(m\nu + \delta\zeta(\mu, \nu, m))d\delta + m\int_0^1 \Psi(\nu + \frac{(1-\delta)}{m}\zeta(\mu, \nu, m))d\delta\right] \\
&\leq \int_0^1 [1 - (s(1-\delta))]\Psi(\mu)d\delta + m\int_0^1 [1 - (s\delta)]\Psi(\nu)d\delta \\
&+ \int_0^1 [1 - s\delta]\Psi(\mu)d\delta + m\int_0^1 [1 - (s(1-\delta))]\Psi(\nu)d\delta \\
&\leq \frac{(2-s)}{2}\left[\Psi(\mu) + \Psi(\mu) + m(\Psi(\nu) + \Psi(\nu))\right] \\
&\leq (2-s)\left[\Psi(\mu) + m(\Psi(\nu))\right].
\end{aligned}$$

This is the required proof. ■

Corollary 1 *If $s = m = 1$ and $\zeta(\mu, \nu, m) = \mu - m\nu$, then we get Hermite-Hadamard inequality in [22].*

Remark 2 *If $m = 1$, then we attain the inequality*

$$\frac{2}{2-s}\Psi(\nu+\frac{1}{2}\zeta(\mu,\nu)) \le \frac{1}{\zeta(\mu,\nu)}\left[\int_{\nu}^{\nu+\zeta(\mu,\nu)}\Psi(x)dx + \int_{\nu+\zeta(\mu,\nu)}^{\nu}\Psi(x)dx\right] \le (2-s)[\Psi(\mu)+\Psi(\nu)].$$

Remark 3 *If $s = 1$, then we get the inequality*

$$2\Psi(m\nu+\frac{1}{2}\zeta(\mu,\nu,m)) \le \frac{1}{\zeta(\mu,\nu,m)}\left[\int_{m\nu}^{m\nu+\zeta(\mu,\nu,m)}\Psi(x)dx + m\int_{\frac{m\nu+\zeta(\mu,\nu,m)}{m}}^{\nu}\Psi(x)dx\right] \le [\Psi(\mu)+m\Psi(\nu)].$$

Remark 4 *If $s = m = 1$, then we get the inequality*

$$2\Psi(\nu+\frac{1}{2}\zeta(\mu,\nu)) \le \frac{1}{\zeta(\mu,\nu)}\left[\int_{\nu}^{\nu+\zeta(\mu,\nu)}\Psi(x)dx + \int_{\nu+\zeta(\mu,\nu)}^{\nu}\Psi(x)dx\right] \le [\Psi(\mu)+\Psi(\nu)].$$

5 Refinements of Hermite–Hadamard type inequality

The main aim of this section is to examine the refinements of Hermite–Hadamard inequality via s–type preinvex functions.

Lemma 1 *Let $\Psi : [\mu, m\mu+\zeta(\frac{\nu}{c},\mu,m)] \to \mathbb{R}$ be a differentiable mapping on $(\mu, m\mu+\zeta(\frac{\nu}{c},\mu,m))$ with $0 < c \le 1$ and $m\mu+\zeta(\nu,\mu,m) > \mu > 0$. If $\Psi' \in \mathcal{L}(\mu, m\mu+\zeta(\frac{\nu}{c},\mu,m))$ and for all $m \in (0,1]$, then*

$$\frac{\Psi(\mu)+\Psi(m\mu+\zeta(\frac{\nu}{c},\mu,m))}{2} - \frac{c}{\zeta(\nu,c\mu,m)}\int_{\mu}^{m\mu+\zeta(\frac{\nu}{c},\mu,m)}\Psi(x)dx = \frac{\zeta(\nu,c\mu,m)}{2c}\int_0^1(1-2\delta)\Psi'\left(m\frac{\nu}{c}+\delta\zeta(\mu,\frac{\nu}{c},m)\right)d\delta. \tag{6}$$

Proof

$$\frac{\zeta(\nu,c\mu,m)}{2c}\int_0^1(1-2\delta)\Psi'\left(\frac{m\nu}{c}+\delta\zeta(\mu,\frac{\nu}{c},m)\right)d\delta = \frac{\zeta(\nu,c\mu,m)}{2c}\left[\frac{(1-2\delta)\Psi(\frac{m\nu}{c}+\delta\zeta(\mu,\frac{\nu}{c}))}{\zeta(\mu,\frac{\nu}{c},m)}\Big|_0^1 + 2\int_0^1\frac{\Psi(\frac{m\nu}{c}+\delta\zeta(\mu,\frac{\nu}{c},m))}{\zeta(\mu,\frac{\nu}{c},m)}d\delta\right]$$

$$= \frac{\zeta(\nu,c\mu,m)}{2c}\left[\frac{c(\Psi(\mu)+\Psi(m\mu+\zeta(\frac{\nu}{c},\mu,m))}{\zeta(\nu,c\mu)} - \frac{2c}{\zeta(\nu,c\mu)}\int_0^1\Psi(\frac{m\nu}{c}+\delta\zeta(\mu,\frac{\nu}{c},m))d\delta\right]$$

$$= \frac{\Psi(\mu)+\Psi(m\mu+\zeta(\frac{\nu}{c},\mu,m))}{2} - \frac{c}{\zeta(\nu,c\mu,m)}\int_{\mu}^{m\mu+\zeta(\frac{\nu}{c},\mu,m)}\Psi(x)dx,$$

which gives the proof. ■

Lemma 2 *Let $\Psi : [\mu, m\mu+\zeta(\frac{\nu}{c},\mu,m)] \to \mathbb{R}$ be a differentiable mapping on $(\mu, m\mu+\zeta(\frac{\nu}{c},\mu,m))$ with $0 < c \le 1$ and $m\mu+\zeta(\nu,\mu,m) > \mu > 0$. If $\Psi' \in \mathcal{L}(\mu, m\mu+\zeta(\frac{\nu}{c},\mu,m))$ and for all $m \in (0,1]$, then*

$$\begin{aligned}&\frac{c}{\zeta(\nu,c\mu,m)}\int_{\mu}^{m\mu+\zeta(\frac{\nu}{c},\mu,m)}\Psi(x)dx - \Psi\left(\frac{2m\mu+\zeta(\nu,\mu,m)}{2c}\right)\\ &= \frac{\zeta(\nu,c\mu,m)}{c}\left\{\int_0^1\delta\Psi'\left(\frac{m\nu}{c}+\delta\zeta(\mu,\frac{\nu}{c},m)\right)d\delta - \int_{1/2}^1\Psi'\left(\frac{m\nu}{c}+\delta\zeta(\mu,\frac{\nu}{c},m)\right)d\delta\right\}.\end{aligned} \tag{7}$$

Proof

$$\begin{aligned}&\frac{\zeta(\nu,c\mu,m)}{c}\left\{\int_0^1\delta\Psi'\left(\frac{m\nu}{c}+\delta\zeta(\mu,\frac{\nu}{c},m)\right)d\delta - \int_{1/2}^1\Psi'\left(\frac{m\nu}{c}+\delta\zeta(\mu,\frac{\nu}{c},m)\right)d\delta\right\}\\ &= \frac{\zeta(\nu,c\mu,m)}{c}\times\left[\frac{\delta\Psi(\frac{m\nu}{c}+\delta\zeta(\mu,\frac{\nu}{c},m))}{\zeta(\mu,\frac{\nu}{c},m)}\Big|_0^1 - \int_0^1\frac{\Psi(\frac{m\nu}{c}+\delta\zeta(\mu,\frac{\nu}{c},m))}{\zeta(\mu,\frac{\nu}{c},m)}d\delta - \frac{\Psi(\frac{m\nu}{c}+\delta\zeta(\mu,\frac{\nu}{c},m))}{\zeta(\mu,\frac{\nu}{c},m)}d\delta\Big|_{\frac{1}{2}}^1\right]\\ &= \frac{\zeta(\nu,c\mu,m)}{c}\left[\frac{c\Psi(\mu)}{\zeta(c\mu,\nu,m)} - \frac{c}{\zeta(c\mu,\nu,m)}\int_0^1\Psi(\frac{m\nu}{c}+\delta\zeta(\mu,\frac{\nu}{c},m))d\delta - \frac{c}{\zeta(c\mu,\nu,m)}\left(\Psi(\mu)-\Psi\left(\frac{(2m\mu+\zeta(\nu,\mu,m))}{2c}\right)\right)\right]\\ &= \frac{c}{\zeta(\nu,c\mu,m)}\int_{\mu}^{m\mu+\zeta(\frac{m\nu}{c},\mu,m)}\Psi(x)dx - \Psi\left(\frac{2m\mu+\zeta(\nu,\mu,m)}{2c}\right),\end{aligned}$$

which gives the proof. ■

Theorem 2 *Let $\mathbb{X}^\circ \subseteq \mathbb{R}$ be an open invex subset w.r.t $\zeta : \mathbb{X}^\circ\times\mathbb{X}^\circ \to \mathbb{R}$ and $\mu, \nu \in \mathbb{X}^\circ$ with $m\nu+\zeta(\mu,\nu,m) \le \nu$. Suppose $\Psi : [m\nu+\zeta(\mu,\nu,m),\nu]$ be a differentiable function on $\mathbb{X}^\circ$. If $|\Psi'|$ is s–type m–preinvex function on $(\mu, m\mu+\zeta(\nu,\mu,m))$ for $m \in (0,1]$ and $s \in [0,1]$, then*

$$\left|\frac{\Psi(\mu)+\Psi(m\mu+\zeta(\frac{\nu}{c},\mu,m))}{2} - \frac{c}{\zeta(\nu,c\mu,m)}\int_{\mu}^{m\mu+\zeta(\frac{\nu}{c},\mu,m)}\Psi(x)dx\right| \le \frac{\zeta(\nu,c\mu,m)}{2c}\left\{\frac{2-s}{4}\left[|\Psi'(\mu)| + m|\Psi'\left(\frac{\nu}{c}\right)|\right]\right\}. \tag{8}$$

Proof According to Lemma 1, one has

$$\left|\frac{\Psi(\mu)+\Psi(m\mu+\zeta(\frac{\nu}{c},\mu,m))}{2}-\frac{c}{\zeta(\nu,c\mu,m)}\int_{\mu}^{m\mu+\zeta(\frac{\nu}{c},\mu,m)}\Psi(x)dx\right|=\frac{\zeta(\nu,c\mu,m)}{2c}\int_0^1|1-2\delta||\Psi'\left(\frac{m\nu}{c}+\delta\zeta(\mu,\frac{\nu}{c},m)\right)|d\delta.$$

Since $|\Psi'|$ is $s-$type $m-$preinvex on $(\mu,\mu+\zeta(\nu,\mu))$, we have

$$\left|\frac{\Psi(\mu)+\Psi(m\mu+\zeta(\frac{\nu}{c},\mu,m))}{2}-\frac{c}{\zeta(\nu,c\mu,m)}\int_{\mu}^{m\mu+\zeta(\frac{\nu}{c},\mu,m)}\Psi(x)dx\right|\leq\frac{\zeta(\nu,c\mu,m)}{2c}\int_0^1|1-2\delta|\left[(1-s(1-\delta))\Psi'(\mu)|+m(1-s\delta)|\Psi'\left(\frac{\nu}{c}\right)|\right]d\delta$$
$$\leq\frac{\zeta(\nu,c\mu,m)}{2c}\left\{|\Psi'(\mu)|\int_0^1|1-2\delta|1-s(1-\delta)d\delta+m|\Psi'\left(\frac{\nu}{c}\right)|\int_0^1|1-2\delta|(1-s\delta)d\delta\right\}. \tag{9}$$

Since,

$$\int_0^1(1-s(1-\delta))|1-2\delta|d\delta=\int_0^1(1-s\delta)|1-2\delta|d\delta=-\frac{s-2}{4}.$$

Putting the value of the above computation in (9), then we obtain the required proof. ■

Theorem 3 *Let $\mathbb{X}^\circ\subseteq\mathbb{R}$ be an open invex subset w.r.t $\zeta:\mathbb{X}^\circ\times\mathbb{X}^\circ\to\mathbb{R}$ and $\mu,\nu\in\mathbb{X}^\circ$ with $m\nu+\zeta(\mu,\nu,m)\leq\nu$. Suppose $\Psi:[m\nu+\zeta(\mu,\nu,m),\nu]$ be a differentiable mapping on $\mathbb{X}^\circ$. If $|\Psi'|^q$ is $s-$type $m-$preinvex on $(\mu,m\mu+\zeta(\nu,\mu,m))$ for $p,q>1$, $\frac{1}{q}+\frac{1}{p}=1$, $m\in(0,1]$ and $s\in[0,1]$, then*

$$\left|\frac{\Psi(\mu)+\Psi(m\mu+\zeta(\frac{\nu}{c},\mu,m))}{2}-\frac{c}{\zeta(\nu,c\mu,m)}\int_{\mu}^{\mu+\zeta(\frac{\nu}{c},\mu)}\Psi(x)dx\right|\leq\frac{\zeta(\nu,c\mu,m)}{2c}\left[\frac{1}{p+1}\right]^{1/p}\left\{\frac{2-s}{2}\left[|\Psi'(\mu)|^q+m|\Psi'\left(\frac{\nu}{c}\right)|^q\right]\right\}^{1/q}. \tag{10}$$

Proof According to Lemma 1 and applying Hölder's inequality, one has

$$\left|\frac{\Psi(\mu)+\Psi(m\mu+\zeta(\frac{\nu}{c},\mu,m))}{2}-\frac{c}{\zeta(\nu,c\mu,m)}\int_{\mu}^{m\mu+\zeta(\frac{\nu}{c},\mu,m)}\Psi(x)dx\right|=\frac{\zeta(\nu,c\mu,m)}{2c}\int_0^1|1-2\delta||\Psi'\left(\frac{m\nu}{c}+\delta\zeta(\mu,\frac{\nu}{c},m)\right)|d\delta$$
$$\leq\frac{\zeta(\nu,c\mu,m)}{2c}\left(\int_0^1|1-2\delta|^pd\delta\right)^{1/p}\left(\int_0^1|\Psi'\left(\frac{m\nu}{c}+\delta\zeta(\mu,\frac{\nu}{c},m)\right)|^qd\delta\right)^{1/q}. \tag{11}$$

Since $|\Psi'|^q$ is s-type $m-$preinvex on $(\mu,m\mu+\zeta(\nu,\mu,m))$, we have

$$\int_0^1|\Psi'\left(\frac{m\nu}{c}+\delta\zeta(\mu,\frac{\nu}{c},m)\right)|^qd\delta=|\Psi'(\mu)|^q\int_0^1(1-s(1-\delta))d\delta+m|\Psi'\left(\frac{\nu}{c}\right)|^q\int_0^1(1-s\delta)d\delta.$$

Now, equation (11) becomes

$$\left|\frac{\Psi(\mu)+\Psi(m\mu+\zeta(\frac{\nu}{c},\mu,m))}{2}-\frac{c}{\zeta(\nu,c\mu,m)}\int_{\mu}^{m\mu+\zeta(\frac{\nu}{c},\mu,m)}\Psi(x)dx\right|$$
$$\leq\frac{\zeta(\nu,c\mu,m)}{2c}\left[\frac{1}{p+1}\right]^{1/p}\left(|\Psi'(\mu)|^q\int_0^1(1-s(1-\delta))d\delta+m|\Psi'\left(\frac{\nu}{c}\right)|^q\int_0^1(1-s\delta)d\delta\right)^{1/q}. \tag{12}$$

Since,

$$\int_0^1(1-s(1-\delta))\,d\delta=\int_0^1(1-s\delta)\,d\delta=-\frac{s-2}{2}\int_0^1|1-2\delta|^pd\delta=\left[\frac{1}{p+1}\right].$$

Putting the value of the above computation in (12), then we obtain the required proof. ■

Theorem 4 *Let $\mathbb{X}^\circ\subseteq\mathbb{R}$ be an open invex subset w.r.t $\zeta:\mathbb{X}^\circ\times\mathbb{X}^\circ\to\mathbb{R}$ and $\mu,\nu\in\mathbb{X}^\circ$ with $m\nu+\zeta(\mu,\nu,m)\leq\nu$. Suppose $\Psi:[m\nu+\zeta(\mu,\nu,m),\nu]$ be a differentiable mapping on $\mathbb{X}^\circ$. If $|\Psi'|^q$ is $s-$type $m-$preinvex on $(\mu,m\mu+\zeta(\nu,\mu,m))$ for $p,q>1$, $\frac{1}{q}+\frac{1}{p}=1$, $m\in(0,1]$ and $s\in[0,1]$, then*

$$\left|\frac{\Psi(\mu)+\Psi(m\mu+\zeta(\frac{\nu}{c},\mu,m))}{2}-\frac{c}{\zeta(\nu,c\mu,m)}\int_{\mu}^{m\mu+\zeta(\frac{\nu}{c},\mu,m)}\Psi(x)dx\right|\leq\frac{\zeta(\nu,c\mu,m)}{c}\left[\frac{1}{2\left(\frac{p+1}{p}\right)}\right]\left\{\frac{2-s}{4}\left[|\Psi'(\mu)|^q+m|\Psi'\left(\frac{\nu}{c}\right)|^q\right]\right\}^{1/q}. \tag{13}$$

Proof According to Lemma 1 and applying Hölder's inequality, one has

$$\left|\frac{\Psi(\mu)+\Psi(m\mu+\zeta(\frac{\nu}{c},\mu,m))}{2}-\frac{c}{\zeta(\nu,c\mu,m)}\int_{\mu}^{\mu+\zeta(\frac{\nu}{c},\mu)}\Psi(x)dx\right|\leq\frac{\zeta(\nu,c\mu,m)}{2c}\int_0^1|1-2\delta||\Psi'\left(\frac{m\nu}{c}+\delta\zeta(\mu,\frac{\nu}{c},m)\right)|d\delta$$
$$=\frac{\zeta(\nu,c\mu,m)}{2c}\int_0^1|1-2\delta|^{1/p}|1-2\delta|^{1/q}|\Psi'\left(\frac{m\nu}{c}+\delta\zeta(\mu,\frac{\nu}{c},m)\right)|d\delta$$
$$\leq\frac{\zeta(\nu,c\mu,m)}{2c}\left(\int_0^1|1-2\delta|d\delta\right)^{1/p}\left(\int_0^1|1-2\delta||\Psi'\left(\frac{m\nu}{c}+\delta\zeta(\mu,\frac{\nu}{c},m)\right)|^qd\delta\right)^{1/q}. \tag{14}$$

Since $|\Psi'|^q$ is s-type $m-$preinvex on $(\mu, m\mu + \zeta(\nu, \mu, m))$, we have

$$\int_0^1 |\Psi'\left(\frac{m\nu}{c} + \delta\zeta(\mu, \frac{\nu}{c}, m)\right)|^q d\delta = |\Psi'(\mu)|^q \int_0^1 (1 - s(1-\delta))d\delta + m|\Psi'\left(\frac{\nu}{c}\right)|^q \int_0^1 (1 - s\delta)d\delta.$$

Now, equation (14) becomes

$$\begin{aligned}&\left|\frac{\Psi(\mu) + \Psi(m\mu + \zeta(\frac{\nu}{c}, \mu, m))}{2} - \frac{c}{\zeta(\nu, c\mu, m)}\int_\mu^{m\mu+\zeta(\frac{\nu}{c},\mu,m)} \Psi(x)dx\right| \\ &\leq \frac{\zeta(\nu, c\mu, m)}{2c}\left(\int_0^1 |1-2\delta|d\delta\right)^{1/p}\left(|\Psi'(\mu)|^q \int_0^1 |1-2\delta|(1-s(1-\delta))d\delta + m|\Psi'\left(\frac{\nu}{c}\right)|^q \int_0^1 |1-2\delta|(1-sk)d\delta\right)^{1/q}. \end{aligned} \tag{15}$$

Since,

$$\int_0^1 |1-2\delta|\,(1-s\,(1-\delta))\,d\delta = \int_0^1 |1-2\delta|\,(1-s\delta)\,d\delta = -\frac{s-2}{4}$$
$$\int_0^1 |1-2\delta|d\delta = \frac{1}{2}.$$

Putting the values of the above computations in (15), then we obtain the required proof. ■

Theorem 5 *Let $\mathbb{X}^\circ \subseteq \mathbb{R}$ be an open invex subset w.r.t $\zeta : \mathbb{X}^\circ \times \mathbb{X}^\circ \to \mathbb{R}$ and $\mu, \nu \in \mathbb{X}^\circ$ with $m\nu + \zeta(\mu, \nu, m) \leq \nu$. Suppose $\Psi : [m\nu + \zeta(\mu, \nu, m), \nu]$ be a differentiable mapping on $\mathbb{X}^\circ$. If $|\Psi'|^q$ is s−type m−preinvex on $(\mu, m\mu + \zeta(\nu, \mu, m))$ for $p, q > 1$, $\frac{1}{q} + \frac{1}{p} = 1, m \in (0, 1]$ and $s \in [0, 1]$, then*

$$\begin{aligned}&\left|\frac{\Psi(\mu) + \Psi(m\mu + \zeta(\frac{\nu}{c}, \mu, m))}{2} - \frac{c}{\zeta(\nu, c\mu, m)}\int_\mu^{m\mu+\zeta(\frac{\nu}{c},\mu,m)} \Psi(x)dx\right| \\ &\leq \frac{\zeta(\nu, c\mu, m)}{2c}\left[\frac{1}{2(p+1)}\right]^{1/p}\left[\left\{\frac{3-2s}{6}|\Psi'(\mu)|^q + \frac{3-s}{6}m|\Psi'\left(\frac{\nu}{c}\right)|^q\right\}^{1/q} + \left\{\frac{3-s}{6}|\Psi'(\mu)|^q + \frac{3-2s}{6}m|\Psi'\left(\frac{\nu}{c}\right)|^q\right\}^{1/q}\right]. \end{aligned} \tag{16}$$

Proof According to Lemma 1 and applying Hölder-Íscan inequality, one has

$$\begin{aligned}&\left|\frac{\Psi(\mu) + \Psi(m\mu + \zeta(\frac{\nu}{c}, \mu, m))}{2} - \frac{c}{\zeta(\nu, c\mu, m)}\int_\mu^{m\mu+\zeta(\frac{\nu}{c},\mu,m)} \Psi(x)dx\right| \leq \frac{\zeta(\nu, c\mu, m)}{2c} \\ &\times\left[\left(\int_0^1 (1-\delta)|1-2\delta|^p d\delta\right)^{1/p}\left(\int_0^1 (1-\delta)|\Psi'\left(\frac{m\nu}{c} + \delta\zeta(\mu, \frac{\nu}{c}, m)\right)|^q d\delta\right)^{1/q} + \left(\int_0^1 \delta|1-2\delta|^p d\delta\right)^{1/p}\left(\int_0^1 \delta|\Psi'\left(\frac{m\nu}{c} + \delta\zeta(\mu, \frac{\nu}{c}, m)\right)|^q d\delta\right)^{1/q}\right]. \end{aligned} \tag{17}$$

Since $|\Psi'|^q$ is s-type $m-$preinvex on $(\mu, m\mu + \zeta(\nu, \mu, m))$, we have

$$\int_0^1 |\Psi'\left(\frac{m\nu}{c} + \delta\zeta(\mu, \frac{\nu}{c}, m)\right)|^q d\delta = |\Psi'(\mu)|^q \int_0^1 (1 - s(1-\delta))d\delta + m|\Psi'\left(\frac{\nu}{c}\right)|^q \int_0^1 (1 - s\delta)d\delta.$$

Now, equation (17) becomes

$$\begin{aligned}&\left|\frac{\Psi(\mu) + \Psi(m\mu + \zeta(\frac{\nu}{c}, \mu, m))}{2} - \frac{c}{\zeta(\nu, c\mu, m)}\int_\mu^{m\mu+\zeta(\frac{\nu}{c},\mu,m)} \Psi(x)dx\right| \\ &\leq \frac{\zeta(\nu, c\mu, m)}{2c}\left[\left(\int_0^1 (1-\delta)|1-2\delta|^p d\delta\right)^{1/p}\left(|\Psi'(\mu)|^q \int_0^1 (1-\delta)(1-s(1-\delta))d\delta + m|\Psi'\left(\frac{\nu}{c}\right)|^q \int_0^1 (1-\delta)(1-s\delta)d\delta\right)^{1/q}\right. \\ &\left. + \left(\int_0^1 \delta|1-2\delta|^p d\delta\right)^{1/p}\left(|\Psi'(\mu)|^q \int_0^1 \delta(1-s(1-\delta))d\delta + m|\Psi'\left(\frac{\nu}{c}\right)|^q \int_0^1 \delta(1-s\delta)d\delta\right)^{1/q}\right]. \end{aligned} \tag{18}$$

Since,

$$\int_0^1 (1-\delta)\,(1-s\,(1-\delta))\,d\delta = \int_0^1 \delta\,(1-s\delta)\,d\delta = -\frac{2s-3}{6}$$
$$\int_0^1 \delta\,(1-s\,(1-\delta))\,d\delta = \int_0^1 (1-\delta)\,(1-s\delta)\,d\delta = -\frac{s-3}{6}$$
$$\int_0^1 \delta|1-2\delta|^p d\delta = \int_0^1 (1-\delta)|1-2\delta|^p d\delta = \left[\frac{1}{2(p+1)}\right].$$

Putting the values of the above computations in (18), then we obtain the required result. ■

Theorem 6 *Let $\mathbb{X}^\circ \subseteq \mathbb{R}$ be an open invex subset w.r.t $\zeta : \mathbb{X}^\circ \times \mathbb{X}^\circ \to \mathbb{R}$ and $\mu, \nu \in \mathbb{X}^\circ$ with $m\nu + \zeta(\mu, \nu, m) \leq \nu$. Suppose $\Psi : [m\nu + \zeta(\mu, \nu, m), \nu]$ be a differentiable mapping on $\mathbb{X}^\circ$. If $|\Psi'|^q$ is s−type m−preinvex on $(\mu, m\mu + \zeta(\nu, \mu, m))$ for $q \geq 1$, $m \in (0, 1]$ and $s \in [0, 1]$, then*

$$\left|\frac{\Psi(\mu) + \Psi(m\mu + \zeta(\frac{\nu}{c}, \mu, m))}{2} - \frac{c}{\zeta(\nu, c\mu, m)} \int_\mu^{m\mu+\zeta(\frac{\nu}{c},\mu,m)} \Psi(x)dx\right| \leq \frac{\zeta(\nu, c\mu, m)}{2c} \left[\frac{1}{4}\right]^{1-1/q}$$
$$\times \left[\left\{\frac{4-3s}{16}|\Psi'(\mu)|^q + \frac{4-s}{16}m|\Psi'\left(\frac{\nu}{c}\right)|^q\right\}^{1/q} + \left\{\frac{4-s}{16}|\Psi'(\mu)|^q + \frac{4-3s}{16}m|\Psi'\left(\frac{\nu}{c}\right)|^q\right\}^{1/q}\right]. \quad (19)$$

Proof According to Lemma 1 and applying Improved power-mean inequality, one has

$$\left|\frac{\Psi(\mu) + \Psi(m\mu + \zeta(\frac{\nu}{c}, \mu, m))}{2} - \frac{c}{\zeta(\nu, c\mu, m)} \int_\mu^{m\mu+\zeta(\frac{\nu}{c},\mu,m)} \Psi(x)dx\right|$$
$$\leq \frac{\zeta(\nu, c\mu, m)}{2c} \left[\left(\int_0^1 (1-\delta)|1-2\delta|d\delta\right)^{1-1/q} \left(\int_0^1 (1-\delta)|1-2\delta||\Psi'\left(\frac{m\nu}{c} + \delta\zeta(\mu, \frac{\nu}{c}, m)\right)|^q d\delta\right)^{1/q}\right.$$
$$\left. + \left(\int_0^1 \delta|1-2\delta|d\delta\right)^{1-1/q} \left(\int_0^1 \delta|1-2\delta||\Psi'\left(\frac{m\nu}{c} + \delta\zeta(\mu, \frac{\nu}{c}, m)\right)|^q d\delta\right)^{1/q}\right]. \quad (20)$$

Since $|\Psi'|^q$ is s-type m−preinvex on $(\mu, m\mu + \zeta(\nu, \mu, m))$, we have

$$\int_0^1 |\Psi'\left(\frac{m\nu}{c} + \delta\zeta(\mu, \frac{\nu}{c}, m)\right)|^q d\delta = |\Psi'(\mu)|^q \int_0^1 (1-s(1-\delta))d\delta + m|\Psi'\left(\frac{\nu}{c}\right)|^q \int_0^1 (1-s\delta)d\delta.$$

Now, equation (20) becomes

$$\left|\frac{\Psi(\mu) + \Psi(m\mu + \zeta(\frac{\nu}{c}, \mu, m))}{2} - \frac{c}{\zeta(\nu, c\mu, m)} \int_\mu^{m\mu+\zeta(\frac{\nu}{c},\mu,m)} \Psi(x)dx\right|$$
$$\leq \frac{\zeta(\nu, c\mu, m)}{2c} \left[\left(\int_0^1 (1-\delta)|1-2\delta|d\delta\right)^{1-1/q} \left(|\Psi'(\mu)|^q \int_0^1 (1-\delta)|1-2\delta|(1-s(1-\delta))d\delta\right.\right.$$
$$\left. + m|\Psi'\left(\frac{\nu}{c}\right)|^q \int_0^1 (1-\delta)|1-2\delta|(1-s\delta)d\delta\right)^{1/q}$$
$$\left. + \left(\int_0^1 \delta|1-2\delta|d\delta\right)^{1-1/q} \left(|\Psi'(\mu)|^q \int_0^1 \delta|1-2\delta|(1-s(1-\delta))d\delta + m|\Psi'\left(\frac{\nu}{c}\right)|^q \int_0^1 \delta|1-2\delta|(1-s\delta)d\delta\right)^{1/q}\right]. \quad (21)$$

Since,

$$\int_0^1 (1-\delta)|1-2\delta|\,(1-s\,(1-\delta))\,d\delta = \int_0^1 \delta|1-2\delta|\,(1-s\delta)\,d\delta = -\frac{3s-4}{16}$$
$$\int_0^1 \delta|1-2\delta|\,(1-s\,(1-\delta))\,d\delta = \int_0^1 (1-\delta)|1-2\delta|\,(1-s\delta)\,d\delta = -\frac{s-4}{16}$$
$$\int_0^1 \delta|1-2\delta|d\delta = \int_0^1 (1-\delta)|1-2\delta|d\delta = \left[\frac{1}{4}\right]$$

Putting the values of the above computations in (21), then we obtain the required proof. ■

Theorem 7 *Let $\mathbb{X}^\circ \subseteq \mathbb{R}$ be an open invex subset w.r.t $\zeta : \mathbb{X}^\circ \times \mathbb{A}^\circ \to \mathbb{R}$ and $\mu, \nu \in \mathbb{X}^\circ$ with $m\nu + \zeta(\mu, \nu, m) \leq \nu$. Suppose $\Psi : [m\nu + \zeta(\mu, \nu, m), \nu]$ be a differentiable mapping on $\mathbb{X}^\circ$. If $|\Psi'|^q$ is s−type m−preinvex on $(\mu, m\mu + \zeta(\nu, \mu, m))$ for $q \geq 1$, $m \in (0, 1]$ and $s \in [0, 1]$, then*

$$\left|\frac{\Psi(\mu) + \Psi(m\mu + \zeta(\frac{\nu}{c}, \mu, m))}{2} - \frac{c}{\zeta(\nu, c\mu, m)} \int_\mu^{m\mu+\zeta(\frac{\nu}{c},\mu,m)} \Psi(x)dx\right| \leq \frac{\zeta(\nu, c\mu, m)}{2c} \left[\frac{1}{2}\right]^{1-\frac{1}{q}} \left\{\frac{2-s}{4}\left[|\Psi'(\mu)|^q + m|\Psi'\left(\frac{\nu}{c}\right)|^q\right]\right\}^{1/q}. \quad (22)$$

Proof According to Lemma 1 and applying Power-mean inequality, one has

$$\left|\frac{\Psi(\mu) + \Psi(m\mu + \zeta(\frac{\nu}{c}, \mu, m))}{2} - \frac{c}{\zeta(\nu, c\mu, m)} \int_\mu^{m\mu+\zeta(\frac{\nu}{c},\mu,m)} \Psi(x)dx\right| \leq \frac{\zeta(\nu, c\mu, m)}{2c} \int_0^1 |1-2\delta||\Psi'\left(\frac{m\nu}{c} + \delta\zeta(\mu, \frac{\nu}{c}, m)\right)|d\delta$$
$$\leq \frac{\zeta(\nu, c\mu, m)}{2c} \left(\int_0^1 |1-2\delta|d\delta\right)^{1-1/q} \left(\int_0^1 |1-2\delta||\Psi'\left(\frac{m\nu}{c} + \delta\zeta(\mu, \frac{\nu}{c}, m)\right)|^q d\delta\right)^{1/q}. \quad (23)$$

Since $|\Psi'|^q$ is s-type m−preinvex on $(\mu, m\mu + \zeta(\nu, \mu, m))$, we have

$$\int_0^1 |\Psi'\left(\frac{m\nu}{c} + \delta\zeta(\mu, \frac{\nu}{c}, m)\right)|^q d\delta = |\Psi'(\mu)|^q \int_0^1 (1-s(1-\delta))d\delta + m|\Psi'\left(\frac{\nu}{c}\right)|^q \int_0^1 (1-s\delta)d\delta.$$

Now, equation (23) becomes

$$\left|\frac{\Psi(\mu)+\Psi(m\mu+\zeta(\frac{\nu}{c},\mu,m))}{2}-\frac{c}{\zeta(\nu,c\mu,m)}\int_{\mu}^{\mu+\zeta(\frac{m\nu}{c},\mu,m)}\Psi(x)dx\right|$$
$$\leq\frac{\zeta(\nu,c\mu,m)}{2c}\left(\int_0^1|1-2\delta|d\delta\right)^{1-1/q}\left(|\Psi'(\mu)|^q\int_0^1|1-2\delta|(1-s(1-\delta))d\delta\ +m|\Psi'\left(\frac{\nu}{c}\right)|^q\int_0^1|1-2\delta|(1-s\delta)d\delta\right)^{1/q}. \tag{24}$$

Since,

$$\int_0^1|1-2\delta|\,(1-s\,(1-\delta))\,d\delta=\int_0^1|1-2\delta|\,(1-s\delta)\,d\delta=-\frac{s-2}{4}$$
$$\int_0^1|1-2\delta|d\delta=\frac{1}{2}.$$

Putting the values of the above computations in (24), then we obtain the required proof. ■

Theorem 8 *Let $\mathbb{X}^\circ\subseteq\mathbb{R}$ be an open invex subset w.r.t $\zeta:\mathbb{X}^\circ\times\mathbb{X}^\circ\to\mathbb{R}$ and $\mu,\nu\in\mathbb{X}^\circ$ with $m\nu+\zeta(\mu,\nu,m)\leq\nu$. Suppose $\Psi:[m\nu+\zeta(\mu,\nu,m),\nu]$ be a differentiable mapping on $\mathbb{X}^\circ$. If $|\Psi'|^q$ is s−type m−preinvex on $(\mu,m\mu+\zeta(\nu,\mu,m))$ for $p,q>1$, $\frac{1}{q}+\frac{1}{p}=1$, $m\in(0,1]$ and $s\in[0,1]$, then*

$$\left|\frac{c}{\zeta(\nu,c\mu,m)}\int_{\mu}^{m\mu+\zeta(\frac{\nu}{c},\mu,m)}\Psi(x)dx-\Psi\left(\frac{2m\mu+\zeta(\nu,\mu,m)}{2c}\right)\right|$$
$$\leq\frac{\zeta(\nu,c\mu,m)}{c}\left[\left(\frac{1}{p+1}\right)^{1/p}\left\{\frac{2-s}{2}[|\Psi'(\mu)|^q+m|\Psi'(\frac{\nu}{c})|^q]\right\}^{1/q}+\left\{\frac{4-3s}{8}[|\Psi'(\mu)|^q+m|\Psi'(\frac{\nu}{c})|^q]\right\}^{1/q}\right]. \tag{25}$$

Proof According to Lemma 2 and applying Hölder's inequality, one has

$$\left|\frac{c}{\zeta(\nu,c\mu,m)}\int_{\mu}^{m\mu+\zeta(\frac{\nu}{c},\mu,m)}\Psi(x)dx-\Psi\left(\frac{2m\mu+\zeta(\nu,\mu,m)}{2c}\right)\right|$$
$$=\frac{\zeta(\nu,c\mu,m)}{c}\left\{\int_0^1\delta\Psi'\left(\frac{m\nu}{c}+\delta\zeta(\mu,\frac{\nu}{c},m)\right)d\delta-\int_{1/2}^1\Psi'\left(\frac{m\nu}{c}+\delta\zeta(\mu,\frac{\nu}{c},m)\right)d\delta\right\}$$
$$\leq\frac{\zeta(\nu,c\mu,m)}{c}\left[\left(\int_0^1\delta^p d\delta\right)^{1/p}\left\{\int_0^1|\Psi'\left(\frac{m\nu}{c}+\delta\zeta(\mu,\frac{\nu}{c},m)\right)|^q d\delta\right\}^{1/q}+\left\{\int_{1/2}^1|\Psi'\left(\frac{m\nu}{c}+\delta\zeta(\mu,\frac{\nu}{c},m)\right)|^q d\delta\right\}^{1/q}\right]$$
$$\leq\frac{\zeta(\nu,c\mu,m)}{c}\left[\left(\frac{1}{p+1}\right)^{1/p}\left\{\int_0^1[1-s(1-\delta)]|\Psi'(\mu)|^q d\delta+m\int_0^1[1-s\delta]|\Psi'\left(\frac{\nu}{c}\right)|^q d\delta\right\}^{1/q}\right.$$
$$\left.+\left\{\int_{1/2}^1[1-s(1-\delta)]|\Psi'(\mu)|^q d\delta+m\int_{1/2}^1[1-s\delta]|\Psi'\left(\frac{\nu}{c}\right)|^q d\delta\right\}^{1/q}\right]$$
$$=\frac{\zeta(\nu,c\mu,m)}{c}\left[\left(\frac{1}{p+1}\right)^{1/p}\left\{\frac{2-s}{2}[|\Psi'(\mu)|^q+m|\Psi'(\frac{\nu}{c})|^q]\right\}^{1/q}+\left\{\frac{4-3s}{8}[|\Psi'(\mu)|^q+m|\Psi'(\frac{\nu}{c})|^q]\right\}^{1/q}\right],$$

which gives the proof. ■

Theorem 9 *Let $\mathbb{X}^\circ\subseteq\mathbb{R}$ be an open invex subset w.r.t $\zeta:\mathbb{X}^\circ\times\mathbb{A}^\circ\to\mathbb{R}$ and $\mu,\nu\in\mathbb{X}^\circ$ with $m\nu+\zeta(\mu,\nu,m)\leq\nu$. Suppose $\Psi:[m\nu+\zeta(\mu,\nu,m),\nu]$ be a differentiable mapping on $\mathbb{X}^\circ$. If $|\Psi'|^q$ is s−type m−preinvex on $(\mu,m\mu+\zeta(\nu,\mu,m))$ for $q\geq1$, $m\in(0,1]$ and $s\in[0,1]$, then*

$$\left|\frac{c}{\zeta(\nu,c\mu,m)}\int_{\mu}^{m\mu+\zeta(\frac{\nu}{c},\mu,m)}\Psi(x)dx-\Psi\left(\frac{2m\mu+\zeta(\nu,\mu,m)}{2c}\right)\right|$$
$$\leq\frac{\zeta(\nu,c\mu,m)}{c}\left[\left(\frac{1}{2}\right)^{1-1/q}\left\{\frac{3-s}{6}|\Psi'(\mu)|^q+\frac{3-2s}{6}m|\Psi'(\frac{\nu}{c})|^q\right\}^{1/q}+\left\{\frac{4-3s}{8}[|\Psi'(\mu)|^q+m|\Psi'(\frac{\nu}{c})|^q]\right\}^{1/q}\right]. \tag{26}$$

Proof From Lemma 2 and applying power-mean inequality, one has

$$\left|\frac{c}{\zeta(\nu,c\mu,m)}\int_{\mu}^{m\mu+\zeta(\frac{\nu}{c},\mu,m)}\Psi(x)dx-\Psi\left(\frac{2m\mu+\zeta(\nu,\mu,m)}{2c}\right)\right|$$
$$=\frac{\zeta(\nu,c\mu,m)}{c}\left\{\int_0^1\delta\Psi'\left(\frac{m\nu}{c}+\delta\zeta(\mu,\frac{\nu}{c},m)\right)d\delta-\int_{1/2}^1\Psi'\left(\frac{m\nu}{c}+\delta\zeta(\mu,\frac{\nu}{c},m)\right)d\delta\right\}$$
$$\leq\frac{\zeta(\nu,c\mu,m)}{c}\left[\left(\int_0^1\delta d\delta\right)^{1-1/q}\left\{\int_0^1\delta|\Psi'\left(\frac{m\nu}{c}+\delta\zeta(\mu,\frac{\nu}{c},m)\right)|^q d\delta\right\}^{1/q}+\left\{\int_{1/2}^1|\Psi'\left(\frac{m\nu}{c}+\delta\zeta(\mu,\frac{\nu}{c},m)\right)|^q d\delta\right\}^{1/q}\right]$$

$$\leq \frac{\zeta(\nu, c\mu, m)}{c} \times \left[\left(\frac{1}{2}\right)^{1-1/q} \left\{\int_0^1 \delta[1-s(1-\delta)]|\Psi'(\mu)|^q d\delta + m\int_0^1 \delta[1-s\delta]|\Psi'\left(\frac{\nu}{c}\right)|^q d\delta\right\}^{1/q}\right]$$

$$+ \frac{\zeta(\nu, c\mu, m)}{c} \times \left\{\int_{1/2}^1 [1-s(1-\delta)]|\Psi'(\mu)|^q d\delta + m\int_{1/2}^1 [1-s\delta]|\Psi'\left(\frac{\nu}{c}\right)|^q d\delta\right\}^{1/q}$$

$$= \frac{\zeta(\nu, c\mu, m)}{c}\left[\left(\frac{1}{2}\right)^{1-1/q}\left\{\frac{3-s}{6}|\Psi'(\mu)|^q + \frac{3-2s}{6}m|\Psi'(\frac{\nu}{c})|^q\right\}^{1/q} + \left\{\frac{4-3s}{8}[|\Psi'(\mu)|^q + m|\Psi'(\frac{\nu}{c})|^q]\right\}^{1/q}\right],$$

which gives the required proof.

■

6 Conclusion

In this work, we showed and investigated a novel idea of preinvex function namely $s-$type $m-$preinvex function and the new sort of Hermite–Hadamard type inequality via newly introduced definition are examined. Further, our attaining results in the order of lemma can be considered as refinements and remarkable extensions to the new family of preinvex functions. In the future, we hope the results of this paper and the new idea can be extended in different directions like fractional calculus, quantum calculus, time scale calculus, etc. We hope the consequences and techniques of this article will energize and inspire the researcher to explore a more interesting sequel in this area.

Declarations

Consent for publication

Not applicable.

Conflicts of interest

The authors declare that there are no conflicts of interest regarding the publication of this paper.

Funding

This research does not receive any external funding.

Author's contributions

M.T.: Conceptualization, Methodology, Software, Writing- Reviewing and Editing. H.A.: Supervision, Investigation, Data Curation, Writing-Original draft preparation. S.K.S.: Visualization, Investigation, Methodology, Software, Writing- Reviewing and Editing. A.A.S.: Conceptualization, Methodology, Software, Supervision, Investigation, Data Curation. B.K.: Methodology, Software, Supervision, Investigation. D.K.: Conceptualization, Methodology, Investigation, Data Curation. All authors discussed the results, approved and contributed to the final manuscript.

Acknowledgements

Not applicable.

References

[1] Hardy, G.H., Little, J.E., & Pólya, G. *Inequalities*, Cambridge, UK. Cambridge University Press. cambridge mathematical library, (1952).
[2] Xi, B.Y., & Qi, F. Some integral inequalities of Hermite-Hadamard type for convex functions with applications to means. *Journal of Function Spaces and Applications*, 2012, Article ID 980438, 1-14, (2012). [CrossRef]
[3] Niculescu, C.P., & Persson, L.E. *Convex functions and their applications* (Vol. 23). Springer, New York, (2006).
[4] Özcan, S., & İşcan, İ. Some new Hermite-Hadamard type integral inequalities for the $s-$convex functions and theirs applications. *Journal of inequalities and applications*, 2019(1), 1-11, (2019). [CrossRef]
[5] Khan, M.A., Chu, Y.M., Khan, T.U., & Khan, J. Some new inequalities of Hermite–Hadamard type for $s-$convex functions with applications. *Open Mathematics*, 15(1), 1414-1430, (2017). [CrossRef]
[6] Sahoo, S.K., Tariq, M., Ahmad, H., Nasir, J., Aydi, H., & Mukheimer, A. New Ostrowski-type fractional integral inequalities via generalized exponential-type convex functions and applications. *Symmetry*, 13(8), 1429, (2021). [CrossRef]
[7] Sahoo, S.K., Ahmad, H., Tariq, M., Kodamasingh, B., Aydi, H., & De la Sen, M. Hermite–Hadamard type inequalities involving k-fractional operator for $(\overline{h}, m)$-convex functions. *Symmetry*, 13(9), 1686, (2021). [CrossRef]
[8] Tariq, M., Ahmad, H., & Sahoo, S.K. The Hermite-Hadamard type inequality and its estimations via generalized convex functions of Raina type. *Mathematical Modelling and Numerical Simulation with Applications*, 1(1), 32-43, (2021). [CrossRef]
[9] Abdeljawad, T., Rashid, S., Hammouch, Z., & Chu, Y.M. Some new local fractional inequalities associated with generalized (s, m) (s, m)-convex functions and applications. *Advances in Difference Equations*, 2020(1), 1-27, (2020). [CrossRef]

[10] Tariq, M., Sahoo, S.K., Nasir, J., Aydi, H., & Alsamir, H. Some Ostrowski type inequalities via n-polynomial exponentially s-convex functions and their applications. *AIMS Mathematics*, 6(12), 13272-13290, (2021). [CrossRef]
[11] Toader, G.H. Some generalizations of the convexity. *In Proceedings of the Colloquium on Approximation and Optimization* (Vol. 329, p. 338). Cluj-Napoca, Romania: University of Cluj-Napoca, (1984, October).
[12] Latif, M. A., & Shoaib, M. Hermite–Hadamard type integral inequalities for differentiable m-preinvex and (α, m)-preinvex functions. *Journal of the Egyptian Mathematical Society*, 23(2), 236-241, (2015). [CrossRef]
[13] Deng, Y., Kalsoom, H., & Wu, S. Some new Quantum Hermite-Hadamard-type estimates within a class of generalized (s, m)-preinvex functions. *Symmetry*, 11(10), 1283, (2019). [CrossRef]
[14] Hanson, M.A. On sufficiency of the Kuhn-Tucker conditions. *Journal of Mathematical Analysis and Applications*, 80(2), 545-550, (1981).
[15] Weir, T., & Mond, B. Pre–inven functions in multiple objective optimization. *Journal of Mathematical Analysis and applications*, 136(1), 29-38, (1998).
[16] Mititelu, S. Invex sets. Studii şi Cercetări Matematice., 46(5), 529–532, (1994).
[17] Antczak, T. Mean value in invexity analysis. *Nonlinear analysis: theory, methods & applications*, 60(8), 1473-1484, (2005). [CrossRef]
[18] Du, T.S., Liao, J.G., & Li, Y.J. Properties and integral inequalities of Hadamard–Simpson type for the generalized (s,m)-preinvex functions. *J. Nonlinear Sci. Appl*, 9(5), 3112-3126, (2016). [CrossRef]
[19] Rashid, S., İşcan, İ., Baleanu, D., & Chu, Y.M. Generation of new fractional inequalities via n polynomials s-type convexity with applications. *Advances in Difference Equations*, 2020(1), 1-20. [CrossRef]
[20] Mohan, S.R., & Neogy, S.K. On invex sets and preinvex functions. *Journal of Mathematical Analysis and Applications*, 189(3), 901-908, (1995). [CrossRef]
[21] Du, T.S., Liao, J., Chen, L., Awan, M.U. Properties and Riemann–Liouville fractional Hermite–Hadamard inequalities for the generalized (α, m)–preinvex functions. *Journal of Inequalities and Applications*, 2016(1), 1-24, (2016). [CrossRef]
[22] Hadamard, J. Étude sur les propriétés des fonctions entières et en particulier d'une fonction considérée par Riemann. *Journal de mathématiques pures et appliquées*, 58, 171-216, (1893).

Mathematical Modelling and Numerical Simulation with Applications (MMNSA) (https://www.mmnsa.org)